UNIVERSITÄT ZU LÜBECK

From the Institute of Biochemistry
of the University of Lübeck
Director: Prof. Dr. Thomas Krey

Immunity and pathogenesis of Ebola virus disease in chimeric mice

Dissertation
For fulfilment of
Requirements
For the Doctoral Degree
Of the University of Lübeck

From the department of Natural Sciences

Submitted by
Monika Rottstegge
from Vreden

Lübeck, 2023

First Referee: Prof. Dr. Lars Redecke

Second Referee: Prof. Dr. Peter König

Date of oral examination: 12.03.2024

Approved for printing: Lübeck, 02.04.2024

Table of Content

List of Figures

List of Abbreviations

ADCC	Antibody-dependent cell-mediated cytotoxicity
ADCP	Antibody-dependent cellular phagocytosis
APC	Antigen-presenting cell
AST	Aspartate aminotransferase
BCR	B cell receptor
BDBV	Bundibugyo Ebola virus
BLT	Bone marrow-liver-thymus
BOMV	Bombali Ebola virus
BSA	Bovine serum albumin
BSL4	Biosafety level 4
CD	Cluster of differentiation
cDC	Conventional dendritic cells
CFR	Case fatality rate
CNS	Central nervous system
CTL	Cytotoxic T lymphocytes
CTLA-4	Cytotoxic T-lymphocyte-associated protein 4
DC	Dendritic cell
DC-SIGN	Dendritic Cell-Specific Intercellular adhesion molecule-3-Grabbing Non-integrin
DMEM	Dulbecco's Modiefied Eagle Medium
DMSO	Dimythylsulfoxid
DNA	Deoxyribonucleic acid
DRC	Democratic Republic of Congo
EBOV	Zaire Ebola virus
EDTA	Ethylenediaminetetraacetic acid
ELISPOT	Enzyme-linked immune-spot
et al.	Et alii, and others
EVD	Ebola virus disease
FACS	Flow-associated cell sorting
FcγR	Fragment crystallizable region gamma receptors
FCS	Fetal calf serum
FFU	Focus forming units
Fig.	Figure
FSC	Forward scatter

g	gram
GM-CSF	Granulocyte-macrophage colony-stimulating factor
GP	Glycoprotein
gpa-EBOV	Guinea pig-adapted Ebola virus
GvHD	Graft versus host disease
h	Hour
HBV	Hepatitis B virus
HCV	Hepatitis C virus
HEK 293T cells	Human embryonic kidney cells
HIS	Human immune system
HIV	Human immunodeficiency virus
HLA	Human leucocyte antigen
HLA-DR	Human leucocyte antigen-DR isotype
HSC	Hematopoietic stem cell
HuPBMC	Human peripheral blood mononuclear cells
IFN	Interferon
IFN-I	Type I interferons
IFNAR-KO	Interferon α/β receptor-knockout
Ig	Immunoglobulin
IL	Interleukin
i.p.	intraperitoneal
IP-10	Interferon gamma-induced protein 10
IRF	Interferon regulatory transcription factor
ISG	Interferon-stimulated genes
i.v.	Intravenous
IVC	Individually ventilated cage
JAK	Janus tyrosine kinase
L	L Protein
l	Liter
LASV	Lassa virus
LN	Lymph node
L-SIGN	Liver/lymph node-specific intercellular adhesion molecule-3-grabbing integrin
MACS	Magnetic-activated cell sorting
maEBOV	Mouse-adapted Ebola virus
MARV	Marburg virus

MCP	Monocyte chemoattractant protein
M-CSF	Macrophage colony-stimulating factor
MDA5	Melanoma differentiation-associated protein 5
MFI	Median fluorescence intensity
MHC	Major histocompatibility complex
µM	micromolar
min	Minutes
MIP	Macrophage inflammatory protein
ml	Milliliter
mM	millimolar
MoDCs	Monocyte-derived dendritic cells
MOI	Multiplicity of infection
mRNA	Messenger ribonucleic acid
MyD88	Myeloid differentiation primary response protein 88
N_{AB}	Neutralizing antibody
NF-κB	Nuclear factor k-light-chain-enhancer of activated B cells
ng	Nanogram
NHP	Non-human primate
NK cell	Natural killer cell
nm	Nanometer
NOD	Non-obese diabetic
NO	Nitric oxide
NP	Nucleoprotein
NPC1	Niemann-Pick C1
ns	Not significant
NSG	Non-obese diabetic/severe combined immunodeficiency-interleukin-2 (IL-2) receptor-γ chain knockout mice
PAMP	Pathogen-associated molecular pattern
PBL	Peripheral blood leucocyte
PBS	Dulbecco's Phosphate Buffered Saline
PBMC	Peripheral blood mononuclear cell
PD	Programmed cell death protein
pDC	Plasmacytoid dendritic cell
PECAM	Platelet and cell adhesion molecule
PFA	Paraformaldehyde
p.i.	Post inoculation

PRR	Pattern recognition receptor
P/S	Penicillin/Streptomycin
RBD	Receptor binding domain
RdRP	RNA-dependent RNA polymerase
RESTV	Reston Ebola virus
RIG	Retinoic acid-inducible gene
RLR	RIG-I-like receptor
RNA	Ribonucleic acid
RNP	Ribonucleoprotein complex
rpm	Rounds per minute
RPMI	Roswell Park Memorial Institute
r.o.	retroorbital
SCF	Stem cell factor
SCID	severe combined immunodeficiency
sGP	Soluble glycoprotein
SSC	Sideward scatter
ssGP	Small soluble glycoprotein
STAT	Signal transducer and activator of transcription
SUDV	Sudan Ebola virus
TAFV	Tai Forest Ebola virus
TCR	T cell receptor
TF	Tissue factor
Th cells	T helper cells
TIM	T-cell immunoglobulin and mucin domain
TIR	Toll/interleukin-1 receptor
TLR	Toll-like receptor
TNF	Tumor necrosis factor
TRIF	TIR-domain-containing adapter inducing interferon β
U	Units
UV	Ultraviolet
V	Volt
VP	Virus protein
WT	Wildtype

1. Abstract

1.1 Abstract

Ebola virus disease (EVD) caused by the Ebola virus species *Zaire ebolavirus* (EBOV) is a deadly disease with up to 90% lethality. Due to the lack of human samples, animal models, and laboratory tools, knowledge about the host immune response against EBOV infection is limited. The hallmarks of EVD include high inflammation, coagulation abnormalities, multiorgan failure, and importantly dysregulation of innate and adaptive immune responses. During fatal EVD, the infection of antigen-presenting cells (APCs) can disrupt the bridge between innate and adaptive immunity and therefore dysregulate T cell response.

To improve our understanding of the interaction between dendritic cells (DCs) and T cells, and their contribution to the pathophysiology of EVD, highly immunodeficient NSG mice were transplanted with human peripheral blood leucocytes (PBLs) and human monocyte-derived dendritic cells (moDCs), referred to as avatar mice.

It was shown that EVD with pathological features could be recreated by the mere addition of human PBLs and EBOV-infected moDCs into NSG mice. The severity was highly dependent on the interaction of the T-cell receptor (TCR) with major histocompatibility complex (MHC)-molecules. The limitations of avatar mice were also highlighted in the context of deciphering the immune response to EBOV infection. The interaction of the host and the xenograft strongly influenced the phenotype of the human cells hampering the analysis by flow cytometry. Finally, it was demonstrated that only the combination of PBLs and immunoglobulins G (IgG) from EVD survivors could prevent avatar mice from succumbing to EBOV infection. The transplantation of PBLs alone was not sufficient to rescue EBOV-infected mice.

The mouse model developed in this study demonstrates that EVD is highly reliant on the interaction between PBLs and EBOV-infected APCs and can occur alone from the interaction. Additionally, this study strongly provided compelling evidence that for the protection against EBOV infection both cellular as well as humoral adaptive immunity are necessary.

1.2 Zusammenfassung

Ebolaviren (EBOV) sind Verursacher des Ebolafiebers (EVD), welches in bis zu 90% der Fälle tödlich verläuft. Die Spezies Zaire ebolavirus (EBOV) weist die höchste Letalität auf. Durch das Fehlen von humanen Proben, Kleintiermodellen und Labormethoden ist das Wissen über die Immunantwort des Wirtes während einer EBOV-Infektion begrenzt. Charakteristische Symptome des Ebolafiebers sind unter anderem starke Entzündungen, Gerinnungsstörungen, Multiorganversagen und vor allem eine Dysregulation der angeborenen und adaptiven Immunantwort. Bei einem tödlichen Krankheitsverlauf kann die Infektion von antigenpräsentierenden Zellen (APCs) die Brücke zwischen angeborener und adaptiver Immunität hemmen und somit die T-Zell-Reaktion dysregulieren.

Um sowohl die Interaktion zwischen dendritischen Zellen (DCs) und T-Zellen als auch ihren Beitrag zur Pathophysiologie von EVD besser zu verstehen, wurden immundefizienten NSG-Mäusen menschliche periphere Blutleukozyten (PBLs) und aus menschlichen Monozyten gewonnene DCs (moDCs) transplantiert, die als Avatar-Mäuse bezeichnet werden.

Es konnte gezeigt werden, dass EVD mit pathologischen Merkmalen durch die bloße Zugabe von menschlichen PBLs und EBOV-infizierten moDCs in NSG-Mäusen nachgebildet werden kann. Der Schweregrad der Erkrankung war stark von der Interaktion des T-Zell-Rezeptors (TCR) mit den Molekülen des Haupthistokompatibilitätskomplexes (MHC) abhängig. Im Zusammenhang mit der Untersuchung der Immunantwort auf eine EBOV-Infektion wurden auch die Grenzen der Avatar-Mäuse aufgezeigt. Die Interaktion zwischen dem Wirt und dem Xenotransplantat beeinflusste den Phänotyp der menschlichen Zellen stark, was die Analyse mittels Durchflusszytometrie erschwerte. Schließlich konnte gezeigt werden, dass nur die Kombination aus PBLs und Immunglobulinen G (IgG) von EVD-Überlebenden verhindern konnte, dass Avatar-Mäuse einer EBOV-Infektion erlagen. Die Transplantation von PBLs allein war nicht ausreichend, um EBOV-infizierte Mäuse zu retten.

Das in dieser Studie entwickelte Mausmodell zeigt, dass EVD in hohem Maße von der Interaktion zwischen PBLs und EBOV-infizierten APCs abhängt und allein durch diese Interaktion entstehen kann. Darüber hinaus lieferte diese Studie Beweise dafür, dass

für den Schutz vor einer EBOV-Infektion sowohl zelluläre als auch humorale adaptive Immunität erforderlich sind.

.

2. Introduction

2.1 The Ebola virus

2.1.1 The virus and its history

2.1.1.1 Ebola virus and its family

The genus *Ebolavirus* belongs to the family *Filoviridae* and to the order *Mononegavirales* (Kuhn et al., 2019). The *Filoviridae* family includes six genera and 11 distinct virus species. Besides Ebolaviruses, Marburg-, Dianlo-, and Cuevaviruses can also infect mammalian hosts, while members of the genera *Striavirus* and *Thamnovirus* were discovered in piscine hosts. The name *Filoviridae* reflects their most apparent morphological feature: the filamentous shape (from the Latin *filum*, meaning thread) (**Fig. 1**). Furthermore, filoviruses are enveloped, single-stranded and negative-sense RNA (ribonucleic acid) viruses (Kuhn et al., 2019). Ebolaviruses are polymorphic, so that the virion can be u-shaped, 6-shaped, and branched. While the diameter is always 80 nanometers (nm), the length can vary up to 14 000 nm (Murphy et al., 1978; Feldmann & Geisbert, 2011).

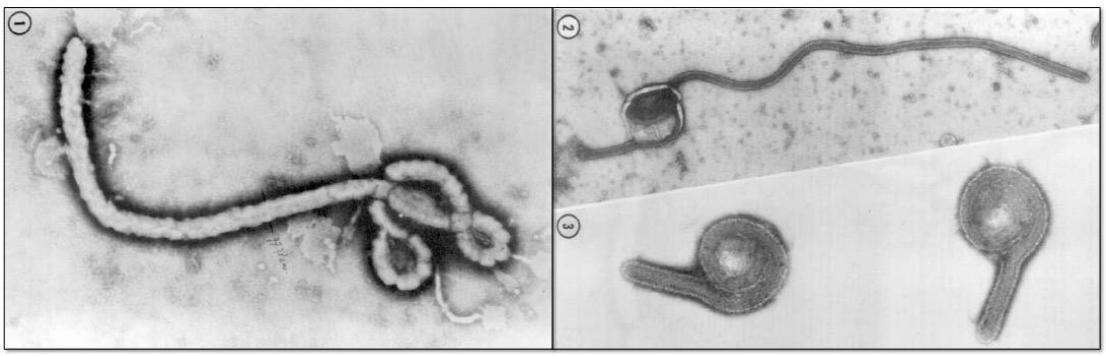

Figure 1: Ebola virus (sp. *Zaire ebolavirus*) morphology. From Murphy et al., 1978.

The *Ebolavirus* genus is comprised of six distinct species: EBOV (species *Zaire ebolavirus*, EBOV), Sudan virus (*Sudan ebolavirus*, SUDV), Bundibugyo virus (*Bundibugyo ebolavirus*, BDBV), Taï Forest virus (*Taï Forest ebolavirus*, TAFV), Reston virus (*Reston ebolavirus*, RESTV), and the recently discovered Bombali virus (*Bombali ebolavirus*, BOMV) (Goldstein et al., 2018; Kuhn et al., 2019). Only EBOV, SUDV, TAFV and BDBV are known to be pathogenic for humans (Le Guenno et al., 1995; Towner et al., 2008). For TAFV only one case of severe, but non-lethal infection was reported and RESTV is pathogenic for non-human primates but probably not for

humans, although seroconversions in individuals exposed have been observed (Cantoni et al., 2016; Jahrling et al., 1990; Le Guenno et al., 1995). It is currently not known whether BOMV may cause disease in humans. EBOV has been the etiological agent responsible for most outbreaks to date. It is also the ebolavirus with highest case-fatality rates in humans and the virus that will be covered in this thesis (https://www.cdc.gov/vhf/ebola/history/summaries.html; 10.10.2023) (De La Vega et al., 2015).

2.1.1.2 Virion structure and viral proteins

EBOV is an enveloped, single-stranded, negative-sense RNA virus. Its genome has a size of 19kb and encodes for seven genes (**Fig. 2A**) (Kuhn et al., 2019). Except for the glycoprotein (GP) all genes are monocistronic leading to nine distinct proteins that are being expressed: nucleoprotein (NP), polymerase cofactor virion protein (VP35), matrix protein VP40, $GP_{1,2}$ (GP consists of two subunits GP1 and GP2), soluble GP (sGP), small soluble GP (ssGP), transcription factor VP30, minor matrix protein VP24, and RNA-dependent RNA polymerase (L) (Sanchez et al., 1993; Mehedi et al., 2011). The complex formation of the EBOV virion requires seven of these proteins, the so-called structural proteins (**Fig. 2B**). Only sGP and ssGP are non-structural. NP and VP30 strongly interact with the viral RNA and form together with L and VP35 the ribonucleoprotein complex (RNP) (Alvarez et al., 2002; Mühlberger et al., 1999; Noda et al., 2010; Volchkov et al., 1995). The RNP is embedded in a matrix primarily consisting of VP40 followed by an outer envelope derived from the host-cell plasma membrane (Jasenosky et al., 2001; Noda et al., 2002). Table 1 summarizes the proteins and their respective functions.

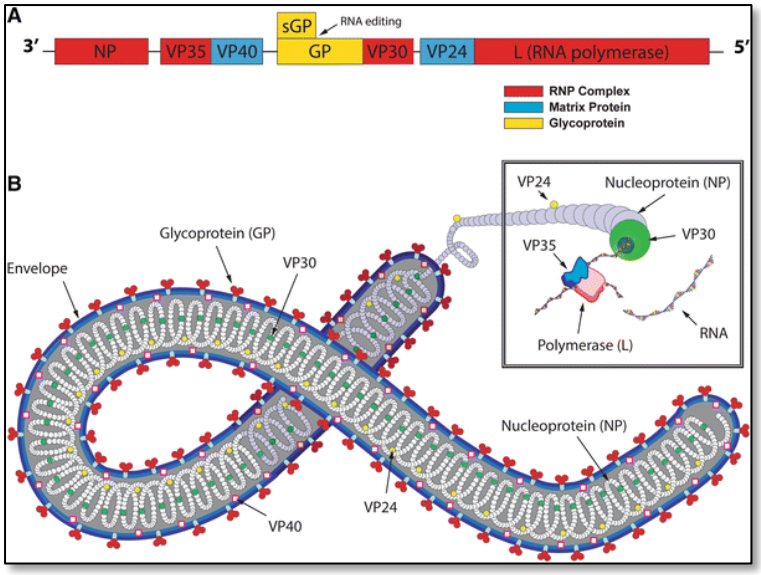

Figure 2: The Ebola virus. A) Schematic representation of the EBOV genome. It contains seven structural proteins (NP, VP24, VP30, VP35, VP40, L, GP) and two non-structural proteins (sGP and ssGP). B) Structure of EBOV particle. During replication NP, VP30, VP35, VP24, nd L protein form ribonucleoprotein (RNP) complex with viral RNA (Choi & Croyle, 2013).

Table 1: Overview of EBOV proteins (Emanuel et al., 2018).

Genome Position	Protein	Protein Functions	Molecular Weight (kDa)
1	Nucleoprotein (NP)	Major nucleoprotein, component of RNP	90 – 104
2	Virion protein 35 VP(35)	Polymerase cofactor, component of RNP, interferon antagonist	35
3	Virion protein 40 (VP40)	Matrix protein, virion assembly, budding	35 – 40
4	Glycoprotein (GP)	Viral entry, receptor binding, membrane fusion	150 – 170
	Soluble glycoprotein (sGP)	Antigenic subversion, restores endothelial barrier function	50 – 55
	Small soluble Glycoprotein (ssGP)	Unknown	50 – 55
5	Virion protein 30 (VP30)	Minor nucleoprotein, component of RNP	27 – 30
6	Virion protein 24 (VP24)	Nucleocapsid condensation, virion assembly, interferon antagonist	24 – 25
7	RNA polymerase (L)	RNA-dependent RNA polymerase, component of the RNP	270

2.1.1.3 Discovery and outbreaks

EBOV can cause outbreaks in humans in central and West Africa with case fatality rates of up to 90% (https://www.cdc.gov/vhf/ebola/history/distribution-map.html, 10.10.2023). EBOV was discovered for the first time in 1976 in the former Republic of Zaire (now Democratic republic of Congo, DRC) (Cox et al., 1983). As the newly discovered pathogen showed the same morphological features and caused similar symptoms in patients as Marburg viruses (MARV), researchers first assumed that these were new cases of MARV infection. The latter virus had been already discovered in 1967 when monkey tissues were imported to Marburg and research personnel fell

ill (Siegert et al., 1967). However, it turned out that an unknown causative agent of viral hemorrhagic fever was isolated being responsible for this outbreak in 1976, which was then named after the Ebola River in northwestern DRC (Emond et al., 1977; Johnson et al., 1977; Pattyn et al., 1977). Since its first emergence with 318 cases (280 deaths) in Zaire, there have been periodical outbreaks of Ebola virus disease (EVD) in several African countries (**Fig. 3**). One noteworthy epidemic happened in Zaire 1995 (now DRC) with 315 cases (250 deaths). Until 2013 most outbreaks originated in middle Africa (Congo, Gabon, DRC) and were quickly under control because small, isolated populations were affected so that population movement outside of the areas was limited and effective contact tracing was possible (https://www.cdc.gov/vhf/ebola/history/chronology.html; 10.10.2023). In 2013 the most devastating outbreak so far started in Guinea and uncontrollably spread across three Western African countries, namely, Guinea, Sierra Leone, and Liberia. It was soon considered as a global public health emergency of international concern. 28 646 cases and 11 323 deaths were reported until 2016. Densely populated areas were affected and supported spreading of the virus (https://www.cdc.gov/vhf/ebola/history/2014-2016-outbreak/index.html; 10.10.2023). This outbreak really emphasized the pandemic potential of EBOV, but also helped to get more insight into the disease itself facilitating the development and licensing of two vaccine candidates (Ervebo, Merck, and Zabdeno/Mvabea, Janssen Pharmaceuticals). Despite the improved surveillance in affected area and vaccination of EVD-patient-contacts, it is still a difficult task to contain outbreaks as the most recent epidemic in DRC and Uganda from 2018 to 2020 indicated (3470 cases, 2287 deaths) (https://www.cdc.gov/vhf/ebola/outbreaks/drc/overview.html; 10.10.2023).

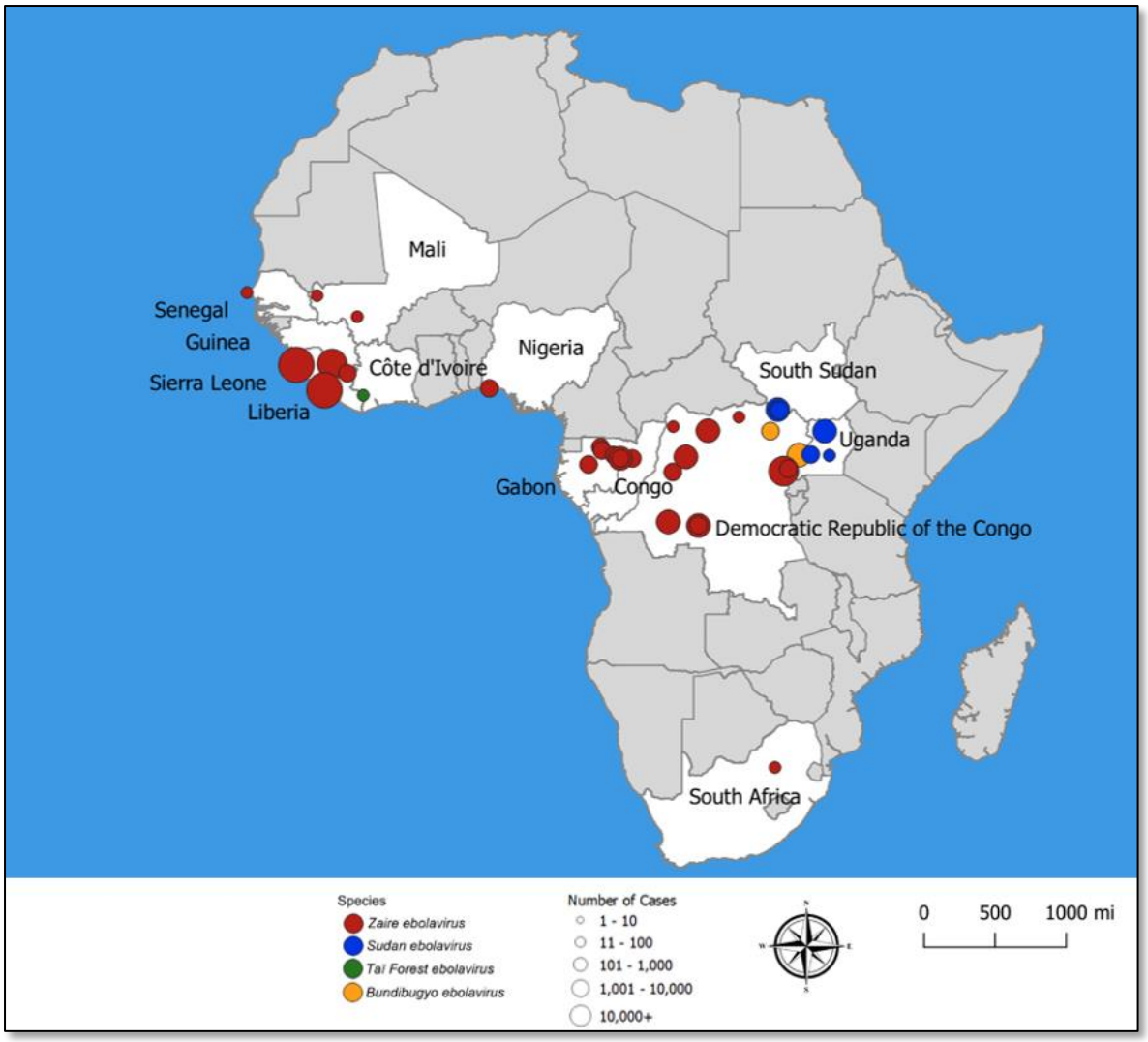

Figure 3: Ebola outbreak distribution map in Africa from 1976 – 2021. This map shows outbreaks of Ebolavirus by species and number of cases in Africa from 1976 – 2021. (https://www.cdc.gov/vhf/ebola/images/Ebola_Africa2021.png; 10.10.2023).

2.1.1.4 Epidemiology and transmission

EBOV is likely endemic in Western and Central Africa. Eastern Africa countries have also reported outbreaks caused by other ebolaviruses such as BDBV and SUDV. RESTV represents an exception and circulates in Eastern and South-eastern Asia. EBOV is a zoonotic pathogen, meaning that it is maintained in animal reservoir species and occasionally are transmitted into humans via zoonotic spillover (Feldmann & Geisbert, 2011; Leroy et al., 2005). Since other filoviruses (MARV and the *Cuevavirus* member Lloviu virus) have been successfully isolated from bat species, namely, *Roussetus aegyptiacus* and *Miniopterus schreibersii* bats respectively, bats are proposed to be also reservoir hosts for EBOV (Towner et al., 2007, 2008). Previous studies have demonstrated the presence of antibodies against EBOV in bats as well

as the presence of viral RNA in some specimens (Leroy et al., 2005). However, until now, infectious EBOV has not been isolated from bats.

Outbreaks are typically initiated by single spillover events followed by human-to-human transmission (**Fig. 4**) (Baize et al., 2014; Dowell et al., 1999a; Gałas, 2014; Roels et al., 1999). Spillovers have been suggested to occur through human contact with living intermediate host (apes or other mammals) or their carcasses, consumption of bushmeat, or directly through contact with putative EBOV bat reservoirs (Baize et al., 2014). Human-to-human transmission requires contact with infected body fluids. The highest risk of contracting EBOV in this setting is through contact with infectious body fluids of sick individuals or cadavers (for example at traditional funerals). Recent data also indicates that EBOV can persist in surviving individuals for long periods of time after recovery and that outbreaks can be initiated via infection of naïve individuals due to contact with survivors (Subissi et al., 2018). In this regard, infectious virus could be detected in survivor semen, breastmilk, cerebrospinal fluid, and aqueous humor. Flare-up events through sexual contacts with EVD survivors had been previously documented (Jacobs et al., 2016; Mate et al., 2015; Moreau et al., 2015; Subissi et al., 2018; Thorson et al., 2021; Varkey et al., 2015; Vetter et al., 2016).

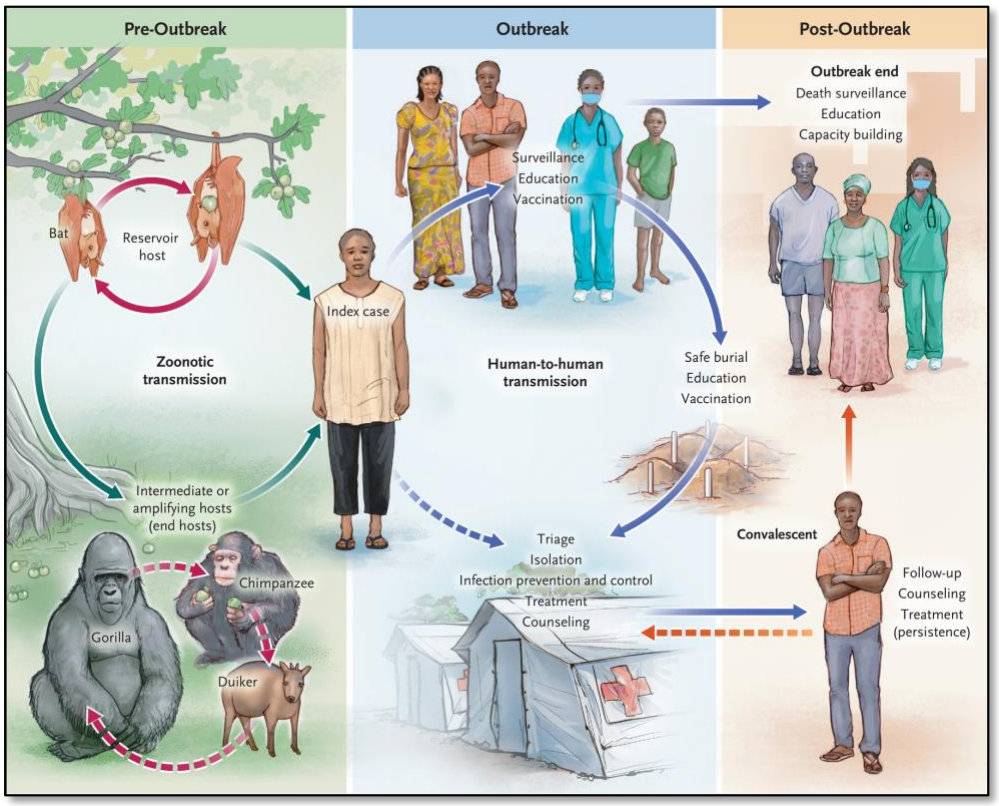

Figure 4: Phases of EBOV outbreaks. EBOV outbreaks usually start with a single spillover event from its reservoir host (putative fruit bats) or an intermediate host, creating the index case. This is followed by human-to-human transmission (Feldmann et al., 2020).

2.1.2 Disease and pathogenesis

2.1.2.1 Clinical timeline and manifestations of Ebola virus disease

EBOV is the causative agent of EVD, formerly known as Ebola hemorrhagic fever (Kuhn et al., 2019; Rojek et al., 2017). EVD is a severe, often fatal disease in humans with a case fatality rate (CFR) of up to 90%. Most of the infections in humans happen through close contact with the blood, secretions, or body fluids of infected individuals (Dowell et al., 1999b; Khan et al., 1999; Leroy et al., 2009; Report of a WHO/International Study Team, 1978; Report of an International Commission, 1978).

After exposure the virion enters the host via lesions in the skin or directly through the mucosa. The incubation period can vary between 2 and 21 days (Velásquez et al., 2015). The clinical progression of EVD can be separated into three distinct phases. The **initial phase** of infection occurs within the first 1 to 3 days and manifests as a non-specific febrile illness characterized by an abrupt onset. Common clinical manifestations during this stage include elevated body temperature, malaise, profound fatigue, and myalgia. A few days later gastrointestinal symptoms ranging from mild to severe occur (**gastrointestinal phase**), predominantly nausea, diarrhea, and vomiting, coupled with anorexia, abdominal discomfort, extreme fatigue, and localized pain (mainly in joints). This is further complicated by substantial fluid loss of up to 5 – 10 l/day leading to extreme dehydration. Following this stage, patients with a mild course of disease will start recovering, while others may go into shock, possibly stemming from hypovolemia (low body fluids) and systemic inflammatory response. This marks the onset of the **final stage of EVD**. In this advanced phase, EVD can lead to liver and kidney failure resulting in a severe metabolic compromise, convulsion, and shock. Death can occur within 16 days after the first symptoms typically because of multi-organ failure. In this final stage **hemorrhagic events** may develop, manifesting as conjunctival bleeding, petechiae (red spots on the skin caused by minor bleeding from damaged capillary blood vessels), gastrointestinal bleeding, mucosal hemorrhage, persistent bleeding at venipuncture sites. Moreover, EVD has the potential to affect the neurological system and may cause confusion, delirium, convulsion, and encephalitis (Baseler et al., 2017; Leligdowicz et al., 2016; Nicastri et al., 2019).

2.1.2.2 Pathogenesis and pathophysiology

The pathophysiology of EVD centers mainly around robust viral replication and the interaction with the host immune system. In fact, most human cells are susceptible to infection, but primary targets are **mononuclear phagocytes** (Kupffer cells, macrophages, microglia) and **DCs** (Schnittler and Feldmann, 1998; Geisbert, et al., 2003b; Geisbert, 2005; Geisbert, et al., 2015; Lüdtke et al., 2017). EBOV $GP_{1,2}$, $GP_{1,2}$ attachment factors on host cells, and endosomal binding to the entry receptor **Niemann-Pick C1 (NPC1)** are predominantly defining cell tropism for EBOV (Carette et al., 2011; Côté et al., 2011). $GP_{1,2}$ mediates the attachment of the virion to cell surface molecules such as C-type lectins among others. The most-described representative of this group is the molecule **dendritic cell-specific intercellular adhesion molecule-3-grabbing non-integrin** (**DC-SIGN**) (Alvarez et al., 2002; Simmons et al., 2003; Takada et al., 2004).

Migratory APCs such as DCs likely facilitate virus dissemination from the initial portals of entry to the draining lymph nodes (**Fig. 5**) (Lüdtke et al., 2017). From here viral particles are released into the circulation (Geisbert, et al., 2003b; Schnittler & Feldmann, 1998). Once EBOV is in peripheral tissues, it can infect many other cells: Kupffer cells, fibroblasts, hepatocytes, cells of adrenal gland tissue, endothelial and epithelial cells. Specifically, lymphoid tissues, liver, and adrenal glands support high levels of viral replication (**Fig. 5**). This manifests itself especially in the liver in the form of necrotic regions (Baize et al., 1999)

Another important aspect, that drives is the high concentration of chemokines and cytokines produced upon interaction of the virus with host immune cells, leading on the one hand to recruitment of more myeloid cells to the entry site, but on the other hand to imbalances regarding their expression (Baize et al., 2002; Gupta et al., 2012; Wauquier et al., 2010a). This so-called **cytokine storm (or hypercytokinemia)** highly impairs the innate and adaptive immune response (McElroy et al., 2015; Ruibal et al., 2016), which is covered in the sections below, and also results in endothelial cell dysfunction accompanied by cell increased vascular permeability and fluid extravasation. Along with inhibition of platelet function and consumption of clotting factors, this leads to coagulopathy. Besides many still unclear facts, a clear connection could be established between severe EVD cases and high concentrations of pro-inflammatory cytokines, pro-inflammatory chemokines, and anti-inflammatory cytokines.

In summary, it can be said that the interaction of many different factors leads to the development of this highly complex disease pattern, which affects different organs. The inability to control viral replication and the host immune response are the key drivers of EVD.

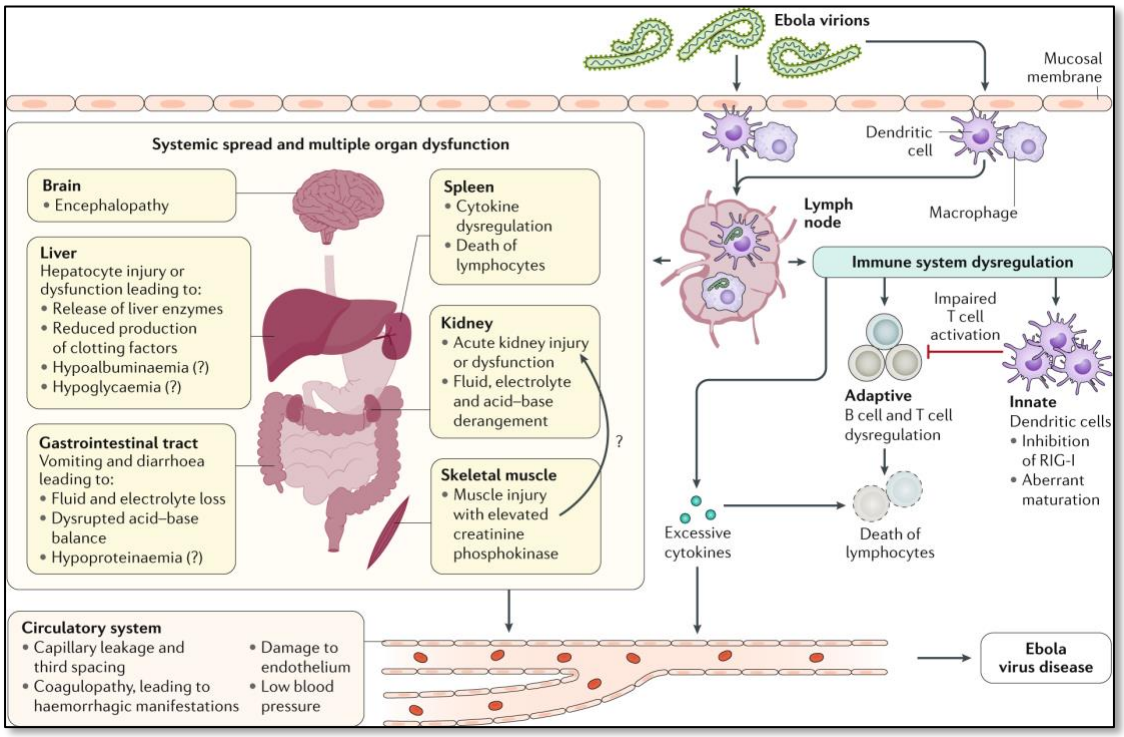

Figure 5: EVD pathogenesis. EBOV virions enter the body through mucosal membranes or lesions in the skin Their first targets are macrophages and certain dendritic cells. These probably facilitate dissemination to lymph nodes, and from there systemic spreading (Jacob et al., 2020).

2.1.2.3 Post-EVD syndrome

The outbreak 2013-2016 facilitated a better insight into post-disease sequelae. Among the survivor community it became clear that a significant number of convalescent patients showed post-disease symptoms such as musculoskeletal pain, headaches, encephalitis, and uveitis, even months and years after discharge. Ocular symptoms include retro-orbital pain, blurry vision, eye pain, sensitivity to light, and conjunctival inflammation. In fact, 14 – 60% of adult survivors were affected by some of these sequelae (Qureshi et al., 2015; Rowe et al., 1999; Tiffany et al., 2016). Arthralgia is reported in 87% of the cases affecting knees, back, hips, fingers, wrists, neck, shoulders, ankles, and elbows (Rowe et al., 1999; Qureshi et al., 2015). Neurological sequelae after EVD infection can include headache, memory loss, mental status changes, seizures, and insomnia. In addition to the above-mentioned long-term physical effects, more and more psychological issues are being revealed (Epstein et al., 2015; Nanyonga et al., 2016). These have a substantial effect on the life of EVD

survivors and are mostly anxiety, depression, and post-traumatic stress disorder. The development of these sequelae is still poorly understood, but the severity of acute disease or exposure to experimental therapies as well as frequency of severity of complication, risk of viral persistence, or disease recrudescence might play roles. Specifically, persistence is increasingly becoming the focus of scientific research since it clearly contributes to long-lasting symptoms (Hugo et al., 2015; Mohammed et al., 2015; Reardon, 2015).

These factors are highlighting the demand on follow up care of EVD survivors after discharge to treat long-term medical (physical and psychological) problems as well as preventing transmission or resurgence of EBOV.

2.2 Immune response to Ebola virus in Humans

The understanding of the immune response to EBOV is still very limited. The vast majority of data comes from *in vitro* experiments. The limited availability of specimen from infected patients and the requirement to work under biosafety level 4 conditions hinders the progression in research as well. The last outbreaks presented a great opportunity to study the human host response to EBOV and to answer some questions regarding correlates of immunity to fatal cases and survivors.

To be able to infect its host, a pathogen must overcome anatomical and chemical barriers, which means that the host must be permissive. The first line of defense includes intrinsic mechanisms as part of the **innate immune response**, which can be initiated almost immediately, and consists of both physical barriers as well as cell-mediated mechanisms to induce an antiviral state in infected and bystander cells. These mechanisms serve on the one hand, to protect cells and thus prevent virus replication and, on the other hand, to induce rapid cell death to eliminate so-called virus factories. In order to achieve this, components of the innate and adaptive immune response including macrophage, neutrophils, T and B cells are being recruited (Akira et al., 2006). The latter cells are part of the so-called **adaptive or acquired immune response**, which is characterized by high specificity to the pathogen. Once the immunological memory is formed, memory T and B cells can be rapidly reactivated upon reinfection with the same pathogen (Guidotti & Chisari, 2001; Iwasaki & Medzhitov, 2004). A major challenge in this context is to restore the baseline situation after clearing the infection, meaning that the immune activation must be suppressed

resulting in immune homeostasis. This is due to the fact, that a highly activated immune system always goes along with the destruction of infected cells and the production of toxic inflammatory mediators. Long-term antiviral responses can result in sustained inflammation, which can in turn cause organ failure, chronic illness, or in the worst case, the death of the affected person (Levy & García-Sastre, 2001; Samuel, 2001). The following part covers a deeper insight into host immune response to EVD and the differences between fatal and non-fatal disease.

2.2.1 Viral recognition and cell signaling

In general, the induction of the immune response cascade requires in the first place the **detection** of a pathogen, followed by **signaling** events. The first processes are part of the intrinsic cellular defense, meaning, that they can be activated immediately or through a signal immediately. The detection procedure must function in such a way that pathogens are recognized as non-self. This is given through a receptor-mediated recognition process that can differentiate unique structure of the respective pathogen, so-called **pathogen-associated molecular patterns (PAMPs)** (Koyama et al., 2008) **(Fig. 7)**. The important task of detecting these structures is carried out by germline-encoded cellular **pattern recognition receptors (PRRs)**, which can be either on cell surfaces or in the cytoplasm. In addition to PAMPs, they can also recognize host components that are released upon cellular damage (Koyama et al., 2008; Meylan et al., 2006). Pathogen recognition rapidly triggers cell signaling cascades for the synthesis of inflammatory cytokines, chemokines, and the transcription of **type I interferon (IFN-I) genes**, which in turn impact cell proliferation, and thus can mobilize immune cells to lymph nodes and activating those (Akira et al., 2006; Ivashkiv & Donlin, 2014). The most prominent and relevant innate sensors for viral infections are **Toll-like receptors (TLRs)** and **retinoic acid-inducible gene I** (**RIG-I)-like receptors (RLRs)**. The detection of virus particles (and intracellular bacteria) is enabled through TLR 3, 7, 8, and 9, recognizing mostly nucleic acid PAMPs (Kumar et al., 2011; Meylan et al., 2006; Saito & Gale, 2007). Ligand binding activates intracellular signaling through adapter proteins causing the first step in the inflammatory response. For antiviral defense two adapter proteins are important: MyD88 (myeloid differentiation primary response protein 88) and TRIF [TIR (Toll/interleukin-1 receptor)-domain-containing adapter inducing interferon β]. Both adapter proteins are inducing conserved downstream pathways that include either NF-κB (nuclear factor k-light-chain-enhancer of activated B cells) or **interferon regulatory transcription factors**

(IRFs), which ultimately results in transcription of genes encoding inflammatory chemokines and cytokines, important proteins for cell signaling, that directly activate or attract more immune cells to the site of infection (**Fig. 6**) (Ivashkiv & Donlin, 2014; Le Bon & Tough, 2002).

The first recognized group of cytokines in terms of innate immunity against viral infections were **interferons (IFNs)**. Three different types of IFNs have been discovered so far. They are classified according to the receptor they signal through. IFN-I were the first being described as important factors involved in antiviral responses (García-Sastre & Biron, 2006; Teijaro, 2016). In fact, they can be produced by all nucleated cells and function as activators of macrophages, NK cells, and DCs (Le Bon and Tough, 2002). Therefore, they play a crucial role in the development of the adaptive immune response. Type II IFNs only represent one member: IFN-gamma (IFNγ), which is produced mainly by NK and T cells. The last group are the type III IFNs and have been only recently discovered (Ye, et al., 2019).

IFNs are secreted, circulate, and bind to their respective receptor, transmembrane heterodimers with an extracellular and intracellular signaling domain. The cascade, which is activated upon binding, is called the JAK (Janus tyrosine kinases) -STAT (signal transducer and activator of transcription) signaling pathway (**Fig. 6**). This results in the relocation of STAT into the nucleus and to the transcription of interferon-stimulated genes (ISGs) being particularly important for the host defense against primary virus infections (Samuel, 2001), since some have the potential for direct antiviral measures to induce the so-called **antiviral state** in bystander cells neighboring the cell affected by the virus (Sadler & Williams, 2008). They can induce apoptosis (cell death) in infected cells and inhibit viral replication.

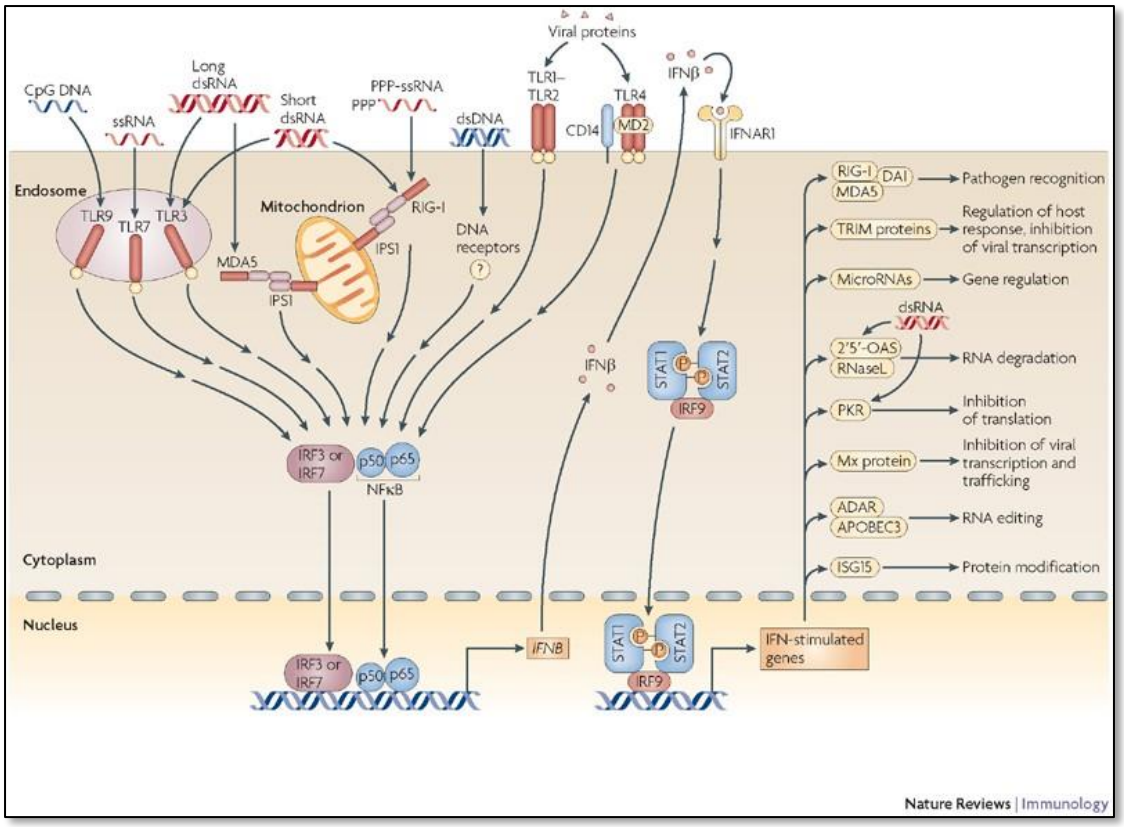

Figure 6: Activation of IFN responses through viral PAMPs. PRRs initiate signaling through NFκB resulting in the transcription of IFN-regulatory factors. This leads to the expression of IFNβ, which initiates an antiviral program, which involves the expression of IFN-stimulated genes (Bowie and Unterholzner, 2008).

2.2.2 Immune evasion mechanisms and innate immunity

Despite innate immune barriers, severe EVD is associated with systemic viral replication and high levels of viremia (De La Vega et al., 2015; Lanini et al., 2015), which means the virus must have developed strategies to circumvent these. In fact, EBOV has evolved mechanisms which effectively counteract **host intrinsic and innate antiviral defenses** in the first place, but also the adaptive arm of immunity (described in 2.2.4).

VP35 and VP24 play a major role in counteracting the hosts innate immune response. *In vitro* findings demonstrated that they downregulate the expression of type I and type III IFN signaling. VP35 impairs the phosphorylation of interferon regulatory factors (IRFs) and inhibits RIG-I signaling through binding viral dsRNA so that recognition by RIG-I is inhibited (Basler et al., 2003; Cárdenas et al., 2006). VP24 interferes with IFN-induced antiviral responses according to *in vitro* data. It inhibits nuclear re-localization of STAT 1, thus impairing JAK-STAT signaling pathways and the production of IFNs

(Basler et al., 2000; Cárdenas et al., 2006; Reid et al., 2006; Zhang et al., 2012). Another important step in viral replication is the final budding of new viral particles from the host cell. This can be inhibited by the host protein tetherin (Neil, 2013), which has been shown to act as an antagonist to VP40. But it seems that GP expression can rescue VP40-induced budding, whereby the mechanism is not elucidated (Jouvenet et al., 2009; Kaletsky et al., 2009).

Fatal cases have not only been associated with high viremia and a cytokine storm resulting in an immunological imbalance (Wauquier et al., 2010a). Infected DCs and macrophages release pro-inflammatory cytokines such as interferons, interleukin 1β (IL1β), IL1-RA, IL-6, IL-8, IL-10, IL-15, macrophage inflammatory protein (MIP)-1α, MIP-1β, monocyte chemoattractant protein-1 (MCP1) and tumor necrosis factor α (TNFα) (Gupta et al., 2001; McElroy et al., 2015; Ruibal et al., 2016) upon EBOV infection. High levels of TNFα favor lymphocyte apoptosis (Baize et al., 1999). In survivors it was shown that cytokines and chemokines (IL1β, IL-6, MIP-1α, MIP-1β, TNFα) are temporarily and moderately upregulated. MIP-1α and MCP1 recruit additional macrophages to the site of infection resulting in more target cells supposing to help the virus to disseminate within the host.

2.2.3 The role of dendritic cells during EVD

DCs are immune cells that bridge innate and adaptive immune response and play a major role during EVD. DCs together with monocytes and macrophages are comprised as phagocytic cells, also referred to as APCs because of their properties of cleaning up debris from dead or dying cells, processing antigens (e.g., pathogens), and presenting those to cells of the adaptive immune system (Banchereau & Steinman, 1998). When speaking about immune cells the **cluster of differentiation (CD)** must be mentioned. This system was introduced to distinguish the very heterogeneous cell populations and is based on the surface marker expression, which results in a specific profile for every single immune cell fraction (Bernard & Boumsell, 1984).

DCs are a very heterogenous, but rare cell populations and their development, ontogeny, and functions are still being discussed. The inclusion of transcriptome data from recent years has revealed the following main DC cell subsets: **Plasmacytoid DCs** (pDCs), **conventional DCs** 1 (cDCs1), cDCs2, and **monocyte derived DCs** (moDCs) (Alcántara-Hernández & Idoyaga, 2021; Villar & Segura, 2020). PDCs function as producers of type I IFNs with poor antigen-presenting capacity and play a

crucial role in viral sensing (Bao & Liu, 2013; Cella et al., 1999; Swiecki & Colonna, 2015), cDC1 and cDC2 are both involved in polarization of naïve CD4 T cells and differentiation of cytotoxic CD8+ T cells (Durand et al., 2019; Jongbloed et al., 2010; Yu et al., 2014). They are effective at antigen-uptake when in a resting, immature state. Upon activation in peripheral tissues such as mucosa or skin, they migrate to draining lymphoid tissues and have the capacity to activate cognate naïve T cells. During this process they upregulate co-stimulatory molecules like CD80, CD86, and major histocompatibility complex (MHC) II, which are in addition to the antigen necessary to activate naïve T cells (Geissmann et al., 2010). MoDCs are a special subset of DCs since they are derived from monocytes and expand tremendously under inflammatory conditions, in contrast to pDCs and cDCs, that originate from the same direct pre-DC precursor (Eguíluz-Gracia et al., 2016; Feng et al., 2022; Jenner et al., 2014). Monocytes are circulating in the blood and are recruited to the site of inflammation, where they can either be differentiated into macrophages or DCs (Askenase et al., 2015; Xiong & Pamer, 2015). Among all APCs DCs are the only cell type capable of priming naïve T cells into antigen-specific memory T cells. This process requires two signals through protein-protein interactions. The first one is the antigen-specific interaction between the TCR and the MHC molecule, which presents the respective antigen after processing by the APC. The second signal is a co-stimulatory signal between CD28 expressed by the T cell and CD80 or CD86 by the APC. Both signals are crucial for priming and activating the T cell (Wherry & Ahmed, 2004). The interaction of DCs and T cells is also referred to as immunological synapse (**Fig. 7**).

It has been hypothesized that EBOV infects DCs, especially DC-SIGN+ DCs, and prevents their further maturation so that as a consequence they can no longer activate T cells. *In vitro* studies further demonstrated that upon infection their function to activate T cells is impaired (Alvarez et al., 2002; Simmons et al., 2003). VP35 blocks RIG-I signaling and therefore type I IFN signaling is affected. As a result, maturation and activation of DCs are blocked so that the upregulation of T cell co-stimulatory molecules is inhibited. Consequently, infected moDCs failed to prime naïve T cells *in vitro* (Basler et al., 2003; Bosio et al., 2003; Mahanty, et al., 2003b). Yet, these mechanisms are not well understood and are also contradictive to human data since human patients that survive and succumb to EVD both produce a substantial amount of IFNs during EVD (McElroy et al., 2015).

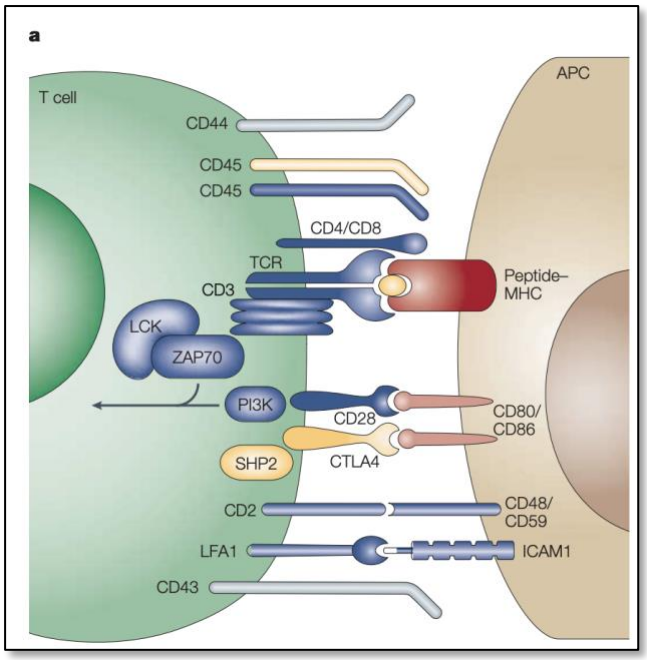

Figure 7: Overview of the immunological synapse. This shows the profile of DC-T-cell interaction during antigen presentation. The stimulatory peptide-MHC molecules are depicted in red, activating/co-stimulatory in blue, inhibitory molecules in yellow. Gray molecules are not involved in signaling (Huppa & Davis, 2003).

2.2.4 Adaptive immunity to EBOV infection

The two arms of adaptive immunity are on the one hand the **humoral immune response** with antibody-producing B cells and on the other hand the **cellular-mediated response** consisting of helper and effector T cells. Both are crucial for antiviral defense. In contrast to the innate immune response, the adaptive is specific for certain antigens. The specificity of both cell types is reflected in the B cell receptor (BCR) and TCR. During their development (B cells in the bone marrow, T cells in the thymus) the receptors undergo random gene rearrangement (V, D, and J genes), so that a high diversity of naïve cells is generated with each single cell being specific for a different pattern (Laydon et al., 2015; Six et al., 2013).

The adaptive immune response seems to be the main driving factor for viral clearance and recovery. Properly regulated humoral and cellular immune responses including the generation of antigen-specific cells are associated with EVD survival (Ruibal et al., 2016; Speranza, et al., 2018).

2.2.4.1 The adaptive immune response to EBOV: Humoral response

B cells are responsible for antibody (Ig) production, which can bind the viral particle in blood and at mucosal surfaces preventing the spread of the pathogen. The BCR is a membrane-bound antibody and recognizes specific parts of the pathogen in intact proteins. Immature B cells are present in the circulation and can travel to lymph nodes (LNs). If the BCR can engage randomly with an epitope, a cascade is activated leading to new gene products and cell division. The offspring cells become either effector plasma cells or a small number become memory B cells. Plasma cells are short lived and secrete their BCR as antibodies, but some migrate to the bone marrow, where they transiently secrete antibodies over a long period of time. Memory B cells are long-lived with a membrane bound BCR (Akkaya et al., 2020; Kurosaki et al., 2015). The produced antibodies can have different functions regarding antiviral defense. They can either directly bind viruses and neutralize them so that they are enabled in finding their specific rectors for cell entry (**neutralizing antibodies, N_{AB}**) or induce killing through nonspecific cells like macrophages and NK cells. They can bind antibody receptors (fragment crystallizable region gamma receptors, FcγR) on the surface of macrophages and NK cells and the antigen-binding site is still free to bind the viral antigens on the surface of the infected cell. Upon antigen binding the NK cell or macrophage can eliminate the infected cell. This FcγR-dependent mechanism is called antibody-dependent cell-mediated cytotoxicity (ADCC) (Lu et al., 2018).

Early studies from 1999 as well as data from the West African epidemic suggested that early development of IgM and isotype switching to IgG is correlated to viral clearance and survival. In contrast to patients that succumbed to EVD, who lack EBOV-specific antibodies during acute phase of disease (Baize et al., 1999; Baize et al., 2002). EBOV-specific IgM is detected in survivors typically within 10 – 18 days post disease onset. In survivors, IgG is detected approximately 19 days to three weeks post-disease onset in coincidence with a reduction of viremia (**Fig. 8**) (Kreuels et al., 2014; Ksiazek et al., 1999; McElroy et al., 2015; Rowe et al., 1999; Wolf et al., 2015). Some more recent studies indicated that high-affinity antibodies with neutralizing capacity as well as FcγR-dependent functions are produced during convalescence (Corti et al., 2016; Davis et al., 2019a; Ellebedy et al., 2016; Koch et al., 2020; Luczkowiak et al., 2018; McElroy et al., 2015). IgG is mainly directed against epitopes within $GP_{1,2}$ (Bornholdt et al., 2016; Corti et al., 2016; McElroy et al., 2015).

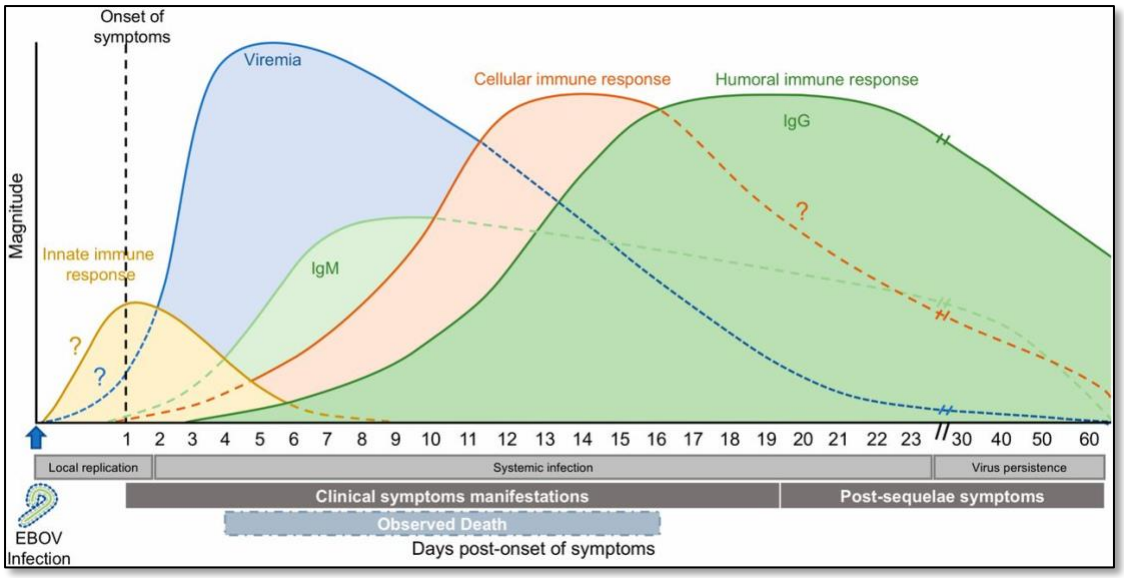

Figure 8: Schematic representation of EBOV infection and immune response. Upon initial EBOV replication after infection the innate immune response is activated (yellow). Viremia rapidly increases (blue) and correlates to the onset of symptoms (fever, abdominal pain), which is self-reported by the patients. After hospitalization, IgM (light green), IgG (humoral response, dark green), and cellular responses (orange) are detected. The virus can persist in immune-privileged sites during recovery phase, even if viremia is no longer detectable. The average period, when patients succumb to EVD, is depicted in the shaded blue box. Interrogation points indicate estimations due to the lack of human data (Ploquin, et al, 2018).

2.2.4.2 The adaptive immune response to EBOV infection: T cell response

T cells can directly recognize and kill virus-infected cells (**cytotoxic T lymphocytes, CTLs**) or induce humoral response (**T helper cells, Th cells**). These two major T cell subsets can be differentiated by their surface protein expression. CTLs express CD8 and Th cells express CD4 on their membranes. CD4 cells are activated by antigens presented on MHCII, which are mainly exogenous antigens like extracellular bacteria. They induce humoral immunity through the release of cytokines activating the production of antibodies by B lymphocytes (Franco et al., 1997; Hale et al., 2013). $CD8^+$ T cells play a major role in viral infections. They can directly induce cell death of infected cells through perforins and granzymes (Guidotti et al., 1996; McMichael et al., 1983; Peters et al., 1991) and are activated by antigens presented on MHC I molecules derived from endogenous pathogens (viruses and intracellular bacteria). The TCR binds in contrast to the BCR short, linear peptides. Once activated through their specific antigen and MHC molecule naïve T lymphocytes differentiate into antigen-specific effector T cells. Most of these cells die after the infection is cleared and the few surviving cells turn into long lived memory T cells. The establishment of immunological memory functions as a long-term protection against antigens. Upon re-infection memory T cells mature into effector memory T cells and can rapidly clear viral

infections. The activation of memory T cells is no longer restricted to dendritic cells and can also be carried out by other APCs (Guidotti & Chisari, 2001; Huber et al., 2014; Iwasaki & Medzhitov, 2004).

Before the West African epidemic of 2013 – 2016 it was assumed that due to massive T lymphocyte loss triggered through apoptosis and the inhibition of DC function that fatal cases were correlated with poor $CD8^+$ T cell activation (Baize et al., 1999; Bradfute et al., 2010; Gupta et al., 2007; Wauquier et al., 2010b). Two studies that were conducted during the epidemic, either evaluating leftover diagnostic samples in West Africa or samples from patients that were treated in the US, disproved the long-accepted hypothesis. They could show that there was **substantial T-cell activation** during acute infection among all patients with the co-expression of activation markers such as CD38 and HLA-DR (Human leukocyte antigen – DR isotype) on $CD4^+$ as well as $CD8^+$ T cells. The upregulation of these two markers is also an indication that the TCR was involved, and therefore initial antigen-presentation by DCs took place during EVD. Furthermore, it was demonstrated in fatal cases that **T cell co-inhibitory markers like programmed cell death-1 (PD-1)** and **cytotoxic T-lymphocyte-associated protein 4 (CTLA-4)** were upregulated on $CD8^+$ T cells und that the formation of antigen specific CD8 T cells was significantly reduced in fatal cases (Ruibal et al. 2016). Another hallmark of T cell response to EBOV infection is **lymphocyte apoptosis** in circulating bystander $CD4^+$ and $CD8^+$ T cells in peripheral blood probably due to poor DC function and massive release of inflammatory mediators (Baize et al., 1999; Geisbert et al., 2000; Reed et al., 2004; Sanchez et al., 2004; Wauquier et al., 2010b). However, lymphopenia was not observed in human studies from 2014 on (Ruibal et al., 2016; McElroy et al., 2015).

On the contrary survival is associated with the development of a robust **antigen-specific cell-mediated immune response**, which is associated with viral clearance (Sanchez et al. 2004; McElroy et al. 2015; Ruibal et al. 2016). EBOV-specific human $CD8^+$ T cells primarily target NP, GP, and to some extent VP40, which was demonstrated by McElroy et al. in patients that were treated in the US, but also by more recent studies by Sakabe et al. and Tipton et al. (McElroy et al., 2015; Sakabe et al., 2018; Tipton et al., 2021).

In summary, the complete picture of the immune response to EVD especially the dysregulated T cell response is not fully understood. Especially, the influence of dysregulated secretion of inflammatory cytokines and chemokines on T cell activation,

T cell apoptosis, up-regulation of co-inhibitory molecules, and the formation of EBOV-specific T cells are important to decipher to develop new treatment strategies.

2.3 Animal models for EBOV

The lack and accessibility of human samples restricts research regarding immunopathology and host response to EVD. Therefore, animal models are necessary to study these aspects. Most common models include non-human primates and rodent models. For the latter, specially adapted EBOV strains had to be developed since these are naturally not susceptible to EVD.

2.3.1 Non-human primates

The gold standard animal models to study EBOV pathogenesis are two species of non-human primates (NHPs): the cynomolgus macaque *(Macaca fascicularis)* and the rhesus macaque *(Macaca mulatta).* Due to their more rapid symptom onset cynomolgus macaques are the preferred model for preclinical development of vaccines (Sullivan et al., 2011), whereas rhesus macaques have been most used for the development of post-exposure therapies (Geisbert et al., 2015). In general, both species recapitulate the human disease in terms of clinical symptoms (fever, anorexia, maculopapular rash) and clinical parameters (increase in liver enzymes, disruption of coagulation). The clinical picture depicts a rapid disease onset with fever, virus dissemination, coagulopathy, high levels of inflammatory cytokines, immune dysregulation, and vascular leakage (Fisher-Hoch et al., 1985, 1992; Geisbert, et al., 2003b; Geisbert, et al., 2003c). In the late stages of disease, euthanasia criteria are typically reached due to the presence of multi-organ failure and shock. The overall lethality in these models is higher than 90% and varies depending on the virus dose and route (intramuscular, inhalation, ocular, oral, intranasal) (Bowen et al., 1978; Fisher-Hoch et al., 1985; Jaax et al., 1996; Johnson et al., 2023; Reed et al., 2011; Twenhafel et al., 2013). Studies with NHPs have led to key discoveries in terms of viral pathogenesis and immunity. For example, the NHP model served to identify DCs and macrophages as early targets of infection, and the role of tissue factor (TF) on EBOV-associated inflammation (Geisbert, et al., 2003a; Geisbert, et al., 2003b; Geisbert, et al., 2003c) There are however several drawbacks when it comes to animal experiments with NHPs. These experiments tend to be inconvenient in the biosafety

level 4 (BLS4) laboratory, there is limited supply availability, and only very few high containment laboratories are appropriately equipped to work with NHP.

2.3.2 Rodent: wild-type mice, Guinea pigs, and hamsters

Rodents are widely used animal models in infectious disease research. Besides their small size and easy reproduction, there are many reagents and experimental tools available, including genetically modified mouse lines. However, immune competent laboratory mice are resistant to EBOV disease, although mice are permissive to EBOV infection. The strategy therefore has been to use immune-suppressed mice or mouse-adapted EBOV.

2.3.2.1 Mouse-adapted EBOV

The first attempts to induce EBOV disease in mice were performed using the strain from the 1976 outbreak in wildtype laboratory strains BALB/c and C57BL/6. It turned out that these mice could get infected with EBOV but did not develop symptoms. Only the infection of newborn mice intracerebral and intraperitoneal were lethal (McCormick et al., 1983; van der Groen et al., 1979). Therefore, mouse models were abandoned to study pathogenesis of EVD and evaluate medical countermeasures for several years. Years later a mouse-adapted EBOV strain (maEBOV) was generated through serial passages of EBOV in old BALB/c and C5BL/6, which was lethal in immunocompetent inbred mice (Bray et al., 1998). This model actually shows similar disease progression as observed in NHPs and humans, so that it is suitable for pathogenicity and host immune response studies (Gupta et al., 2005; Warfield et al., 2003). MaEBOV infects the same primary target cells (monocytes, macrophages, DCs) and affects the same organs (liver, LN, spleen) with additional lymphopenia and elevated systemic viral titers (Gibb et al., 2001). However, further studies showed that not all aspects of disease could be modelled in mice, especially profound coagulation abnormalities were absent and only intraperitoneal challenge resulted in fatal disease. Other routes were not effective independent of the dose (Bray et al., 2001; Mahanty, et al., 2003a). Subsequent sequencing revealed mutations in coding regions of all EBOV proteins including mutations affecting the functions of NP and IFN-I antagonist proteins (Ebihara et al., 2006), which are very important aspects regarding immunological studies.

2.3.2.2 EBOV infection in hamsters and guinea pigs

Another extensively used small animal model for infectious diseases are Syrian gold hamsters (*Mesocricetus auratus*) since they appear to reflect a different susceptibility spectrum than mice, why they were also tested for EBOV infection. The infection with maEBOV is lethal in hamsters and resembles many features of human disease including uncontrolled viral replication, cytokine and chemokine storm, splenic disorganization and hepatic necrosis as seen in NHPs. In contrast to murine models, signs of coagulopathy were also observed (Ebihara et al., 2013). However, hamsters are resistant to infection with WT (wildtype) EBOV but can be rendered susceptible if $CD4^+$ T cells are depleted (Prescott et al., 2015).

Guinea pigs (*Cavia porcellus*) were also tested for their potential use in studying EBOV infections and it has turned out that an adapted virus must also be used here. The infection with WT EBOV results in a transient febrile illness, which is partial lethal. Passaging the virus 6 – 9 times results in a guinea pig-adapted variant (gpa-EBOV), which is uniformly lethal. On day 4 – 7 the animals develop high fever and succumb to the infection 8 – 12 days later. Disease progression is accompanied by high viral burdens, lymphopenia, hepatic and splenic degeneration and necrosis, coagulopathy, and hemorrhage (Connolly et al., 1999; Cross et al., 2015). Since the guinea pig model resembles the disease very close to what has been shown in NHPs and humans it is used for pathogenesis, transmission, and route of infection studies (Cross et al., 2015; Wong et al., 2015). One disadvantage is that species specific reagents are very limited compared to those for mice studies.

2.3.3 Immunocompromised mouse models

2.3.3.1 Immunodeficient mice

Mice with different degrees of immunosuppression in the innate immune response such as INF α/β receptor-knockout (IFNAR-KO) mice (Bray et al., 2001) or STAT1-knockout (Raymond et al., 2011) are susceptible to infection with WT EBOV. These mice recapitulate some important clinical features (rapid disease onset and high viral titers in spleen and liver) and show differences in outcome when infected with different Ebola virus species such as TAFV and BDBV (Brannan et al., 2015; Bray, 2001; de Wit et al., 2011; Raymond et al., 2011). These mice lack critical components of interferon signaling cascades and the studies emphasize again the importance of IFNs in EBOV immunity (Bray et al., 2001). Precisely, this point makes it very difficult to

study EBOV immunology because IFN has an important role for the innate and adaptive immune response.

2.3.3.2 Humanized mouse models

Humanized mouse models (also Human immune system mice, HIS mice) are based on a highly immunodeficient mouse strain, which can be engrafted with human cells after a sublethal irradiation, so that the human immune system can be reconstituted. NOD.Cg-Prkdc^{scid}Il2rg^{tm1Wjl}/SzJ SCID mice (NOD-scid IL2Rγ^{null}; NSG mice) act as a platform for this mouse model. These mice are deficient in NK-, T- and B-cell development so that a reconstitution of innate and adaptive immune system with human cells is possible (Ishikawa et al., 2005). For EBOV three different HIS mice platforms have been developed so far all of them using human CD34$^+$ hematopoietic cells (HSC). In addition to HSCs these mice are transgenic for human immune genes or are also transplanted with human immune organs. NSG mice without any administration of human cells develop disease after WT EBOV infection around six weeks post infection (Bird et al., 2015; Lüdtke et al., 2015; Spengler et al., 2016). Lüdtke and colleagues developed the first humanized mouse model for EBOV research, the huNSGA2 mouse (Lüdtke et al., 2015). Later similar studies were published (Bird et al., 2015). Human hematopoietic CD34$^+$ stem cells obtained from umbilical cord blood of HLA-A2$^+$ donors and are applied to human HLA-A2-transgenic NSG mice resulting in a lethal model for EBOV infection. The mice showed histological changes in the liver and upregulation of cytokines and chemokines. Furthermore, important hallmarks of EVD like coagulation and signs of hemorrhage could be observed. In later studies, this mouse model was infected with different Ebola virus strains and recapitulated relative case-fatality rates as seen in humans (Escudero-Pérez et al., 2019).

NSG-BLT (bone marrow-liver-thymus) mice were also successfully infected with EBOV. This mouse model is in addition to the engraftment with HSCs also transplanted with fetal liver and thymus fragments (Bird et al., 2016). Disease progression is dose- and donor-dependent, while infection with high-dose EBOV results in rapid and lethal EVD. Despite lacking signs of hemorrhage or coagulopathy, elevated human cytokine and chemokine levels are recapitulated in this mouse model, including high expression of M-CSF (macrophage colony-stimulating factor), IL-6, IL-8, TNF-α, interferon-gamma induced-protein 10 (IP-10), and MCP-1 (Bird et al., 2015; Kerber et al., 2018; Villinger et al., 1999; Wauquier et al., 2010b). The third HIS mouse model for EBOV

infection is based on Hu-NSG-SCM3 mice. They are also transplanted with HSCs and are furthermore transgenic for human IL-3, stem cell factor (SCF), and granulocyte/monocyte colony-stimulating factor (GM-CSF), which are supposed to support better reconstitution of the myeloid compartment (Nicolini et al., 2004). They reflect the highest levels of engraftment including high levels of myeloid cells as well as T and B lymphocytes. They show 67% lethality and liver and spleen pathology (Spengler et al., 2016, 2017).

3. Aim of this thesis

The interaction between DCs and T cells bridges innate and adaptive immune responses, and it constitutes an important checkpoint in EVD. The information about this crosstalk is scarce due to limited human samples and inadequate small animal models. The caveat of HIS mice developed to study EBOV infection so far are that they do not adequately reflect human immune response to EBOV infection due to limited T cell responses. To overcome these issues, the aim of this thesis was to develop a humanized mouse model with the following characteristics:

1) It should be susceptible to EVD
2) It should facilitate the evaluation of the contribution of the DC-T cell crosstalk to EBOV pathogenesis
3) It should facilitate the investigation of immunological aspects of EVD
4) It should help to evaluate the immunological memory of EVD survivor

To achieve these objectives, the aim is to generate a humanized mouse model based on the transplantation of mature human PBLs (peripheral blood leucocytes) into immune-suppressed NSG mice, which should ensure the maintenance of the immunological memory of the respective donor.
To allow for manipulation of the DC fraction, EBOV-infected myeloid cells are sequentially transplanted after PBL administration. The combination of human PBLs including T cells and *ex vivo* EBOV-infected moDCs is intended to make these mice susceptible to EVD.

The key objective is to assess the immunological memory of EBOV-specific long-term cellular and humoral immunity in the proposed avatar mouse model to study the correlates of protection against EBOV infection.

4. Results

4.1 Establishment of a donor-specific humanized mouse model susceptible to EBOV disease

Humanized mice provide an easily manipulable platform for studying human cell functions during infections and the resulting inflammatory response. The generation of humanized mice can happen either through transplantation of hematopoietic stem cells or through the administration of mature human PBMCs into highly immunodeficient mice. In previous studies, NSG mice engrafted with human $CD34^+$ HSCs showed immunological as well as pathological features of EVD (Lüdtke et al., 2015; Escudero-Perez et al., 2019). The main limitation of this approach is the loss of immune information of the donor since the immune system is generated *de novo*. However, recent studies have shown that T cells are crucial for survival of EVD and together with DCs play an important role in the pathophysiology of EVD (Ruibal et al., 2016; Lüdtke et al., 2016).

In order to investigate the role of the T cell – DC interaction during EBOV pathogenesis a humanized mouse model was sought to be developed using a strategy previously developed by Harui et al. (Harui et al., 2011). In this study, NSG mice transgenic for the human HLA-A2 molecule were reconstituted with PBLs from HLA-A2+ donors also referred to as avatar mice. This resulted in a detectable population of human immune cells in the spleen and peripheral blood of the mice. The use of NSG-A2 mice was supposed to improve the engraftment of human cells and to facilitate CD8 T cell responses in this model. Another crucial aspect that Harui and colleagues demonstrated in their study was that a subsequent adoptive transfer of antigen-loaded *ex-vivo*-generated donor-matched moDCs into these NSG mice resulted in antigen-specific T cell formation. Donor-matched moDCs were transduced with an adenoviral vector and injected into avatar mice. Spleenocytes recovered from these mice and challenged with transduced moDCs expanded and secreted a cytokine profile characteristic of antigen-specific CD8+ T cells (Harui et al., 2011). These findings strongly suggested that avatar mice can be utilized to study T cell-DC interactions during infection.

During my master thesis, I have tested several protocols to see which one would be more suitable to assess DC-T cell interactions during EBOV infection (Rottstegge, 2016). The first steps were always as following: after obtaining peripheral blood from HLA-A2+ healthy donors, peripheral blood mononuclear cells (PBMCs) were isolated by density gradient centrifugation, and $CD14^+$ and $CD14^-$ cells were separated by magnetic-activated cell sorting (MACS) (**Fig. 9**).

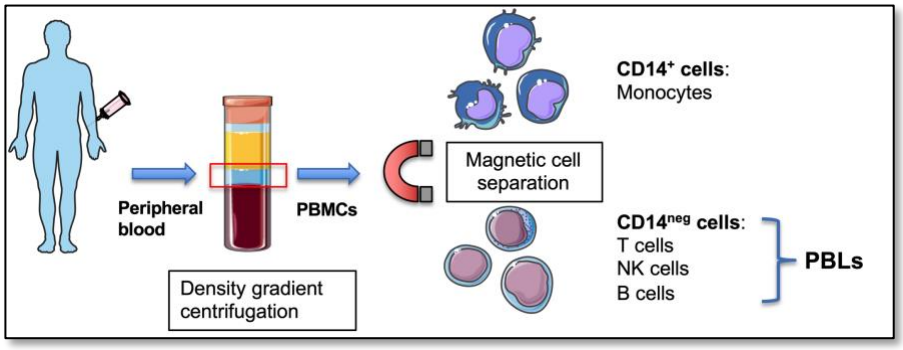

Figure 9: Processing and separation of peripheral blood. EDTA (ethylenediaminetetraacetic acid) blood was drawn from healthy HLA-$A2^+$ donors and PBMCs were separated through density gradient centrifugation. PBMCs were sorted into $CD14^+$ monocytes and $CD14^{neg}$ peripheral blood lymphocytes (PBLs) using $CD14^+$ magnetic beads.

CD14- cells also referred to as PBLs consist mainly of T-, B, and NK cells. These were utilized to evaluate the administration route of human cells in NSG mice and to analyze the retaining cell subsets in avatar mice. Briefly, the inoculation through the retroorbital route (r.o.) elucidated the most consistent engraftment of human cells (**Fig. 10**). It was also demonstrated that mainly T cells (up to 95% 28 days after inoculation), of which up to 90% were effector memory T cells, repopulated in the mice (Rottstegge, 2016). Previous studies had already come to similar conclusions (King et al., 2008; Ali et al., 2012; Harui et al., 2011). CD14+ cells (monocytes) were cultured under different conditions to optimize the protocol for the generation of immature moDCs to our needs (**Fig. 10**). Immature moDCs are infectable with EBOV (Mahanty et al., 2003b).

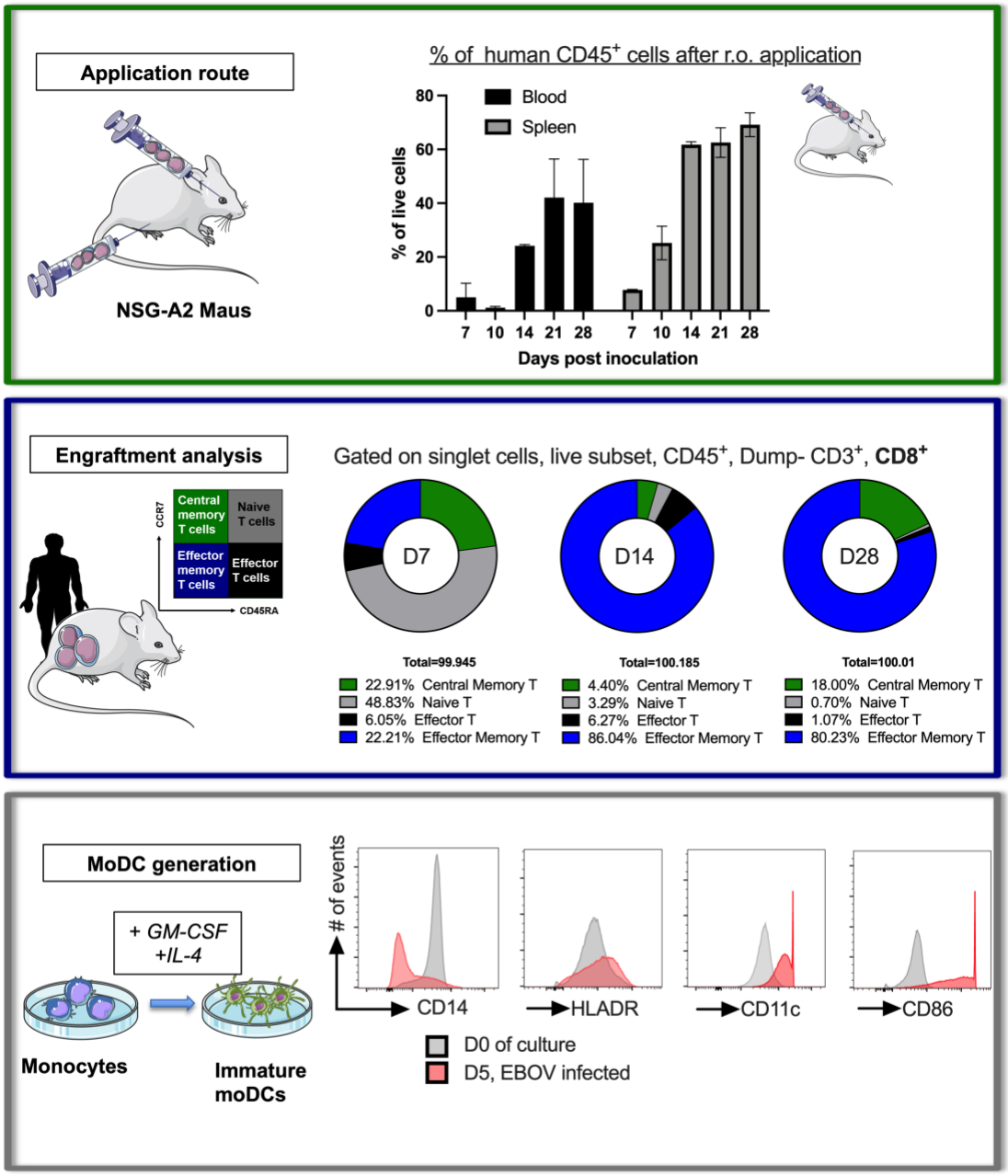

Figure 10: Preliminary study results. Intraperitoneal and retroorbital application routes were tested for the administration of CD14- human PBMCs into NSG mice and evaluated for their efficiency. Retroorbital administration of huPBLs was higher and more consistent in blood and spleen. The engraftment was analyzed for its T cell composition and showed a skewing towards an effector memory T cell phenotype. Monocytes (CD14+ cells) were derived into monocyte-derived dendritic cells under different culture conditions and their phenotype was evaluated by flow cytometry.

The results of these experiments led to the following experimental procedure, which was used as a starting point for all subsequent experiments in this study (**Fig. 11**): $CD14^+$ cells were cultured for five days in moDC differentiation media in the presence of IL-4 and GM-CSF. On the same day recipient mice were inoculated with 10^7 PBLs through the r.o. route. After five days cultured monocytes displayed an immature moDC phenotype ($CD14^-$, HLA-DR^+, $CD11c^+$, $CD86^{low}$) and showed the highest

viability in this protocol. These cells were infected with EBOV *ex vivo* for 60 min and also administered into the mice through the r.o. route.

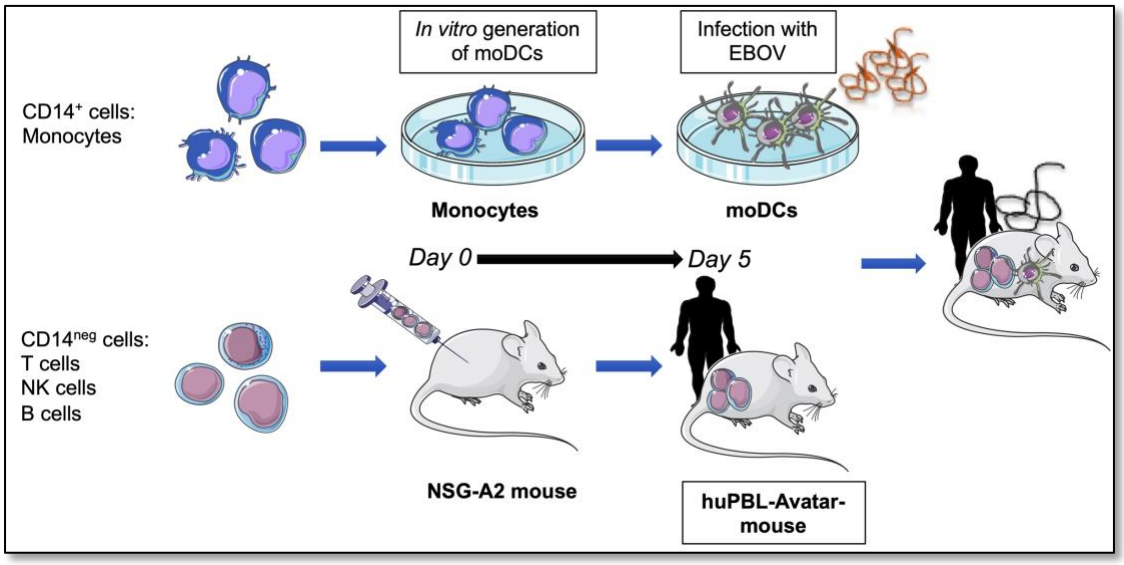

Figure 11: Final setup for the generation of avatar mice. Monocytes were differentiated into immature moDCs in the presence of human granulocyte-macrophage colony-stimulating factor (GM-CSF) and IL-4 for five days *in vitro*. 10^7 huPBLs were transplanted into recipient NSG-A2 mice at day 0 to generate avatar mice. Five days after transplantation moDCs were infected with EBOV (MOI = 1) or mock-infected *ex vivo* and 5 * 10^5 moDCs were administered into avatar mice.

4.1.1 Infection with EBOV-infected moDCs renders avatar mice susceptible to EVD

To evaluate the response of avatar mice to EBOV infection, 10^7 PBLs from a healthy HLA-A2$^+$ donor were administered r.o. into 10 NSG mice respectively. Five days later moDCs were infected with EBOV at a multiplicity of infection (MOI) of 1 or mock-infected with PBS. Mice received either 5*10^5 EBOV-infected moDCs or 5*10^5 mock-infected moDCs r.o. Weight and temperature were monitored for 12 days on a daily basis to evaluate morbidity and mortality. Blood samples were drawn on days 2, 4, 7, 9, and on the respective day of euthanasia to measure aspartate aminotransferase (AST) levels, a marker of cell damage, and determine viremia **(Fig 12A)**. Viral titers were also measured in organs during necropsies.

Infected mice started to lose weight and showed signs of shock (dropped temperature) around day 7 post-infection and succumbed to the disease at either day 10 or day 11 by reaching euthanasia criteria (e.g., weight loss) (**Fig. 12B-D**). This is comparable to the incubation period observed in humans, which ranges between 2 to 21 days, but typically lasts 6 to 10 days (Baseler et al., 2017; Leligdowicz et al., 2016). High viremia

and organ titers in liver, kidney, and spleen indicated that these mice suffered high levels of viral replication, which developed into a systemic infection. Consistent with this, the levels of viremia peaked around day 7 (**Fig. 12E/F**). Additional morbidity signs included ruffled fur and lethargy which are signs of severe disease in mice.

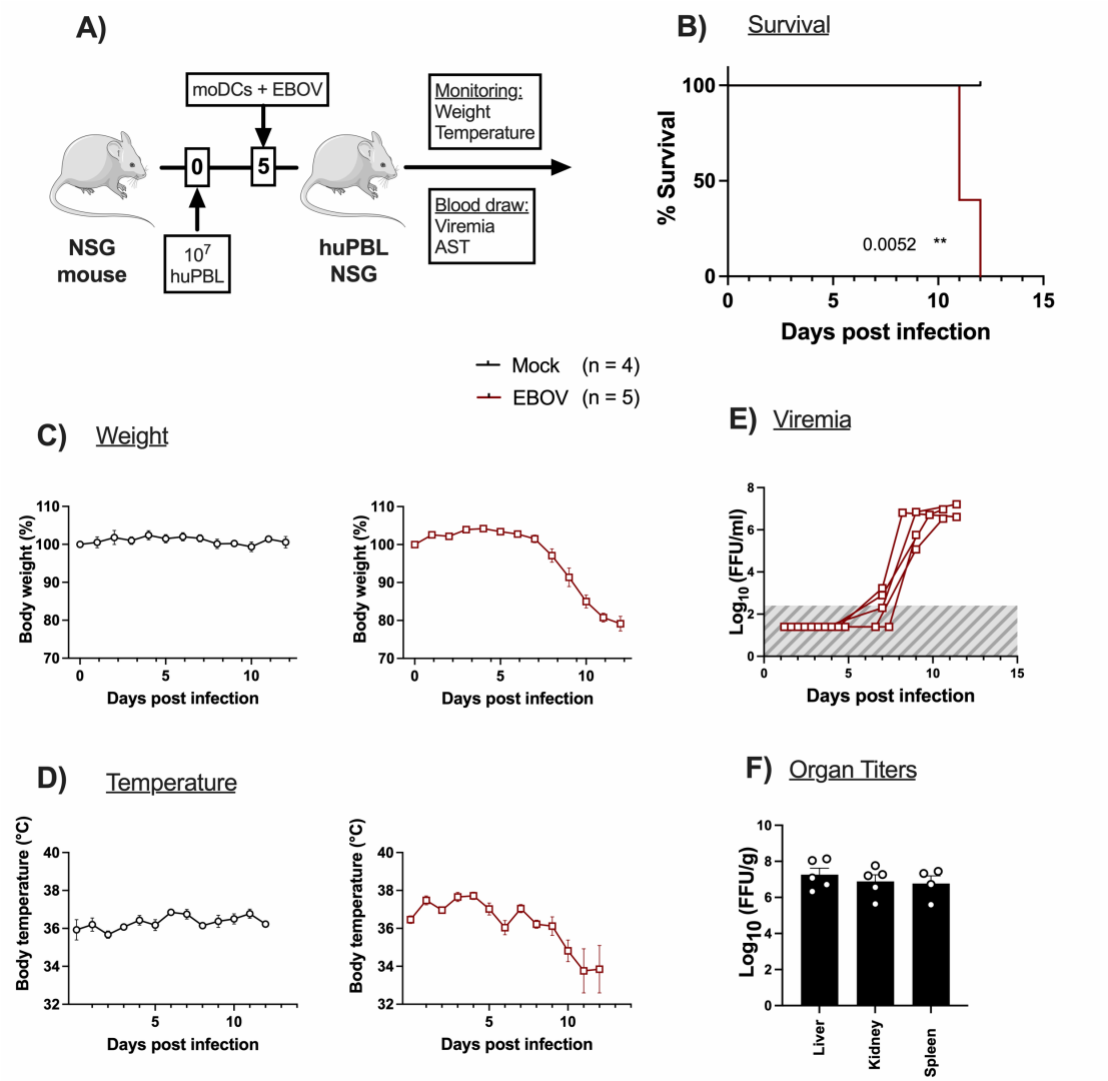

Figure 12: Avatar mice are susceptible to EBOV infection. (A) Ten mice were inoculated with 10^7 PBLs from a healthy donor. 5 days post inoculation mice were transplanted with $5*10^5$ *in vitro* generated either mock-infected (black; n = 4) or EBOV-infected moDCs (red; n = 5) from the same donor. Survival, weight, and temperature were monitored daily (B – D), blood and serum were collected at indicated time points for detection of AST levels and viremia E. The limit of detection for viremia is shaded in grey. Organ viral titers were determined at day of death (F). Mean and SEM are shown unless individual data points are depicted. Statistical significance was analyzed using LogRank (Mantel-Cox) test. Levels of significance were interpreted as follows: NS (not significant) $p > 0.05$, * $p \leq 0.05$, ** $p \leq 0.01$, *** $p \leq 0.001$, and **** $p \leq 0.0001$.

Compared to the mock group, infected mice displayed higher levels of serum AST levels starting at d7 (**Fig. 13A**) suggesting cellular damage (liver damage). Examination of the deceased animals indicated signs of hemorrhage in the intestine

and fatty liver (liver steatosis) (**Fig. 13B**). This was consistent with the presence of bloody stool and / or urine in four out of five mice.

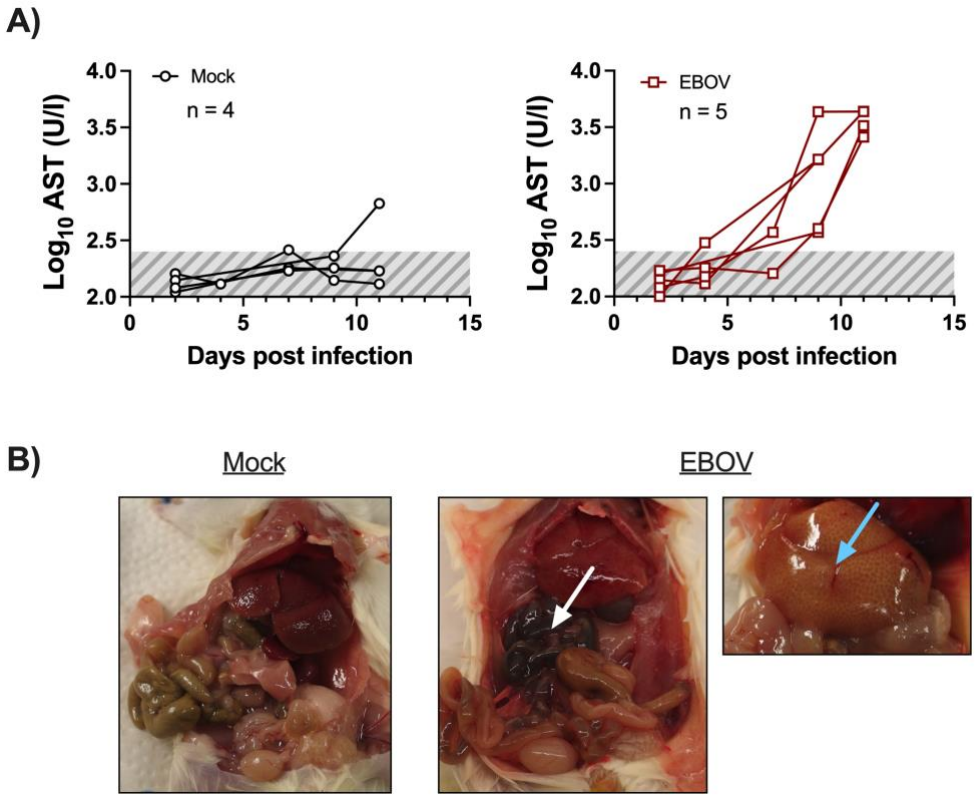

Figure 13: Avatar mice reproduced main features of human EBOV infection. (A) AST levels in serum were analyzed with a commercial kit and using a Fujifilm machine in mock (black) and EBOV-infected mice (red). The normal range for AST is shaded in grey. Graphs show mean and SEM. (B) Necropsies of mock and EBOV infected avatar mice are shown. Gastrointestinal bleeding (left EBOV, white arrow) and liver steatosis (right EBOV, light blue arrow) are indicated the picture.

In summary, the generation of avatar mice using HLA-A2$^+$ T cells from naïve donors and EBOV-infected donor-matched moDCs, resulted in a model that was 100% lethal. These results indicated that the transplantation of T cells and matched DCs alone in the context of EBOV infection was sufficient to recapitulate the main features of EVD.

4.1.2 Donor-specific EVD manifestations in avatar mice

Next, the effect of donor variability was assessed in the model and whether the course of EVD and its severity was donor-dependent. Bird et al., had already shown in their NSG-BLT mouse model that EVD progression varied depending on the donor cells utilized (Bird et al., 2016). To assess this in this system, 10 avatar mice from two

different donors (donor 2, D2, and donor 3, D3) were generated and infected with EBOV using donor-matched moDCs. The results were then compared with those of the previous experiments (donor 1, D1). Weight and temperature were monitored for 24 days on a daily basis to evaluate morbidity and mortality. Blood samples were drawn on indicated days and on the respective day of death to measure AST levels and determine viremia. Viral titers were also measured in organs during necropsies.

For D1 and D3 100% of the EBOV-infected animals had to be euthanized after reaching euthanasia criteria. D2-avatar mice showed a delay in the time of death (euthanasia) so that all mice reached this point after day 15 post-infection (**Fig. 14A/B**). One mouse in this group survived infection until the experiment was terminated on day 24. Moreover, while D1 and D3 showed similar viremia and AST levels, D2-avatars displayed two peaks of viremia around day 12 and day 25. Overall, the levels of circulating serum ASTs were lower compared to the other groups (**Fig. 14C/D**). As described above for D1, four mice showed signs of hemorrhage (bloody urine and/or stool). Signs of bleeding could be observed in two out of five mice for D1 and for three out of five mice for D2.

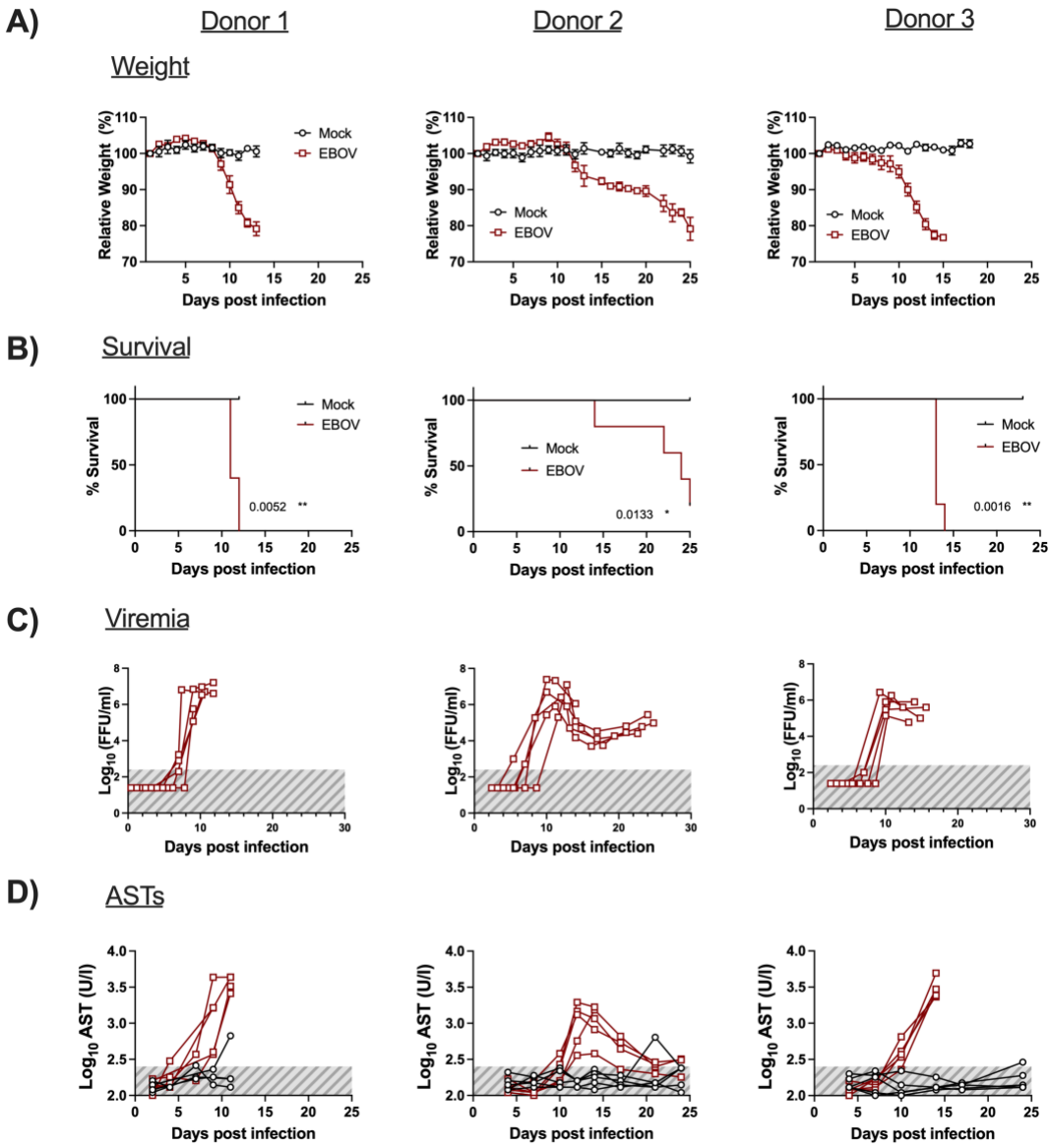

Figure 14: Donor-specificity in avatar mice. Ten (9 mice for donor 1) avatar mice of three different donors were generated (donor 1 see section 5.1.2). 5 days post-inoculation mice were transplanted with $5*10^5$ *in vitro* generated either mock-infected (black; n = 4 or n = 5) or EBOV-infected moDCs (red; n = 5) from the same donor. Weight (A) and survival (B) were monitored daily, blood and serum were collected at indicated time points for detection of viremia (C) and ASTs (D). The limit of detection for viremia is shaded in grey. Mean and SEM are shown unless individual data points are depicted. Statistical significance was analyzed using LogRank (Mantel-Cox) test. Levels of significance were interpreted as follows: NS (not significant) $p > 0.05$, * $p \leq 0.05$, ** $p \leq 0.01$, *** $p \leq 0.001$, and **** $p \leq 0.0001$.

In summary, this experiment that this model was reproducible with cells from different donors and indicated that the disease progression in EBOV-infected avatar mice is highly dependent on the donor. This is in line with the hypothesis that this model is suitable to investigate donor-specific T-cell responses to EBOV infection.

4.1.3 Avatar mice recapitulate ebolavirus pathogenesis but not Lassa virus pathogenesis

Recently, it was shown that NSG-A2 mice engrafted with $CD34^+$ human HSCs could recapitulate the case-fatality ratios of different ebolaviruses reported during outbreaks in humans (Escudero-Pérez et al., 2019). Accordingly, the next step was to evaluate the response of avatar mice to infection with other members of the *Ebolavirus* genus. Reston virus was selected (species *Reston ebolavirus*, RESTV), of which no case of human infection has yet been recorded (Cantoni et al., 2016; Jahrling et al., 1990). Furthermore, to evaluate if the model could also be applied to other hemorrhagic fever virus, avatar mice were exposed to Lassa virus (LASV) the causative agent of Lassa fever in humans (Frame et al., 1970). **Both LASV and RESTV have been previously shown to be able to infect human moDCs** (Mahanty et al., 2003b; Escudero-Perez et al., 2019). To evaluate RESTV and LASV infection, five mice were inoculated with RESTV-infected moDCs (MOI = 1) and five with LASV-infected moDCs (MOI = 1). In addition, as controls five mice were infected with $5*10^5$ EBOV-infected moDCs and five mice received $5*10^5$ mock-infected moDCs. Weight and temperature were monitored for 24 days on a daily basis to evaluate morbidity and mortality. Blood samples were drawn on days 3, 6, 9, 14, 17, and on the respective day of euthanasia to measure AST levels and determine viremia **(Fig. 15A)**. Viral titers were also measured at necropsy.

While EBOV infection of avatar mice resulted in 100% lethality, 3 out of 5 mice infected with RESTV survived the infection and displayed moderate weight loss over the course of infection. LASV-infection in avatar mice was asymptomatic with no changes in weight loss or body temperature, and 100% survival (**Fig. 15B-D**). One of the RESTV-infected mice had to be euthanized due to neurological manifestations (limb paralysis). AST serum levels in RESTV-infected mice were lower than in EBOV-infected animals, reached a plateau around day 12 and decreased around day 17. Among the LASV-infected group AST levels were under the range of detection (**Fig. 15E**). In EBOV-infected mice viremia reached uniformly high levels and peaked at day 7 and slightly decreased until the euthanasia endpoint. RESTV-infected animals that succumbed to disease showed high titers similar to EBOV-infected mice, while viremia in survivors gradually increased over time until the endpoint (**Fig. 15F**). Viral titers in liver, kidney, lung, heart, and spleen were determined at necropsy. For EBOV, high viral titers could be detected in all organs evaluated. RESTV-infected mice showed significantly lower titers than their EBOV counterparts and virus replication could not be detected in the heart. LASV replication was detectable in the liver, lung, and spleen, with titers in the

lung comparable to those observed in EBOV-infected mice. These data indicate that avatar mice are susceptible to LASV infection but that the presence of donor-matched T cells and moDCs is not sufficient to recapitulate human Lassa fever. The data obtained with RESTV mimics that obtained in HSC-based humanized mice and strongly suggest differences in pathogenesis between EBOV and RESTV associated to the T cell-DC interface. (**Fig. 15G**).

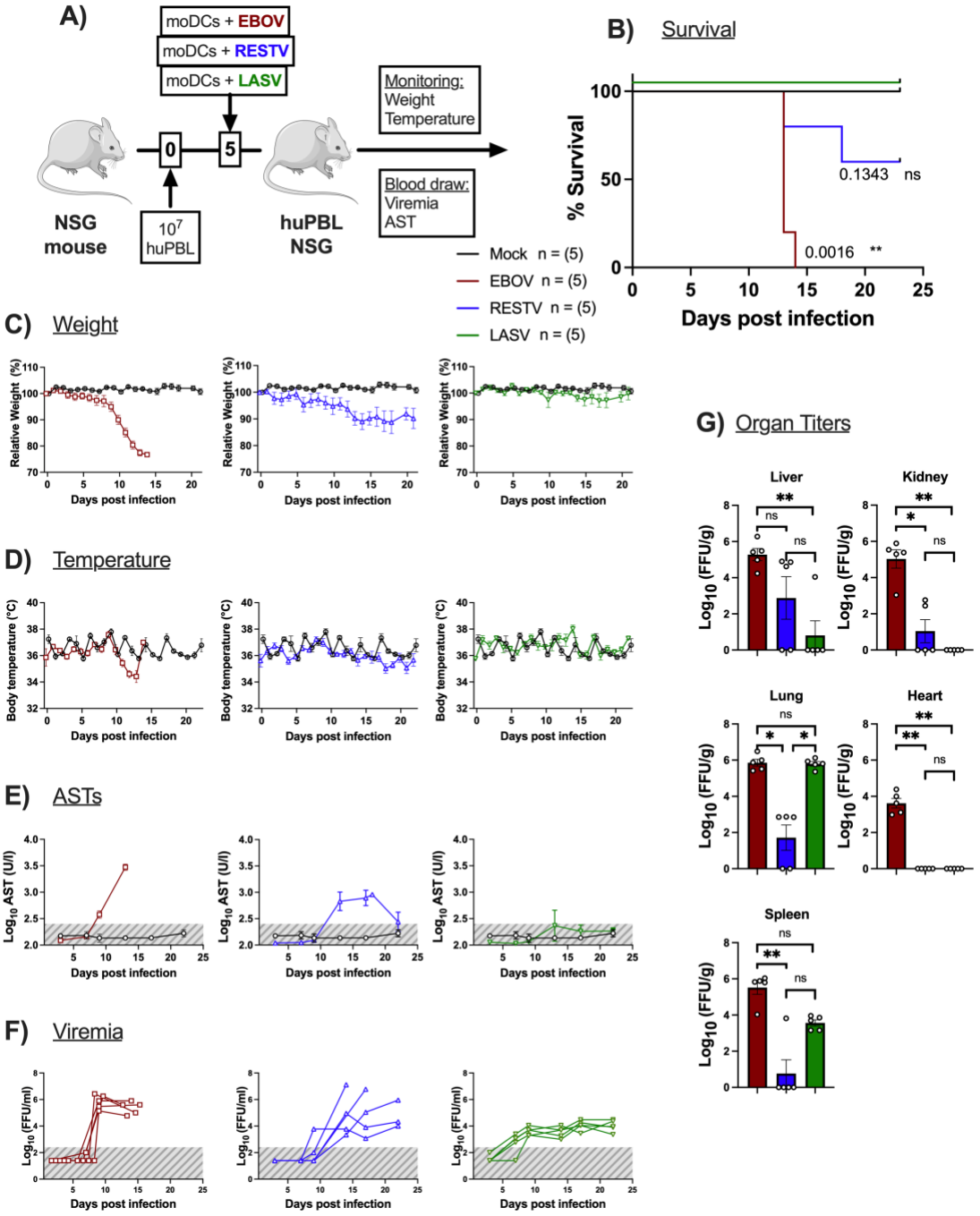

Figure 15: Infection of avatar mice with different viruses. (A) Twenty mice were engrafted with 10^7 PBLs from a healthy donor. 5 days post-inoculation mice were transplanted with $5*10^5$ *in vitro* generated either mock-infected (black; n = 5), EBOV-infected moDCs (red; n = 5), RESTV-infected moDCs (blue; n = 5), or LASV-infected moDCs (green; n = 5) from the same donor. Survival, weight, and temperature were monitored daily (B – D), blood and serum were collected at indicated time points for detection of AST levels and viremia (E / F). The normal range for AST and the limit of detection for viremia are shaded

in grey. Organ viral titers were determined at day of euthanasia (G). Mean and SEM are shown unless individual data points are depicted. Statistical significances were analyzed using either LogRank (Mantel-Cox) test or one-way ANOVA (Kruskal-Wallis test) followed by Dunn's multiple comparison test. Levels of significance were interpreted as follows: NS (not significant) $p > 0.05$, * $p \leq 0.05$, ** $p \leq 0.01$, *** $p \leq 0.001$, and **** $p \leq 0.0001$.

These findings also suggest that avatar mice could be used to test the pathogenicity of other poorly characterized ebolaviruses in humans.

4.1.4 Disease progression is dependent on the DC input

After entering the host, EBOV infects DCs and exploits their migratory capacity to spread from the site of infection within the host (Lüdtke et al., 2017). Since the interaction between DCs and T cells can easily be manipulated in avatar mice, these could facilitate a more in-depth analysis of how these interactions impact the progression of EVD. The first aspect to investigate was EBOV transport by DCs. It was hypothesized that if EBOV transport by DCs is linked to disease severity, reducing the input of infected DCs could also in turn reduce EVD symptoms. To prove this hypothesis, three experimental avatar mouse groups were established in which decreasing amounts of EBOV-infected DCs were transplanted. Therefore, mice were inoculated with $5*10^5$, $5*10^4$ or $5*10^3$ EBOV-infected moDCs. A mock group transplanted with $5*10^5$ non-infected DCs was kept as control. Weight and temperature were monitored for 24 days on a daily basis to evaluate morbidity and mortality. Blood samples were drawn on days 3, 6, 9, 14, 17, and on the respective day of death to measure AST levels and determine viremia **(Fig 16A)**. Viral titers were also measured in organs at necropsy.

Mice transplanted with $5*10^5$ EBOV-infected moDCs lost weight rapidly and succumbed to infection within two weeks post-infection. Conversely, in mice transplanted with $5*10^4$ or $5*10^3$ moDCs four out of five mice survived infection (**Fig. 16B**). In the group transplanted with $5*10^3$ EBOV-infected moDCs we also observed substantial reduction of morbidity and body scoring parameters, namely weight loss and body temperature, whereas mice inoculated with $5*10^4$ -EBOV-infected moDCs still experienced weight loss between days 10 and 15 (**Fig. 16C/D**). AST serum levels in mice infected with $5*10^5$ and $5*10^4$ EBOV-infected moDCs peaked on day 13 and decreased again in the surviving mice of the middle dose group, while AST serum levels in the mice that received $5*10^3$ EBOV-infected moDCs steadily increased from day 10 on until the end of the experiment (**Fig. 16E**). Viremia peaked on day 10 post-infection and slightly decreased until the euthanasia endpoint in mice transplanted with

$5*10^5$ EBOV-infected moDCs (**Fig. 16F**). In the medium-infection dose group, viremia also increased by day 10 and remained at that level until the end of the experiment. Of note, viremia among the low-infection dose group varied between subjects. This was also reflected when assessing organ titers (**Fig. 16G**). While mice infected with $5*10^5$ or $5*10^4$ EBOV-infected moDCs had consistent viral titers within groups, mice that received $5*10^3$ EBOV-infected moDCs exhibited slightly reduced titers with a high variability and no detectable virus in some mice in liver, kidney, lung, and heart. Only in spleen virus was detected in all mice.

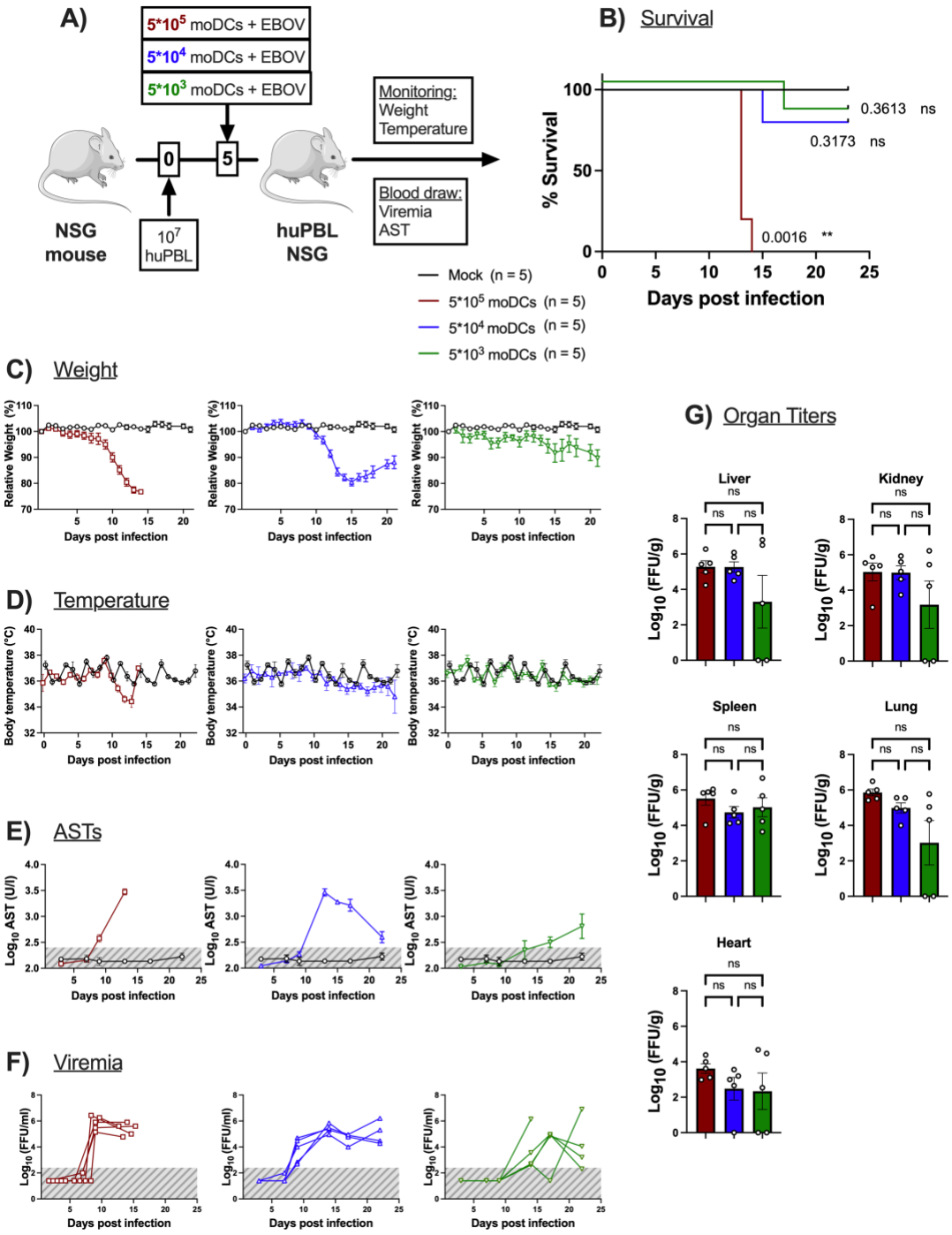

Figure 16: Infection of avatar mice with different doses of infected moDCs. (A) 20 mice were engrafted with 10^7 PBLs from a healthy donor. 5 days post-inoculation mice were transplanted with $5*10^5$ *in vitro* generated either mock-infected (black; n = 5), $5*10^5$ EBOV-infected moDCs (red; n = 5), $5*10^4$ EBOV-infected moDCs (blue; n = 5), or $5*10^3$ EBOV-infected moDCs (green; n = 5) from the same donor. Survival, weight, and temperature were monitored daily (B – D), blood and serum were collected at indicated time points for detection of AST levels and viremia (E / F). The normal range for AST and the limit of detection for viremia are shaded in grey. Organ viral titers were determined at day of euthanasia (G). Mean and SEM are shown unless individual data points are depicted. Statistical significances were analyzed using either LogRank (Mantel-Cox) test or one-way ANOVA (Kruskal-Wallis test) followed by Dunn's multiple comparison test. Levels of significance were interpreted as follows: NS (not significant) $p > 0.05$, * $p \leq 0.05$, ** $p \leq 0.01$, *** $p \leq 0.001$, and **** $p \leq 0.0001$.

In summary, it was shown that the amount of infected DCs administered to avatar mice influenced disease progression and outcome. These data strongly suggest that DCs play an important role in EBOV dissemination.

4.1.5 DC subsets derived from MUTZ-3 cell line can induce EVD in avatar mice

DCs represent a highly diverse category of immune cells, exhibiting variations in their roles as APCs and their distribution within the body, including expression of different surface molecules (Haniffa et al., 2013; Helft et al., 2010). DC-SIGN-expressing moDCs have been extensively utilized to study DCs in the context of EBOV research. The aim was to employ avatar mice to investigate the contribution of other DC subsets during EVD pathogenesis.

To investigate this, the **HLA-A2+ MUTZ-3 cell line**, which is CD34+ human acute myeloid leukemia cell line and can be differentiated into different DC subsets using different cytokine cocktails, was utilized. For this experiment interstitial-like DC-SIGN$^+$ DCs and Langerhans cell-like Langerin$^+$ DCs were generated. After differentiation, cells were infected with EBOV and inoculated into mice as described. In total 4 groups of 5 avatar mice were generated with either mock-infected moDCs, EBOV-infected moDCs, EBOV-infected DC-SIGN$^+$-MUTZ-3 cells, or EBOV-infected Langerin$^+$-MUTZ-3 cells (all MOI=1). Weight and temperature were monitored for 24 days on a daily basis to evaluate morbidity and mortality. Blood samples were drawn on days 3, 6, 9, 14, 17, and on the respective day of euthanasia to measure AST levels and to determine viremia **(Fig. 17A)**. Viral titers were also measured in organs on the day of euthanasia.

All infected groups lost weight rapidly, body temperature dropped, reached high levels of serum ASTs and viremia, and succumbed to infection. There were also no differences in viral titers among the groups (**Fig. 17B-G**).

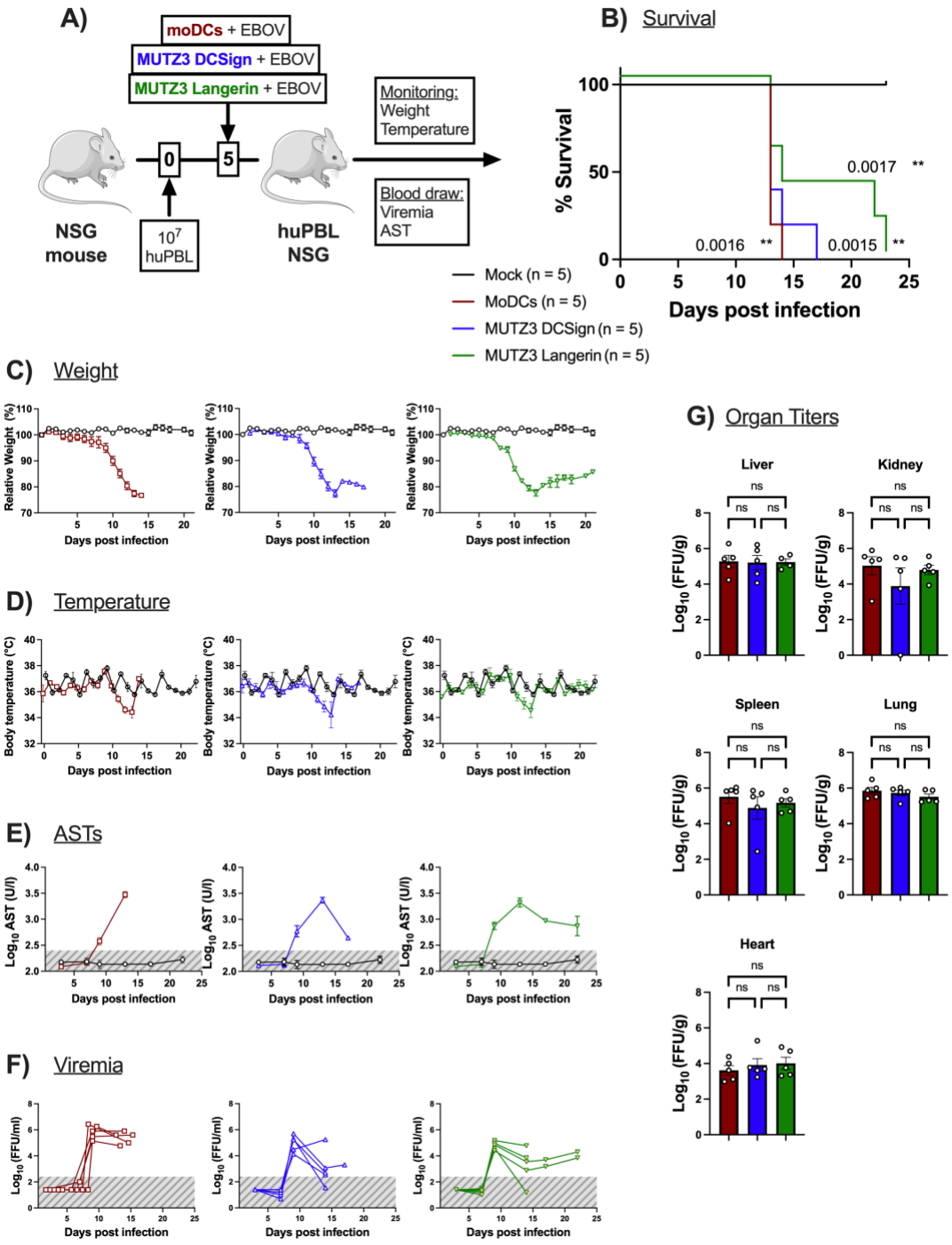

Figure 17: EBOV-Infection of avatar mice with different dendritic cells. (A) 20 mice were engrafted with 10^7 PBLs from a healthy donor. 5 days post-inoculation mice were transplanted with $5*10^5$ *in vitro* generated either mock-infected (black; n = 5), $5*10^5$ EBOV-infected moDCs (red; n = 5) from the same donor, $5*10^5$ EBOV-infected DC-SIGN-expressing MUTZ3 cells (blue; n = 5), or $5*10^5$ EBOV-infected Langerin-expressing MUTZ3 cells (green; n = 5). Survival, weight, and temperature were monitored daily (B – D), blood and serum were collected at indicated time points for detection of AST levels and viremia (E / F). The normal range for AST and the limit of detection for viremia are shaded in grey. Organ viral titers were determined at day of euthanasia (G). Mean and SEM are shown unless individual data points are depicted. Statistical significances were analyzed using either LogRank (Mantel-Cox) test or one-way ANOVA (Kruskal-Wallis test) followed by Dunn's multiple comparison test. Levels of significance were interpreted as follows: NS (not significant) $p > 0.05$, * $p \leq 0.05$, ** $p \leq 0.01$, *** $p \leq 0.001$, and **** $p \leq 0.0001$.

These results indicated that EVD in avatar mice could be induced with EBOV-infected DC subsets derived from MUTZ-3 cells independent of the specific subtype of transplanted DC.

4.1.6 Both T cells and DCs are required to recapitulate EVD in avatar mice

So far, the conducted experiments demonstrated that EVD can be recapitulated in avatar mice utilizing PBLs from a healthy donor and EBOV-infected moDCs from the same donor or a HLA-A2+ DC cell line (4.1.5). The amount of EBOV-infected moDCs influenced disease progression and different DC subsets were equally capable of inducing EVD in avatar mice. Since infected DCs seemed to affect disease severity very strongly in avatar mice, the next step was to investigate whether transplantation of infected DCs alone could be sufficient to recapitulate EVD in avatar mice.

To test this, $5*10^5$ EBOV-infected or mock-infected moDCs were transplanted into two groups (n=5) NSG-A2 mice which had **not** been previously transplanted with huPBL. Weight and temperature were monitored for 22 days on a daily basis to evaluate morbidity and mortality. Blood samples were drawn on days 3, 6, 9, 14, 17, and on the respective day of euthanasia to measure AST levels and to determine viremia **(Fig. 18A)**. Viral titers were also measured in organs on the day of necropsy.

None of the infected mice showed any signs of disease and all mice survived (**Fig. 18B-D**). Nevertheless, mice developed significant levels of viremia and showed elevated levels of serum AST that peaked at day 14 post infection, which coincided with viremia peaking at the same time and reaching a plateau (**Fig. 18E/F**). Organ titers were also comparable to previous experiments with transplanted avatar mice (**Fig. 18G**).

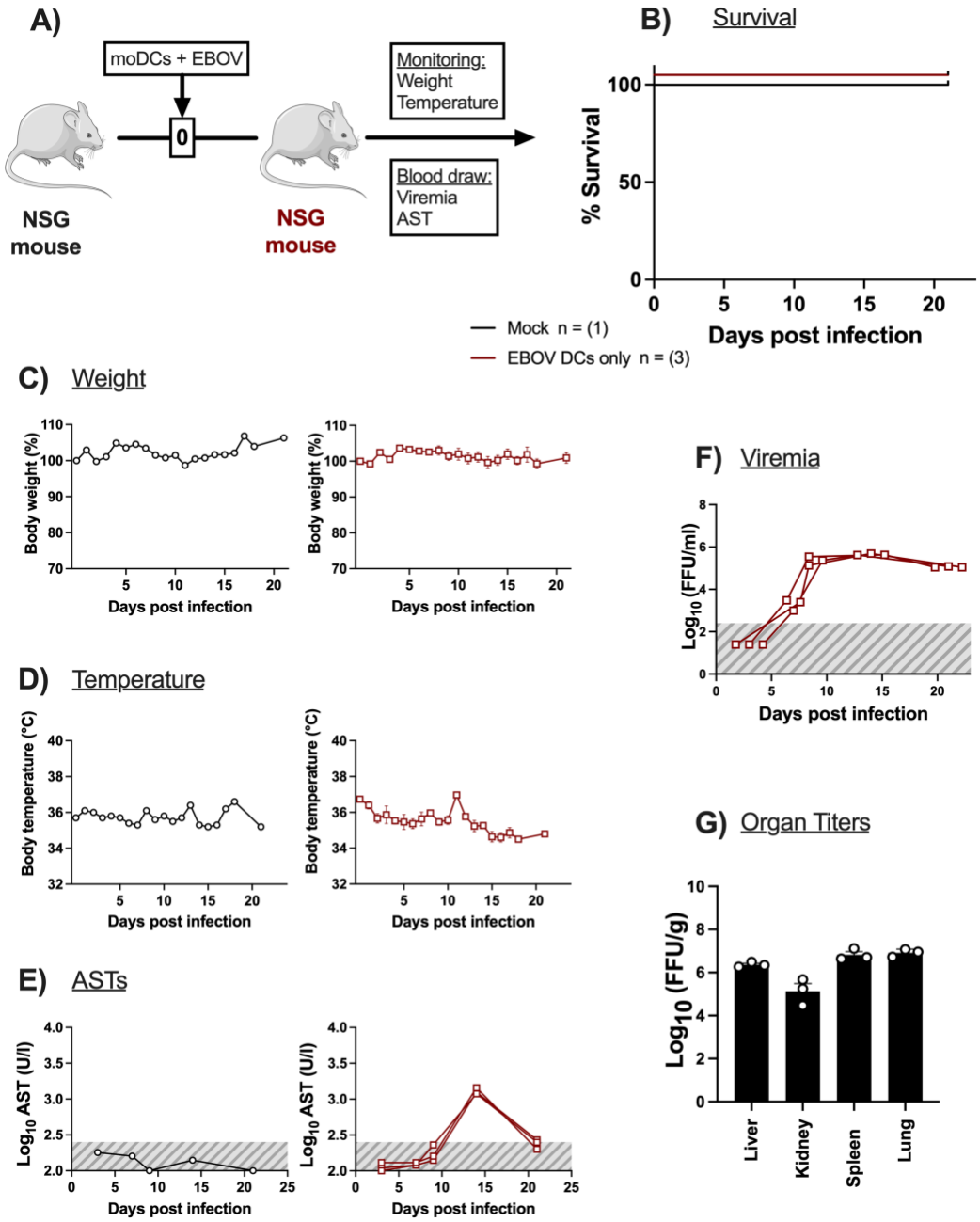

Figure 18: Infection of NSG mice with EBOV-infected moDCs. (A) 10 NSG mice were transplanted with $5*10^5$ *in vitro* generated either mock-infected (black; n = 1) or EBOV-infected moDCs (red; n = 3). Survival, weight, and temperature were monitored daily (B – D), blood and serum were collected at indicated time points for detection of AST levels and viremia (E / F). The normal range for AST and the limit of detection for viremia are shaded in grey. Organ viral titers were determined at day of euthanasia (G). Mean and SEM are shown unless individual data points are depicted. Statistical significance was analyzed using LogRank (Mantel-Cox) test. Levels of significance were interpreted as follows: NS (not significant) $p > 0.05$, * $p \leq 0.05$, ** $p \leq 0.01$, *** $p \leq 0.001$, and **** $p \leq 0.0001$.

These findings demonstrated that, in order to recapitulate EVD in the avatar model, both human PBLs and human EBOV-infected moDCs are required.

4.1.7 TCR – MHC interaction is required to induce EVD in avatar mice

After showing that EBOV-infected moDCs alone were not sufficient to induce EVD in avatar mice, the nature of the crosstalk between EBOV-infected moDCs and T cells was investigated. Antigen presentation requires interaction between HLA-peptide complexes on the surface of DCs and the TCR (Huppa and Davis, 2003). To evaluate the importance of HLA-TCR interactions in the model, EBOV pathogenesis in mice inoculated with HLA-matched DCs and T cells as well as in mice in which T cells and DCs were from donors with mismatched HLAs was evaluated.

Ten mice were transplanted with 10^7 huPBLs from an HLA-$A2^+$ donor. Meanwhile, moDCs from the same donor and an HLA-A2-negative donor were generated *in vitro*, infected with EBOV 5 days later, and administered to 5 mice respectively. Weight and temperature were monitored for 22 days on a daily basis to evaluate morbidity and mortality. Blood samples were drawn on days 3, 6, 9, 14, 17, and on the respective day of euthanasia to measure AST levels and determine viremia **(Fig. 19A)**.

Weight and temperature of mice that received EBOV-infected HLA-matched cells dropped around day 7 and 4 out of 5 mice succumbed to the infection. The weight of the animals that were administered EBOV-infected HLA-mismatched cells decreased gradually over the course of infection (**Fig. 19B-D**). Despite similar levels of viremia and elevated serum ASTs, 4 out of 5 HLA-TCR mismatched avatar mice survived EBOV infection (**Fig. 19E/F**).

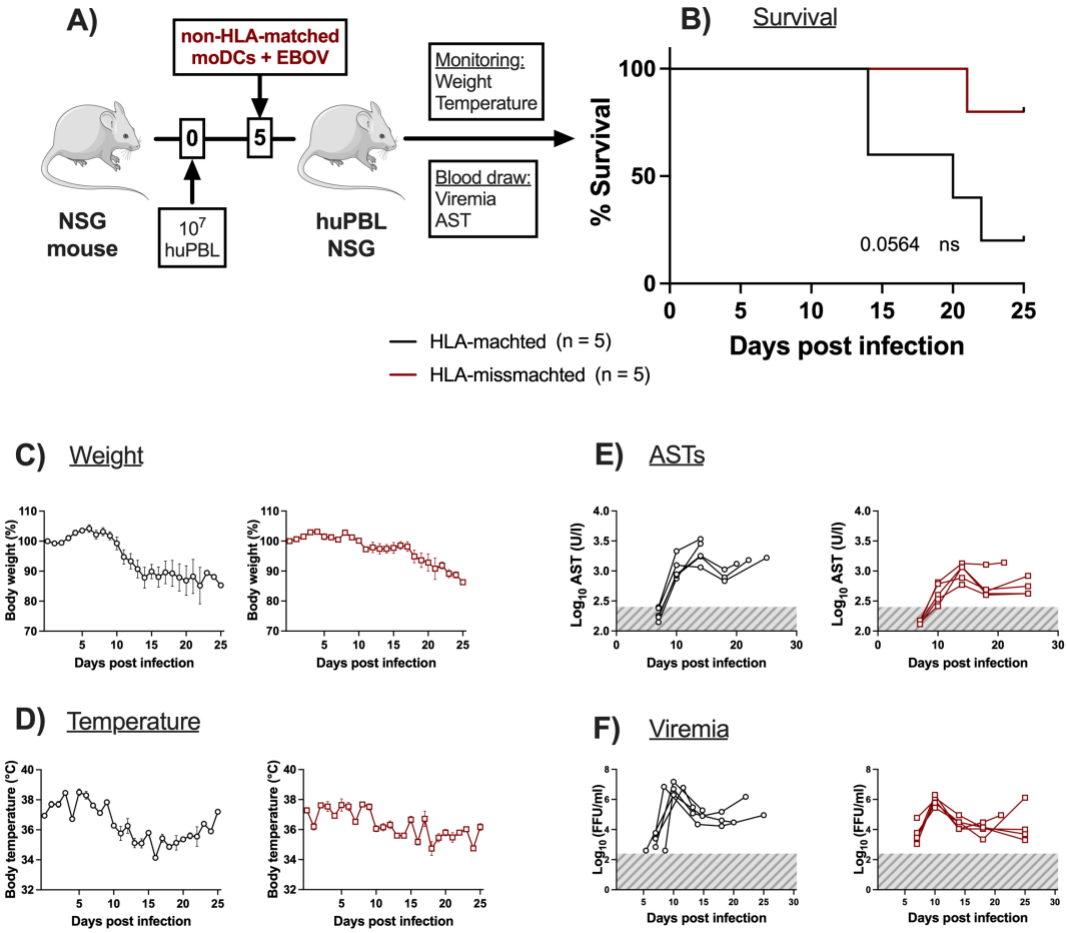

Figure 19: EBOV infection of avatar mice with non-HLA-matched moDCs. (A) 10 mice were inoculated with 10^7 PBLs from a healthy donor. 5 days post-inoculation mice were transplanted with $5*10^5$ *in vitro* generated EBOV-infected moDCs either from the same donor (black; n = 5) or from a non-HLA-matched donor (red; n = 5). Survival, weight, and temperature were monitored daily (B – D), blood and serum were collected at indicated time points for detection of AST levels and viremia (E / F). The normal range for AST and the limit of detection for viremia are shaded in grey. Mean and SEM are shown unless individual data points are depicted. Statistical significance was analyzed using LogRank (Mantel-Cox) test. Levels of significance were interpreted as follows: NS (not significant) $p > 0.05$, * $p \leq 0.05$, ** $p \leq 0.01$, *** $p \leq 0.001$, and **** $p \leq 0.0001$.

Taken together, these findings indicated that, in avatar mice, lethal EBOV infection can be achieved by transplantation of both PBLs and DCs. The severity of the model is dependent on HLA-TCR interactions.

4.2 Investigation of EVD determinants in avatar mice

EVD is a complex disease involving the disruption of the host immune response. Immune dysregulation leading to defective adaptive immune responses seem to play a central role in EVD pathophysiology. Clinical immunology data obtained during outbreaks strongly suggest that **upregulation of T cell activation- as well as co-inhibitory markers, T cell apoptosis**, **uncontrolled secretion of pro-inflammatory**

cytokines, and the lack of **formation of EBOV-specific T cells are hallmarks of severe EVD** (Ruibal et al., 2016; McElroy et al., 2015; Villinger et al., 1999; Baize et al., 2002; Wauquier et al., 2010; Kreuels et al., 2014; Wolf et al., 2015). Thus, the next step was to explore whether the avatar model would recapitulate these immune features and would serve to study. This would likely facilitate the development of T cell-based therapies in the future. To be able to investigate immunological features and their kinetics in this model, human cells and especially T cells were tracked in blood, spleen, and lung over the course of infection.

4.2.1 Engrafted human cells are reduced in blood of EBOV-infected avatar mice

Systemic EBOV infection is associated to high production of pro-inflammatory mediators, also referred to as 'cytokine storm', which is common in severe EVD (Wauqier et al., 2010; Gupta et al., 2001; McElroy 2015; Ruibal et al., 2016). This is likely related with the high levels of T cell activation observed in severe EVD (Ruibal et al., 2016; McElroy et al., 2015). The consequence of this excess T cell activation is likely lymphocyte apoptosis, which is a hallmark of EVD pathophysiology (Wauquier et al., 2010; Baize et al., 2002; Villinger 1999).

To investigate whether EBOV infection causes lymphopenia in avatar mice, repopulation of human PBLs was assessed over time in peripheral blood, spleen, and lung. PBMCs from a healthy HLA-A2$^+$ donor were separated into CD14$^+$ (monocytes) and CD14$^-$ (PBLs) cells subsets. 36 avatar mice were generated by transplanting 10^7 huPBLs. Meanwhile, moDCs from the same donor were generated *in vitro*, infected with EBOV 5 days later, and finally $5x10^5$ cells were administered to 18 mice respectively. Mock mice received the same amount non-infected moDCs. On days 1, 2, 6, 10, 13, and 16 three mice from each group were euthanized, and organs and blood were harvested.

The investigation of different immunological determinants in avatar mice was assessed through flow cytometry. Human PBLs were identified using the human hematopoietic cell marker CD45, which is also known as lymphocyte common antigen and is expressed on cells of hematopoietic origin, therefore on all leucocytes (Altin & Sloan, 1997). Human CD45$^+$ cells were traced over the course of infection as the percentage of live cells (**Fig. 20A**). The percentage of human CD45$^+$ cells in blood, spleen, and lung stayed equal until d6 between mock and infected mice **(Fig. 20B)**. On day 10

mice exposed to EBOV showed differences in human cell repopulation compared to mock-infected mice. EBOV-infected mice showed lower levels of human $CD45^+$ cells in peripheral blood and lung compared to mock mice (not significant). On days 13 and 16 the differences in blood between these two groups became even more pronounced. No clear trend could be identified in the spleen, as the variability of the percentages of $CD45^+$ cells in EBOV- infected mice was high.

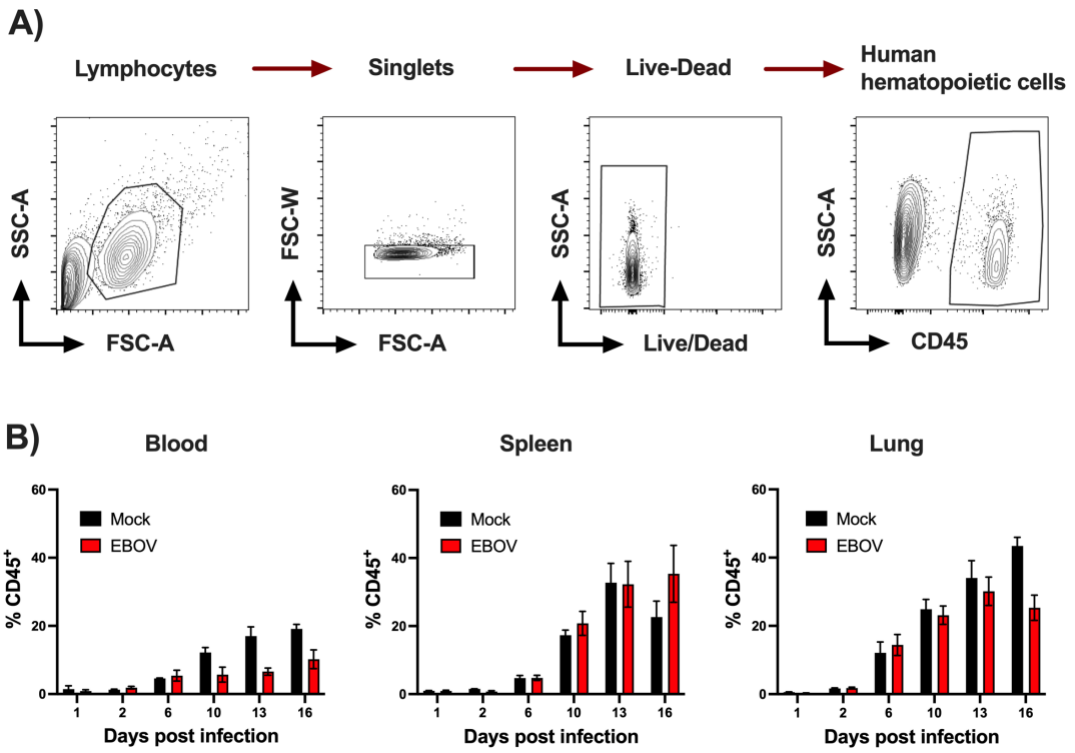

Figure 20: Repopulation of human cells in avatar mice in different organs. Avatar mice were infected with EBOV-infected moDCs 5 days post-transplantation and euthanized on days 1, 2, 6, 10, 13, and 16 post-infection. Mock mice received mock-infected moDCs. Blood, spleen, and lung were harvested and analyzed for the presence of human cells with flow cytometry using antibodies directed against human cell surface markers. **A)** The first gate excludes debris, the second doublets, and the third dead cells. In the fourth gate human CD45 hematopoietic cells are selected. **B)** Graphs represent the frequencies of $CD45^+$ cells within the live population in different organs over time. Mock group (n=3) is depicted in black and EBOV-infected mice (n=3) are depicted in red. Mean and SEM are shown.

In summary, differences in human cell repopulation could be observed especially in peripheral blood with lower percentages (not significant) of human CD45-expressing cells in EBOV-infected mice compared to mock-infected animals. Based on this data, however, it is not possible to say whether this is due to lymphopenia or migration to other organs that have not been investigated.

4.2.2 EBOV-infected avatar mice exhibit activated CD4$^+$- and CD8$^+$ T cells

In the same experiment, the T cell response in avatar mice was sought to be characterized, especially if they reflect the upregulation of activation and inhibitory markers. Two studies conducted with samples from the 2013-2016 West African outbreak detected the co-expression of activation markers like CD38 and HLA-DR on a significant amount of CD4 and CD8 T cells through flow cytometry on acute samples. It was shown that there was substantial T-cell activation during acute infection among all patients on CD4$^+$ as well as CD8$^+$ T cells (Ruibal et al., 2016; McElroy et al., 2015).

To study the levels of T cell activation in EBOV-infected avatar mice, flow cytometry to look for the presence of HLADR$^+$ CD38$^+$ T cells was utilized (**Fig. 21A)** during the same experiment as in 4.2.1. T cells co-expressing these two markers have been previously defined as activated T cells (Lindgren et al., 2011; McElroy et al., 2015; Miller et al., 2008; Ruibal et al., 2016).

Mock-infected avatar mice showed a basal co-expression of activation markers over the course of the experiment, reaching a plateau between days 6 and 10 in blood, spleen, and lung (**Fig. 21C**). Compared to mock-infected animals, EBOV-infected mice showed a higher percentage of activated T cells. This difference became visible at day 10 post-infection in blood, spleen, and lung, and was most pronounced around day 13 (not significant). In peripheral blood the median of frequencies of HLADR$^+$ CD38$^+$ T cells in EBOV-infected mice reached 71.4% compared to 40.8% in mock mice ($p = 0.1$), in spleen 71.7% (EBOV) and 35.2% (mock) ($p=0.1$).

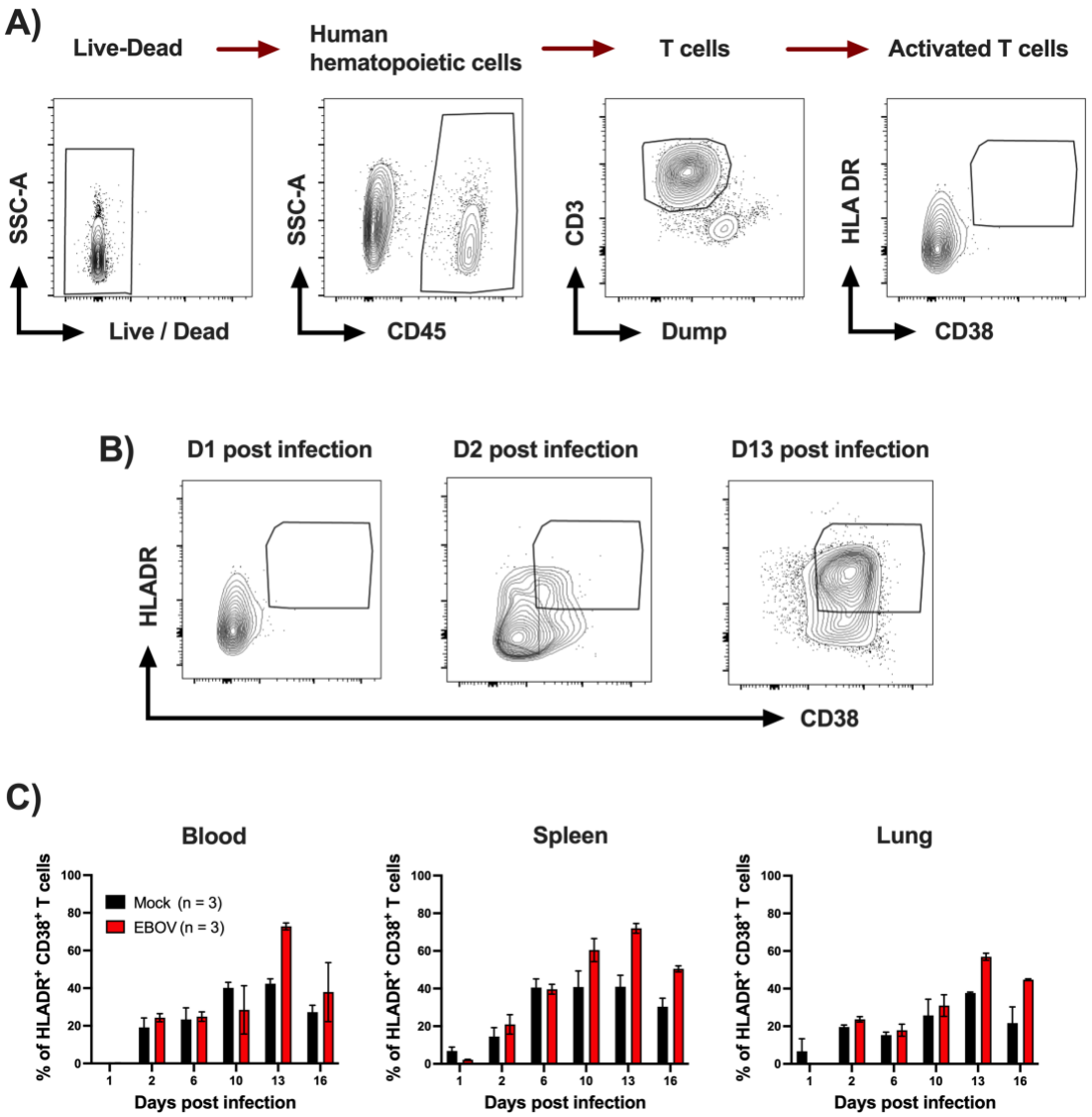

Figure 21: T cell activation in avatar mice. Avatar mice were infected with EBOV-infected moDCs 5 days post transplantation and sacrificed on days 1, 2, 6, 10, 13, and 16 post infection. Mock mice received mock-infected moDCs. Blood, spleen, and lung were harvested and analyzed for the presence of activated T cells with flow cytometry. Activated T cells were defined as $CD38^+$ and $HLADR^+$. **A)** The first gate excluded debris, the second doublets (both gates are not shown), and the third dead cells. In the fourth gate human CD45 hematopoietic cells were selected. T cells were defined as $CD3^+$ and dump negative. The dump channel included CD19 (B cells), CD56 (NK cells), CD14 and CD16 (macrophages and monocytes). $CD3^+$ cells were then stained for HLADR and CD38. **B)** Representative flow cytometry plots show activated T cells in blood from D1, D2, and D13 from EBOV-infected mice. **C)** Graphs represent the frequencies of activated T cells within the T cell population in different organs over time. Mock group (n=3) is depicted in black and EBOV-infected mice (n=3) are depicted in red. Mean and SEM are shown.

T cell activation was observed in human studies in fatal cases as well as in survivors at similar levels, and therefore not correlated to viral clearance. Indeed, it was demonstrated in fatal cases that co-inhibitory markers PD-1 and CTLA-4 were upregulated on $CD8^+$ T cells (Ruibal et al. 2016; McElroy et al., 2015). High expression of these two markers could be related to a nonfunctional, but reversible status named

“T cell exhaustion” (Wherry, 2011). It involves defects in molecular mechanisms that control the transition from activation to immune homeostasis. PD-1 and CTLA-4 are moreover upregulated in certain tumor cells and immunotherapeutic approaches to block these receptors are already available (Sharma & Allison, 2015).

To investigate whether avatar mice are a suitable model to study T cell dysregulation, the co-expression of PD-1 and CTLA-4 was monitored through flow cytometry over the course of infection during the same experiment (**Fig. 22A/B**). A population of T cells expressing both CTLA-4 and PD-1 markers was detected as early as day 2 post infection in blood, lung, and spleen of both mock-infected and EBOV-infected mice (**Fig. 22C**). Around 40% of T cells exhibited dual marker expression. By day 10, the percentage increased to 80% in both groups. In blood this increased gradually until day 10 to 80% of all T cells in both groups. The spleen showed a peak in CTLA-4 and PD-1 expressing T cells on day 10, with a notable increase between days 6 and 10. No significant difference was observed between mock- and EBOV-infected mice until day 10, but later on, mock-infected mice had slightly higher expression. However, on days 13 and 16, a higher percentage of T cells co-expressed both markers in EBOV-infected animals, although the difference was not statistically significant. CD4+ and CD8+ T cells showed no distinction in marker expression (data not shown).

Moreover, the formation of EBOV-specific T cells was investigated through flow cytometry. For this, a tetramer specific for the HLA-A2-restricted peptide FLSFASLFL was used that has been shown to be able to detect NP-specific T cells during the West African pandemic. However, the detection of antigen-specific T cells in surviving animals from the experiments in section 5.1.5 and 5.1.6 was not successful with this specific tetramer (**Supp. Fig. 1**).

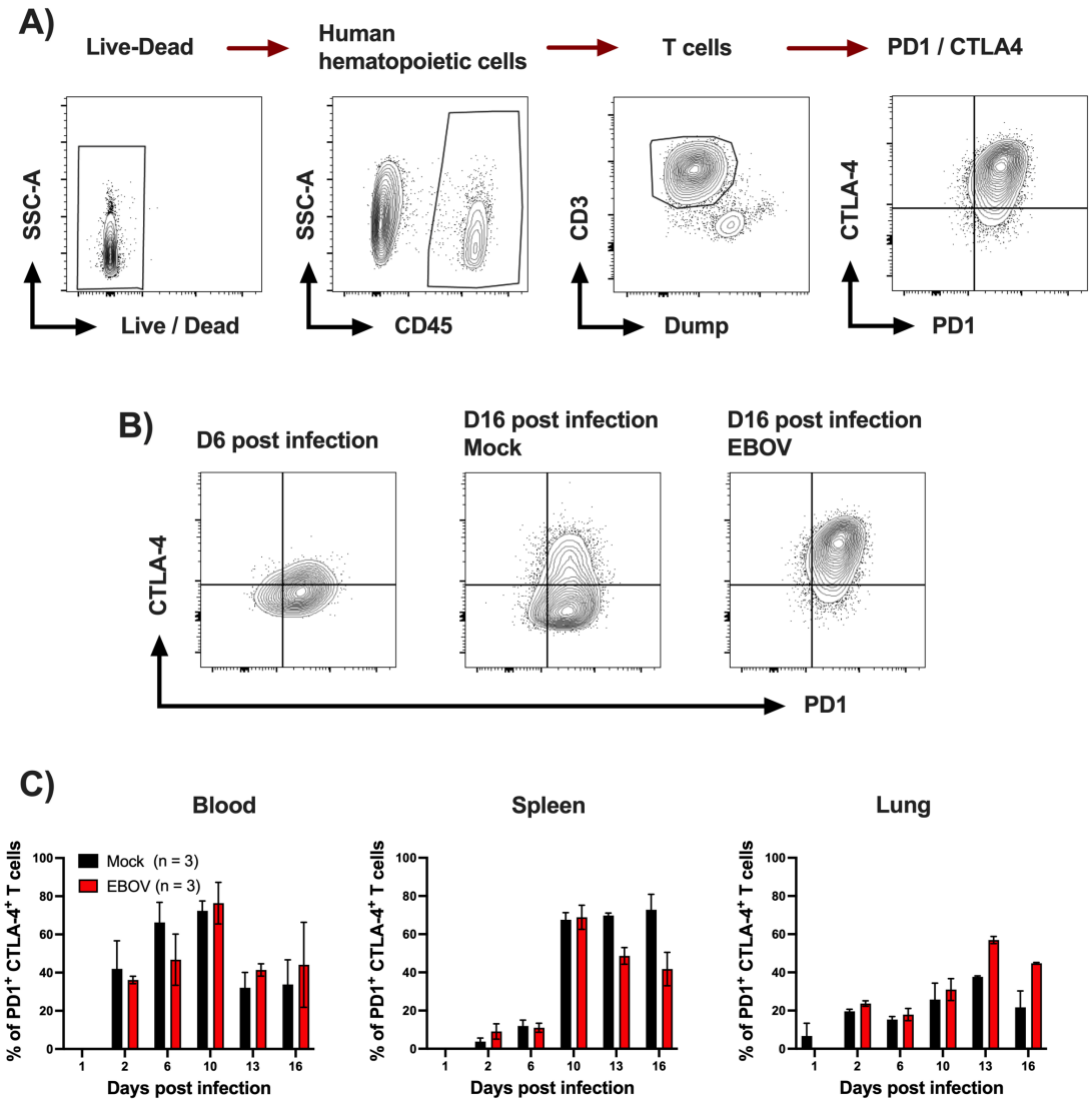

Figure 22: CTLA-4 and PD-1 expression in avatar mice. Avatar mice were infected with EBOV-infected moDCs 5 days post transplantation and sacrificed on days 1, 2, 6, 10, 13, and 16 post infection. Mock mice received mock-infected moDCs. Blood, spleen, and lung were harvested and analyzed for the presence of exhaustion markers PD1 and CTLA-4 within the T cell population with flow cytometry. **A)** The first gate excluded debris, the second doublets (both gates are not shown), and the third dead cells. In the fourth gate human CD45 hematopoietic cells were selected. T cells were defined as $CD3^+$ and dump negative. The dump channel included CD19 (B cells), CD56 (NK cells), CD14 and CD16 (macrophages and monocytes). $CD3^+$ cells were then stained for CTLA-4 and PD1. **B)** Representative flow cytometry plots show blood cells from D6 and D16 (mock and EBOV). **C)** Graphs represent the frequencies of $CTLA\text{-}4^+$ and $PD1^+$ cells within the T cell population in different organs over time. Mock group (n=3) is depicted in black and EBOV-infected mice (n=3) are depicted in red. Mean and SEM are shown.

In summary, T-cell activation could be observed in EBOV-infected avatar mice (not significant), while there was no difference in PD-1 and CTLA-4 co-expression between mock- and EBOV-infected animals. The detection of NP-specific T cells with a tetramer was not successful either. These results may indicate the limitations of the mouse model regarding the study of T cell response in the context of EBOV infection.

4.2.3 Infection of avatar mice with EBOV leads to increase in inflammation

It has been shown that an infection with EBOV results in prolific, uncontrolled secretion of pro-inflammatory cytokines and chemokines resulting in an immunological imbalance, also referred to as cytokine storm (Wauqier et al., 2010). Similar to what has been observed during septic shock, infected monocytes, DCs, and macrophages release pro-inflammatory meditators such as IFNs, IL1β, IL1-RA, IL-6, IL-8, IL-10, IL-15, MIP-1α, MIP-1β, MCP1, and TNFα (Gupta et al., 2001; McElroy 2015; Ruibal et al., 2016) upon infection with EBOV, in particular in fatal cases. In survivors it was shown that cytokines and chemokines (IL1β, IL-6, MIP-1α, MIP-1β, TNFα) are temporarily and moderately upregulated.

As this uncontrolled production of soluble mediators also triggers T cell activation, T cell exhaustion, and lymphocyte apoptosis (Wauquier et al., 2010; Baize et al., 2002; Villinger 1999), the next step was to evaluate whether EBOV-infected avatar mice exhibited an altered cytokine and chemokine profile compared to mock-infected animals. Chemokine and cytokine levels in the serum were measured through a Luminex-bases analysis in EBOV-infected and mock-infected avatar mice on D13 post infection, since both groups exhibited the biggest differences in human cell repopulation and T cell activation. To determine specific contribution of human PBLs during EBOV infection in this model, panels were utilized that included human cytokines, chemokines, and coagulation markers.

PBMCs from a healthy HLA-A2$^+$ donor were separated into CD14$^+$ (monocytes) and CD14$^-$ (PBLs) cells subsets. Avatar mice were generated by transplanting 10^7 huPBLs r.o. into recipient mice. Meanwhile, moDCs from the same donor were generated *in vitro*, infected with EBOV 5 days later, and finally $5x10^5$ EBOV-infected moDCs were administered. Mock mice received the same amount mock-infected moDCs (n=18). Weight and temperature were monitored for on a daily basis. On day 13, three mice from each group were euthanized and blood was harvested to obtain serum.

As the heatmap demonstrates, mock-infected and EBOV-infected mice showed high variability of cytokine and chemokine levels within groups (**Fig. 23A**). Some parameters were nevertheless indicating that there were possible differences between groups. Pro-inflammatory mediators MIP1α, IP10, MIP1β, Pecam1 (platelet and endothelial cell adhesion molecule 1), sCD40L, and E-selectin were slightly up-regulated in infected animals (not significant), while the anti-inflammatory cytokine IL-

10 seemed to be higher in mock-infected mice (not significant), therefore down-regulated in EBOV-infected mice (**Fig. 23B**).

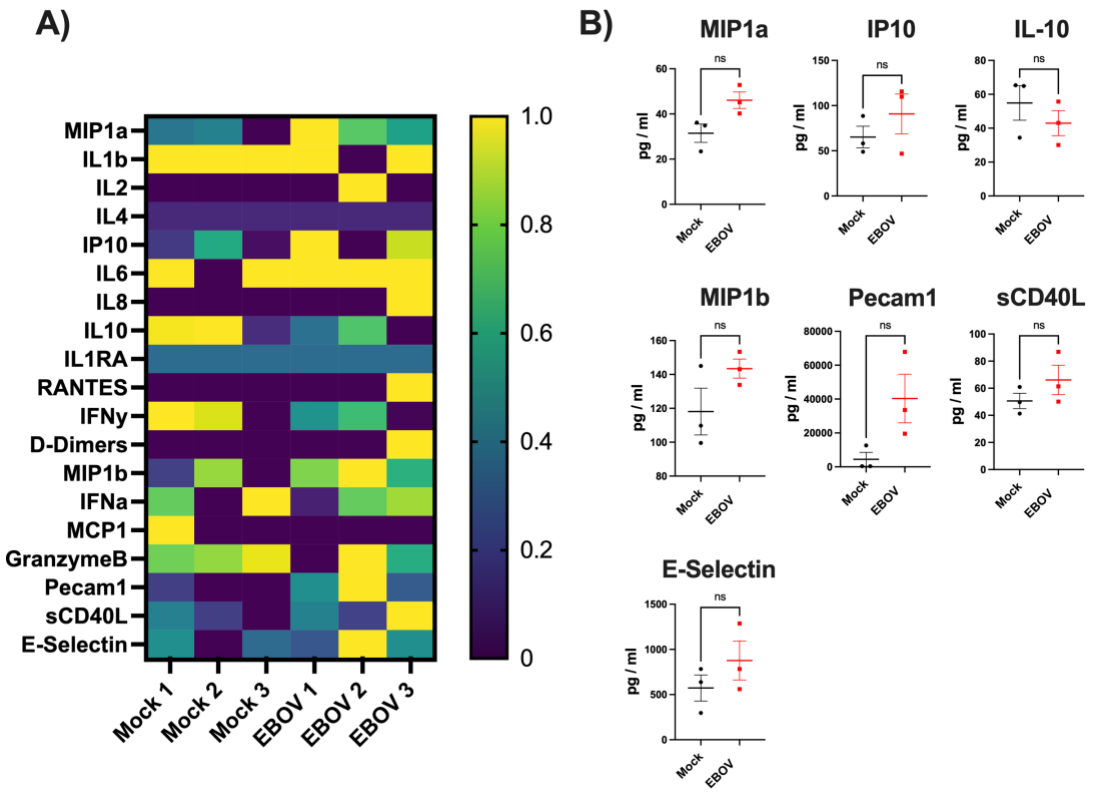

Figure 23: Cytokine and Chemokine profile of EBOV-infected and mock-infected avatar mice on day 13 post infection. Avatar mice were infected with EBOV-infected moDCs 5 days post transplantation and sacrificed on days 13 post infection. Mock mice received mock-infected moDCs. Analytes were measured through Luminex multiplex assay in plasma. **A)** Heatmap shows levels of indicated chemokines and cytokines in plasma of mice on day 13 post infection. Collected data was analyzed using min-max normalization, which normalized concentrations between 1 and 0. **B)** Concentrations of selected analytes are shown in infected (red) and mock mice (black). Statistical significance was analyzed using nonparametric Mann-Whitney U test. Levels of significance were interpreted as follows: NS (not significant) $p > 0.05$, * $p \leq 0.05$, ** $p \leq 0.01$, *** $p \leq 0.001$, and **** $p \leq 0.0001$.

4.3 Application of the model to study EVD survivor immunity

In the following experiments avatar mice were evaluated whether they could serve to study EVD survivor immunity. In particular, whether a natural infection with EBOV provided protection against re-infection. Previous studies had suggested that EVD survival required both T cell and antibody responses (Ruibal et al., 2016; McElroy et al., 2015), so we wanted to address whether this was the case. In order to perform these experiments, Prof. Miles Carroll provided us with PBMC and plasma samples from Guinean EVD surviving patients from the 2013 – 16 West Africa epidemic. PBMC

samples selected were those that showed higher levels of effector T cell activation in IFNγ GP ELISPOT (enzyme-linked immune-spot) analyses (Tipton et al., 2021).

4.3.1. PBLs from EVD survivors alone do not protect from EBOV infection

First, it was investigated whether transfer of huPBLs from EVD survivors was sufficient to rescue avatar mice from lethal EBOV infection. To do so, PBMCs from 5 HLA-A2$^+$ EVD survivors were thawed and PBMCs from 5 HLA-A2$^+$ healthy controls were separated into CD14$^+$ (monocytes) and CD14$^-$ (PBLs) cells subsets. 5 huPBL-Avatar mice were generated from survivor PBMCs (one mouse per survivor) and 9 mice from EBOV naïve controls. Of these 9 controls, 2 mice were left uninfected (mock). Meanwhile, moDCs from HLA-A2 matched donors were generated *in vitro*, infected with EBOV 5 days later, and finally 5x10^5 cells/mouse were injected. Mock mice received the same amount non-infected moDCs (n=2). This strategy was based on the finding that HLA-A2-matched DCs could be used to generate avatar mice instead of autologous moDCs (Suppl. Fig. 1).

Weight and temperature were monitored for 24 days on a daily basis. Blood samples were drawn on days 3, 7, 10, 13, 16, 20, and on the respective day of death to measure AST levels and determine viremia **(Fig 24A)**. Viral titers were also measured in organs on day of death. Mice were euthanized according to the termination criteria.

In both groups, survivor avatar mice and control avatar mice lost weight rapidly, showed elevated serum AST levels, and high viremia (**Fig. 24C/E/F**). All mice within both groups, except for one survivor avatar mice, succumbed to EBOV-infection. While the control group rapidly died of the infection around day 11 / 12, survivor avatar mice showed a slight delay (d14 – d20) (**Fig. 24B**). More profound differences could be observed when measuring body temperature (**Fig. 24D**). As already demonstrated in previous sections EBOV-infection of avatar mice reconstituted with PBLs from healthy control donors, body temperature decreases strongly before death, even down to 30 – 32 °C in some mice. This was also observed in this experiment among the control group. In contrast to avatar mice generated with EVD survivor PBLs. These animals exhibited a stable body temperature between 35 and 37 °C during the experiment (**Fig. 24D**). Moreover, organ titers were significantly lower in liver (p=0.0013), kidney (p=0.0303), spleen (p=0.0051), and heart (p=0.0043) in survivor avatar mice. The lung showed a slight reduction (p=0.202) (**Fig. 24G**).

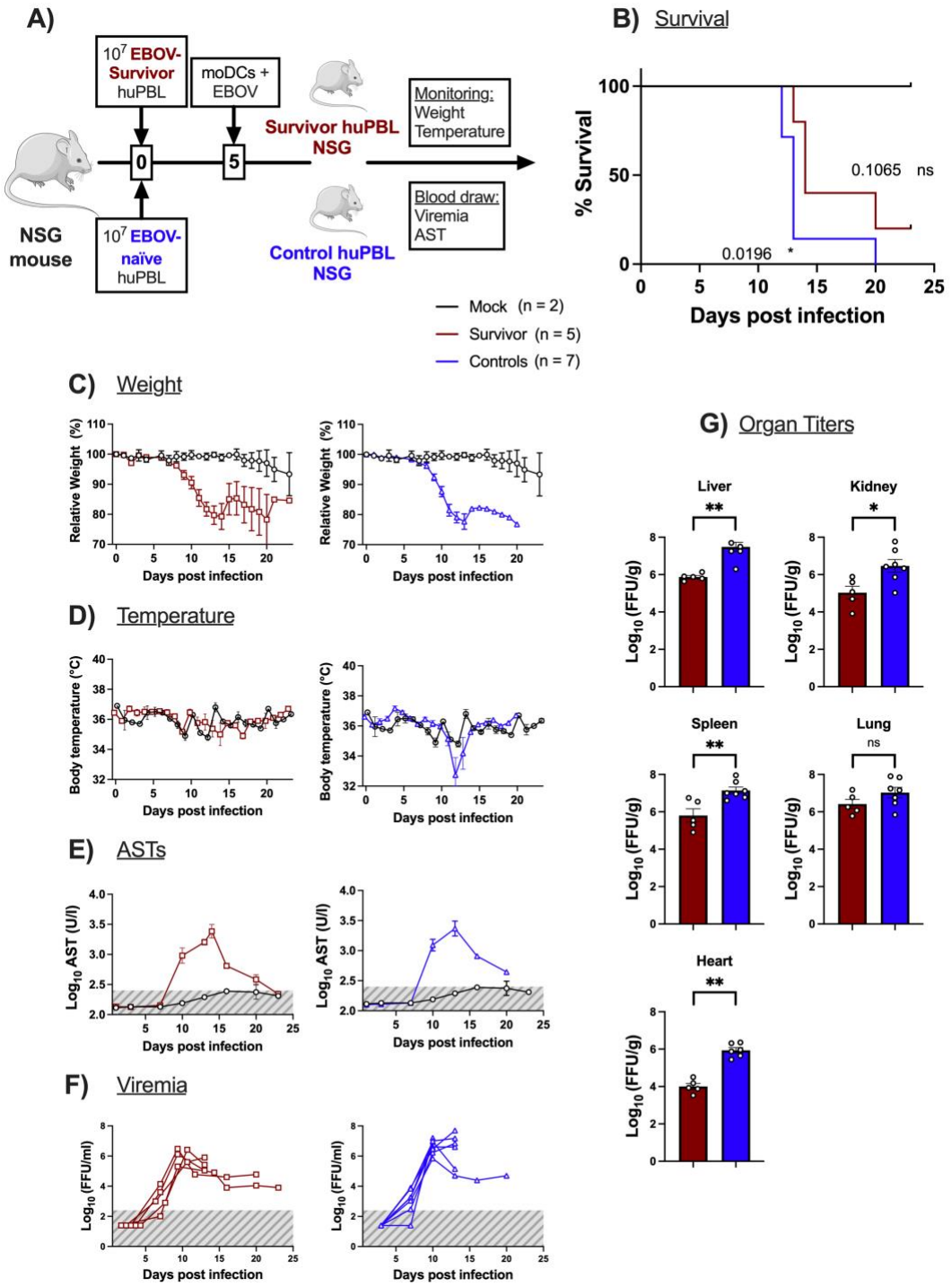

Figure 24: Infection of avatar mice generated with EVD survivor PBLs. (A) Five mice were engrafted with 10^7 PBLs from EVD survivors (one mouse per survivor; n = 5, red) and 9 were engrafted with 10^7 PBLs from healthy donors (2 mock (n = 2; black); 7 EBOV-infected (n = 7; blue)). Five days post inoculation mice were transplanted with $5*10^5$ *in vitro* generated either mock-infected or $5*10^5$ EBOV-infected moDCs from one healthy donor. Survival, weight, and temperature were monitored daily (B – D), blood and serum were collected at indicated time points for detection of AST levels and viremia (E / F). The normal range for AST and the limit of detection for viremia are shaded in grey. Organ viral titers were determined at day of death (G). Mean and SEM are shown unless individual data points are depicted. Statistical significances were analyzed using either LogRank (Mantel-Cox) test or one-way ANOVA (Kruskal-Wallis test) followed by Dunn's multiple comparison test. Levels of significance were interpreted as follows: NS (not significant) $p > 0.05$, * $p \leq 0.05$, ** $p \leq 0.01$, *** $p \leq 0.001$, and **** $p \leq 0.0001$.

In addition to the above-mentioned parameters, flow cytometry was also performed on peripheral blood on each time point. Since T cell activation was demonstrated to be upregulated in previous experiments, we wanted to investigate, whether a difference in the level of activation or cell subsets, that express activation markers, can be observed in huPBL-Avatar mice from EVD survivors compared to mice transplanted with EVD-naïve PBLs. Co-expression of CD38 and HLAD-R was again used to determine activated T cells.

The percentage of activated T cells started to differ around D10 between mock, survivor, and control avatar mice, with the latter group showing highest percentage of activated T cells, followed by avatar mice reconstituted with survivor PBLs, and mock mice the lowest (**Fig. 25A**). The biggest difference was observed on D13. Even though the differences were not statistically significant, a clear trend could be seen (**Fig. 25B**). However, when T cells were subdivided into CD4 and CD8 T cell subsets, significant differences between control and survivor avatar mice were observed on days 10 and 13 (**Fig. 25C**). In avatar mice engrafted with EVD survivor PBLs $CD4^+$ T cells elicited significantly lower co-expression of HLA-DR and CD38 comparable to levels measured in mock mice. Among $CD8^+$ T cells no difference was detectable. Previous clinical data suggested that the adaptive immune response to EBOV is mostly driven by NP-specific $CD8^+$ T cells (McElroy et al., 2015; Sakabe et al., 2018; Sundar et al., 2007). These might be specifically re-activated after EBOV-infection in survivor avatar mice and thus bystander $CD4^+$ T cells might be less affected.

In summary, avatar mice transplanted with PBLs from EVD surviving patients showed a reduction in virus replication in organs at the time of euthanasia. Nevertheless, transfer of survivor T cells alone was not sufficient to provide protection against EBOV challenge.

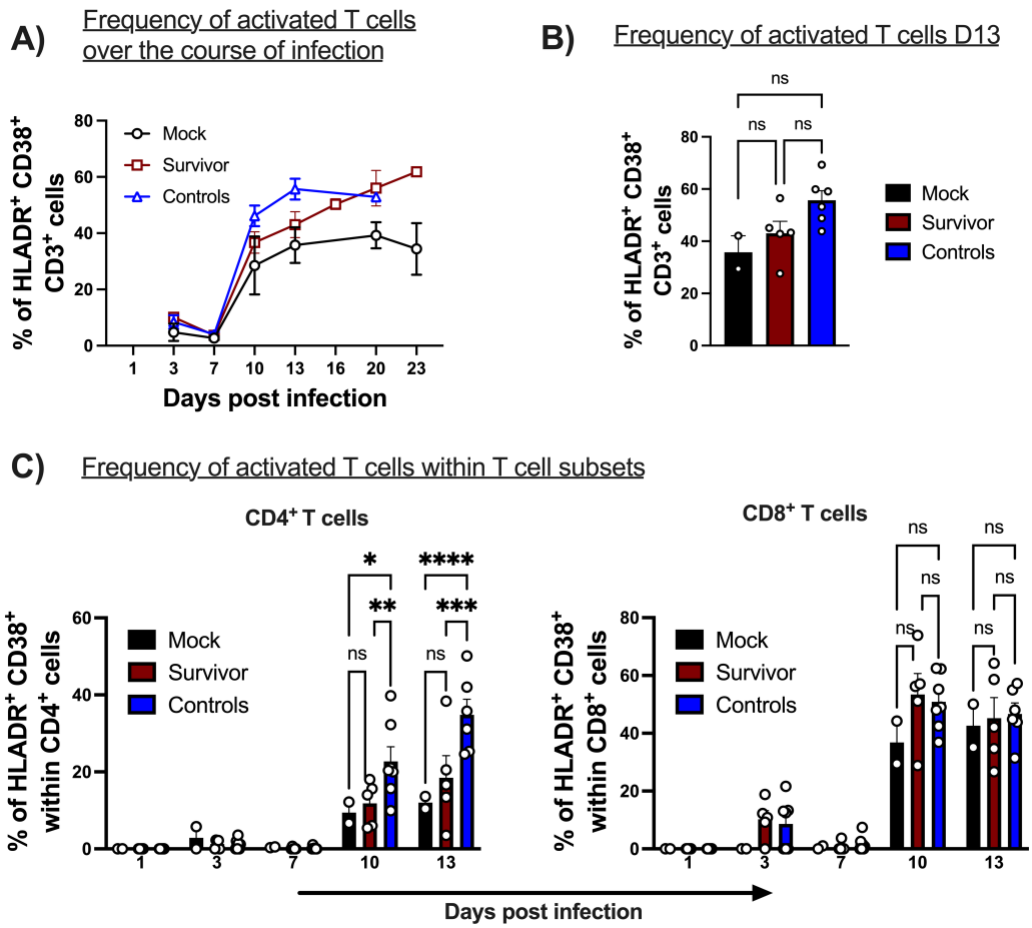

Figure 25: T cell activation in avatar mice from EVD-survivor. Five mice were engrafted with 10^7 PBLs from EVD survivors (one mouse per survivor; n = 5, red) and 9 were engrafted with 10^7 PBLs from healthy donors (2 mock (n = 2; black); 7 EBOV-infected (n = 7; blue)). Five days post inoculation mice were transplanted with $5*10^5$ *in vitro* generated either mock-infected or $5*10^5$ EBOV-infected moDCs from one healthy donor. Blood was drawn on different time points post infection and analyzed for the presence of activated T cells with flow cytometry. Activated T cells were defined as $CD38^+$ and $HLADR^+$. A) Graph represents frequencies of activated T cells within the T cell population over the course of infection. B) Bar graphs show activated T cells in blood on D13. C) Graphs represent frequencies of activated T cells within the $CD4^+$ and $CD8^+$ T cell populations separately over the course of infection. Statistical significances were analyzed using one-way ANOVA (Kruskal-Wallis test) followed by Dunn's multiple comparison test. Levels of significance were interpreted as follows: NS (not significant) $p > 0.05$, * $p \leq 0.05$, ** $p \leq 0.01$, *** $p \leq 0.001$, and **** $p \leq 0.0001$.

4.3.2 PBLs and IgG from EVD survivors can protect avatar mice from EBOV infection

In the following experiment it was evaluated whether the transplantation of both T cells and antibodies from survivors could protect avatar mice from lethal EVD. In addition to PBMCs from EVD survivor plasma from two different survivors, of which one showed low neutralizing capacity and the other high neutralizing capacity, was utilized. Bulk IgG was extracted from these plasma samples through affinity-purification using

Protein G beads. As an antibody control the commercially available monoclonal anti-EBOV antibody KZ52 was utilized (Maruyama et al., 1999; Parren et al., 2002).

The experimental setup was as follows. PBMCs from HLA-A2$^+$ EVD survivors were thawed and PBMCs from HLA-A2$^+$ healthy controls were separated into CD14$^+$ (monocytes) and CD14$^-$ (PBLs) cells subsets. Ten avatar mice were generated from survivor PBMCs and 13 mice from controls, two of which functioned as mock mice. Meanwhile, moDCs from one healthy donor were generated *in vitro*, infected with EBOV 5 days later, and finally 5x10^5 cells were administered r.o. to 21 mice respectively. Mock mice received the same amount non-infected moDCs (n=2). On the same day either isolated low-neutralizing, high-neutralizing, or KZ52 was injected into the mice with a concentration of 10 mg/kg of body weight i.p. directly after infection, as previously described (Duehr et al., 2017) **(Fig. 26A)**. This resulted in 8 different experimental groups: control avatar mice + mock-infected moDCs, untreated control avatar mice + EBOV-infected moDCs, control avatar mice + EBOV-infected moDCs + KZ52, control avatar mice + EBOV-infected moDCs + low neutralizing IgG, control avatar mice + EBOV-infected moDCs + high neutralizing IgG, survivor avatar mice + EBOV-infected moDCs + KZ52, survivor avatar mice + EBOV-infected moDCs + low neutralizing IgG, and survivor avatar mice + EBOV-infected moDCs + high neutralizing IgG. Weight and temperature were monitored for 24 days on a daily basis. Blood samples were drawn on days 7, 10, 13, 16, 20, and on the respective day of death to measure AST levels and determine viremia. Viral titers were also measured in organs on day of death. Mice were killed according to termination criteria.

Avatar mice transplanted with PBLs from healthy donors lost weight and dropped body temperature rapidly (**Fig. 26C/D**). Independently of the treatment, all control mice reached euthanasia criteria within the first two weeks post infection (**Fig. 26B**). Interestingly, KZ52, which showed protective functions in rodent models but not in NHP models before, had no benefit either (Oswald et al., 2007; Parren et al., 2002). On the contrary, avatar mice engrafted with PBLs from EVD survivor survived after infusion with IgG or KZ52 until day 18 post infection. Only one mouse treated with KZ52, and one mouse of the high neutralizing group reached euthanasia criteria before the experiment was terminated (**Fig. 26B**). Moreover, survivor PBL-transplanted avatar mice presented stable body temperatures over the course of the whole experiment (**Fig. 26D**).

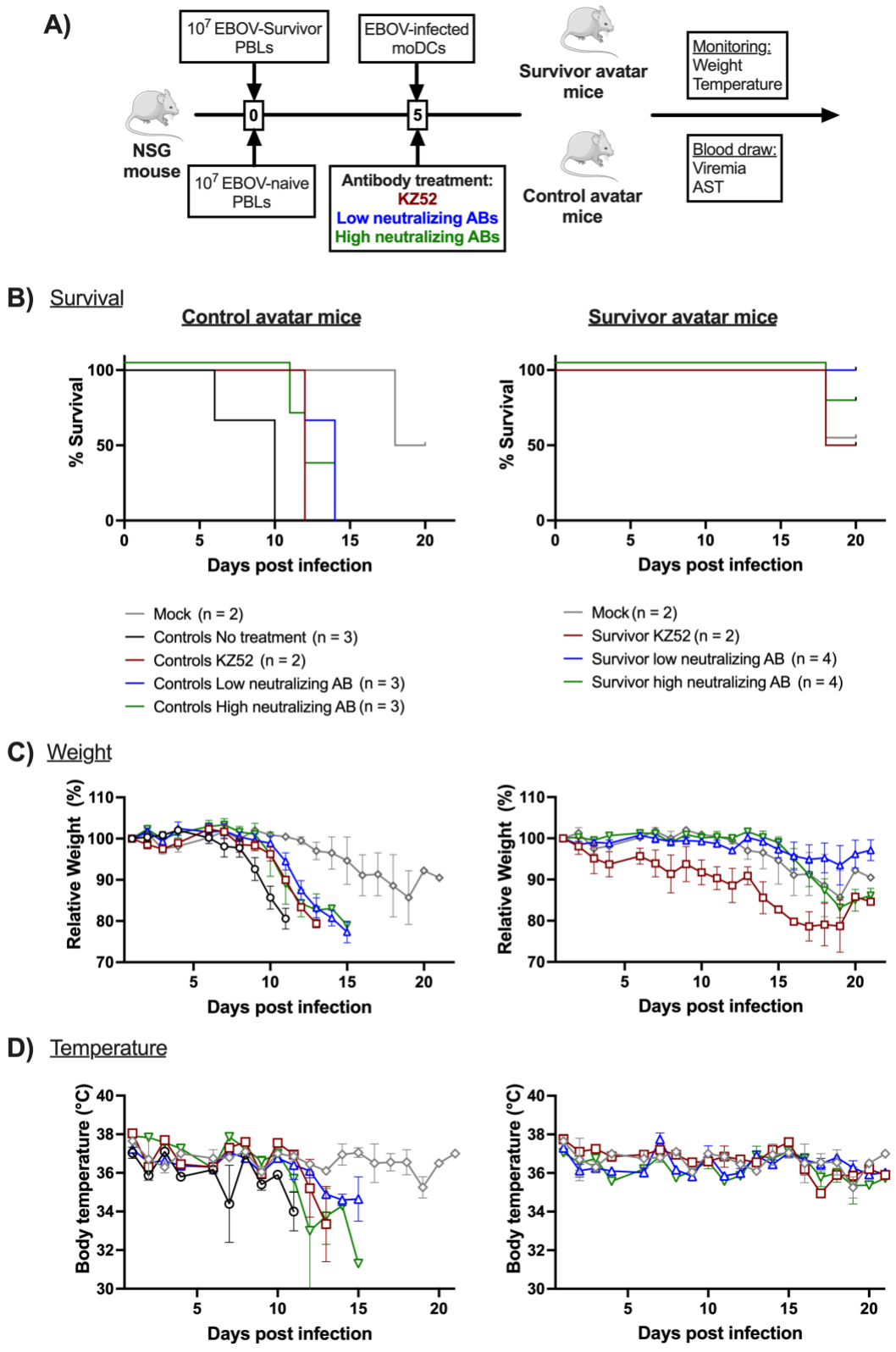

Figure 26: EBOV infection of avatar mice inoculated with EVD-survivor PBLs and treated with antibodies. (A) NSG mice were either engrafted with 10^7 PBLs from EVD survivors or with 10^7 PBLs from healthy donors. Five days post inoculation mice were transplanted with $5*10^5$ *in vitro* generated either mock-infected or $5*10^5$ EBOV-infected moDCs from one healthy donor. At the same time, mice from each group received i.p. either PBS (untreated, black), 10 mg/kg KZ52 (red), 10 mg/kg low neutralizing IgG from a EVD survivor (blue), or 10 mg/kg high neutralizing IgG from a EVD survivor (green), Survival, weight, and temperature were monitored daily (B – D). Mean and SEM are shown.

To further characterize the impact of survivor PBLs and antibody treatment on EVD pathogenicity, AST levels, viremia, and viral titers lung, spleen, heart, kidney, and liver were measured (**Fig. 27**). AST serum levels uniformly peaked on day 11 in all groups containing avatar mice engrafted with PBLs from healthy donors independent of antibody treatment (**Fig. 27A**). AST levels of antibody-treated survivor avatar mice peaked between days 14 and 17 at lower levels compared to control mice and dropped again. A similar progression could be observed when detecting viremia. In all control groups, it peaked on day 10, while viremia in avatar mice transplanted with EVD survivor PBLs reached a plateau around day 14 and only minimally decreased again until the end of the experiment (**Fig. 27B**). Organ titers were determined when animals reached endpoint criteria or the experimental endpoint. Groups with survivor avatar mice showed overall lower organ titers compared to their control counterparts with the same antibody treatment, albeit not significant (**Fig. 27C**). This trend could be seen among all organs.

In summary, mice that received PBLs from EVD survivors showed higher survival and an overall lower expression of disease symptoms completely independent on the neutralizing capacity of the IgG transferred. These results indicated that both cellular and humoral memory were required for controlling EBOV infection, and that avatar mice could be used in the future to dissect the relative contribution of both arms of immune response to infection and to identify correlates of immunity.

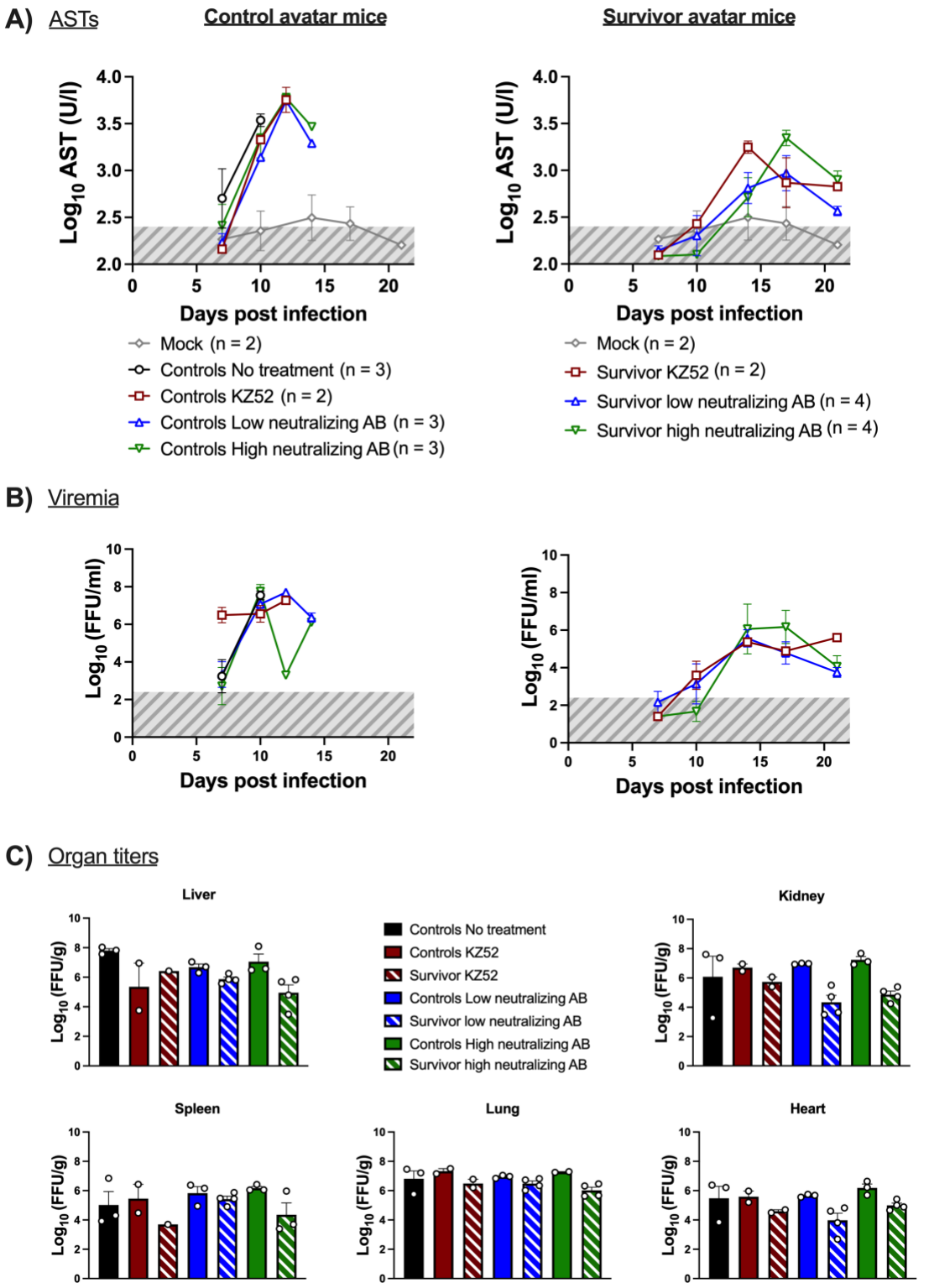

Figure 27: ASTs and EBOV replication in avatar mice transplanted with survivor or control PBLs under AB treatment. Blood and serum were collected at indicated time points for detection of AST levels and viremia (A/ B). The normal range for AST and the limit of detection for viremia are shaded in grey. Organ viral titers were determined at day of death (C). Mean and SEM are shown. Statistical significances were analyzed using either LogRank (Mantel-Cox) test or one-way ANOVA (Kruskal-Wallis test) followed by Dunn's multiple comparison test. Levels of significance were interpreted as follows: NS (not significant) $p > 0.05$, * $p \leq 0.05$, ** $p \leq 0.01$, *** $p \leq 0.001$, and **** $p \leq 0.0001$.

4.3.3 Combination of antibodies and PBLs from EVD survivor reduce secretion of pro-inflammatory mediators in EBOV-infected avatar mice

As previously shown pro-inflammatory mediators like MIP1α, MIP-1β, and MCP-1 were upregulated in EBOV-infected avatar mice transplanted with PBLs from healthy donors that succumbed to infection. The next step was to investigate whether any differences in mice injected with survivor PBLs in combination with antibody treatment compared to control mice could be detected. In fact, in human survivors it was shown that cytokines and chemokines were temporarily and moderately upregulated in contrast to fatal cases, which were associated with prolific, uncontrolled secretion of pro-inflammatory cytokines and chemokines (McElroy et al., 2015; Ruibal et al., 2016; Kerber et al., 2018).

In order to investigate the differences between EBOV-infected mice transplanted with cells from healthy donors and cells from EVD survivors and the influence of the addition of antibodies to disease outcome, Luminex-based analysis of immune mediators was performed. To evaluate specific contribution of human PBLs in our model, panels to assess expression of human cytokines, chemokines, and coagulation markers were utilized. Serum samples from avatar mice were obtained on their respective day of death when euthanasia criteria were reached.

Since antibody-treated showed a similar disease progression, they were not analyzed separately but were grouped according to their transplanted cells. Thus, four different groups could be compared: control avatar mice, antibody-treated control avatar mice, survivor avatar mice, and antibody-treated avatar mice. Heatmap of serum levels showed that there were no group-specific patterns with respect to the measured parameters, except for pro-inflammatory mediators MIP1α, MIP-1β, and MCP-1 (**Fig. 28A**). These were significantly upregulated in avatar mice transplanted with control PBLs treated as well as untreated with antibodies compared to avatar mice that received survivor PBLs and antibodies (**Fig. 28B**). These prof-inflammatory cytokines were previously associated with severe EVD in humans (Ruibal et al., 2016; Kerber et al., 2018).

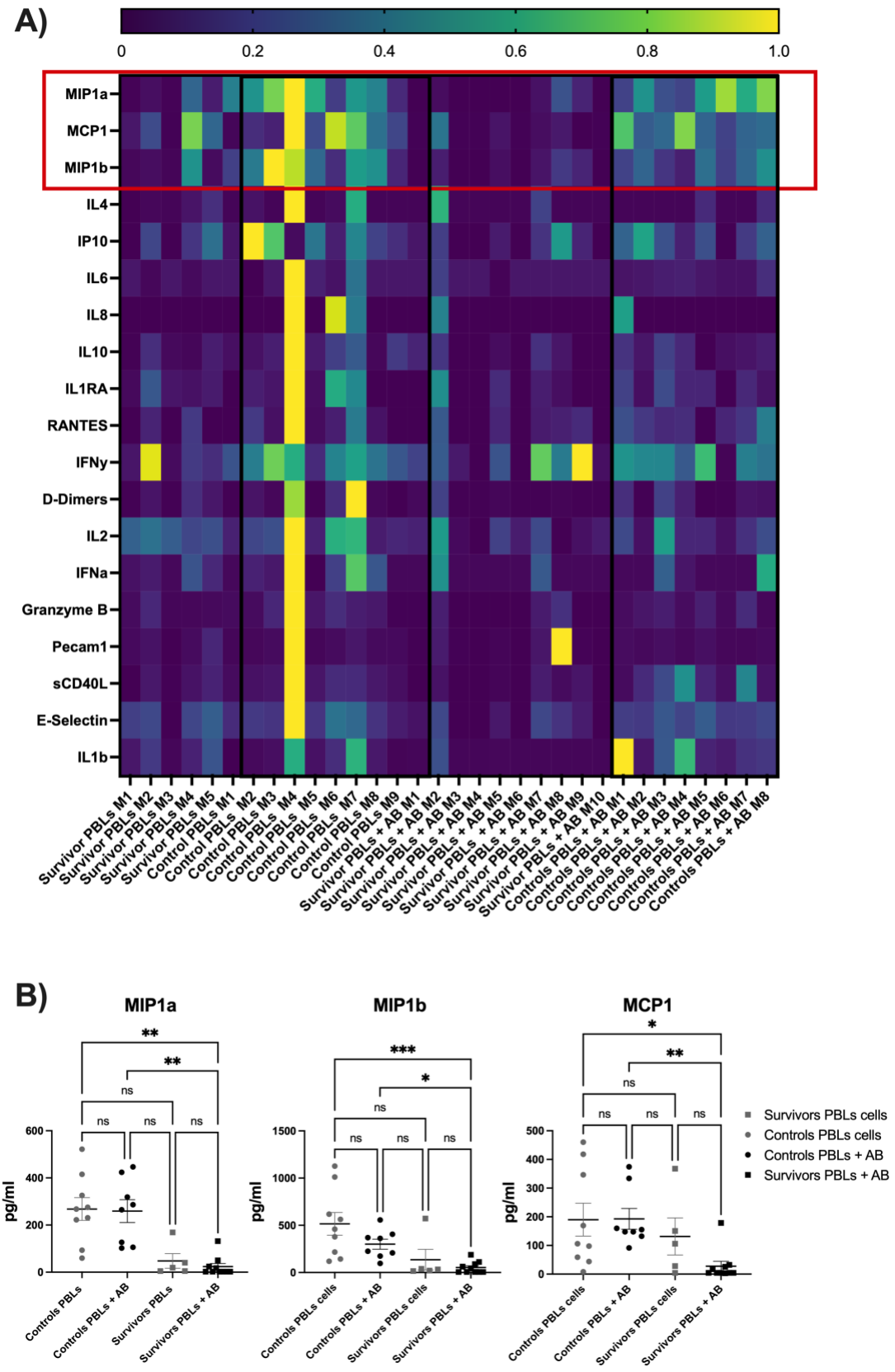

Figure 28: Cytokine and Chemokine profile of EBOV-infected avatar mice transplanted with control PBLs or survivor PBL on their day of death. NSG mice were either engrafted with 10^7 PBLs from EVD survivors or with 10^7 PBLs from healthy donors. Five days post inoculation mice were transplanted with $5*10^5$ *in vitro* generated either mock-infected or $5*10^5$ EBOV-infected moDCs from one healthy donor. At the same time, mice from each group received i.p. either PBS or 10 mg/kg antibody treatment. Analytes were measured through Luminex multiplex assay in plasma. A) Heatmap shows levels of indicated

chemokines and cytokines in plasma on their respective day of death. Collected data was analyzed using min-max normalization, which normalized concentrations between 1 and 0. B) Concentrations of selected analytes are shown in EBOV-infected control avatar mice without (grey dots) or with (black dots) antibody treatment, and in EBOV-infected survivor cell-transplanted avatar mice without (grey cubes) or with (black cubes) antibody treatment. Statistical significance was analyzed using nonparametric Mann-Whitney U test. Levels of significance were interpreted as follows: NS (not significant) $p > 0.05$, * $p \leq 0.05$, ** $p \leq 0.01$, *** $p \leq 0.001$, and **** $p \leq 0.0001$.

5. Discussion

EBOV, the causative agent of EVD, causes sporadic epidemics in West Africa with a mortality of up to 90%. Due to the lack of patient samples and EBOV considered as a BSL4 pathogen, the immune response to EBOV infection and its influence on EVD pathophysiology, is still not fully understood. What is known is that DCs as well as EBOV-specific T cells play an important role in pathogenesis and immunity.

The goal of this thesis was to develop a humanized mouse model susceptible to EVD based on the sequential transplantation of human PBLs and moDCs from individual donors in HLA-A2-transgenic NSG mice (avatar mice), which could retain the immunological memory of its donor. With the aid of this model the contribution of DC-T cell crosstalk to EVD pathogenesis was dissected. Furthermore, the immune response during EBOV infection was investigated in avatar mice, and in the end the protective function of EBOV-specific immunological memory from EVD survivor was evaluated.

5.1 Establishment of a donor-specific humanized mouse model susceptible to EVD

Several humanized mouse models for EBOV have been developed in recent years since the generation of the NSG triple knockout mice with severe defects in innate and adaptive immunity (Shultz et al., 2005). This facilitates the engraftment of human cells, which can be done either by using administration of hematopoietic stem cells or mature PBMCs. In filovirus research, three different platforms based on the engraftment of human hematopoietic stem cells (HSC) have been developed and extensively used to study mainly filovirus pathogenesis (Bird et al., 2015; Lüdtke et al., 2015; Spengler et al., 2016; Sprengler et al., 2017).

They recapitulate human case fatality rates and several important features of human EVD, in particular high viremia, elevated AST levels, and hypercytokinemia. A caveat of these models is that they typically require transplantation of HSCs and therefore do not retain any memory information. Especially, the huNSG-A2 model, that was developed in our laboratory has poor T cell development due to the lack of thymic T cell selection (Lüdtke et al., 2015).

To establish a humanized mouse platform, that enables the characterization of DC and T cell interaction, which plays a central role in viral hemorrhagic fevers, we adapted a protocol by Harui and colleagues (Harui et al., 2011). In NSG mice transgenic for human HLA-A2 transplanted with human PBLs from HLA-A2 positive donors, they could induce antigen-specific T cells by inoculating these mice with *ex vivo* generated moDCs loaded with the respective antigen. As it has been shown in previous studies moDCs can be infected with EBOV *in vitro* (Mahanty et al., 2003b; Bosio et al., 2003). Furthermore, certain DCs play an important role in virus dissemination within the host (Lüdtke et al., 2017). Preliminary work from my master thesis elucidated that the engraftment consisted of up to 95% of T cells in blood predominantly with an effector memory phenotype already 10 days post inoculation and inclined to nearly 100% on day 28.

This study is the first to use avatar mice in the context of WT EBOV infection. Bradfute and colleagues already infected mice transplanted with PBLs with maEBOV in 2012. They were able to show that human lymphocytes underwent apoptosis and that several human cytokines were increased in infected animals (Bradfute et al., 2012). However, this model was not used in further studies. When *in vitro* generated moDCs were introduced, that were infected *ex vivo* with EBOV, from the same donor into avatar mice 5 days post PBL administration, it turned out very quickly that these were highly susceptible to EVD. EBOV-infected avatar mice were highly viremic, exhibited high viral titers in several organs, and high AST levels. The infection was 100% lethal. Especially high viremia and high AST levels were characterized as a marker for poor outcome during human EVD (Vernet et al., 2017). Furthermore, several pathological symptoms, which can also be found in human EVD, were also reflected in this mouse model, such as liver steatosis and hemorrhage, which appeared in form of blood found in urine as well as in stool. Moreover, we noticed that the disease progression was varying between donors but was always accompanied by rapid weight loss and severe reduction in body temperature (hypothermia).

Through these experiments, it could be shown that PBLs and DCs are already sufficient to induce EVD in avatar mice and that they play a significant role in EVD pathophysiology. This is consistent with studies in EVD patients and non-human primates. Studies by Speranza and colleagues have shown that disease severity is associated with altered expression of genes related to T cell and DC function (Speranza, et al., 2018a; Speranza, et al., 2018b). Furthermore, data from acute EVD

patients during outbreaks in Gabon in 1996 and the West African pandemic indicated that dysregulation of T cell immunity is associated with severe EVD (Ruibal et al., 2016; Baize et al., 1999).

The rate of loss of body weight and body temperature in EBOV-infected avatar mice were also depended on the respective donor. Human donor variability was already demonstrated in BLT mice infected with EBOV by Bird and colleagues (Bird et al., 2016). They argued that this feature might be perceived as a drawback since it creates high variability within the data. On the other hand, this could also be an advantage since it represents the variability present in the human population. In fact, for EVD it seems that specific T cell clonality may have an effect on the severity of the disease. During the 2013 – 2016 outbreak it was demonstrated that a high T cell receptor diversity was correlated with survival (Speranza et al., 2018). This indicates that avatar mice could help to better understand correlates of protection of EVD.

So far avatar mice reflected crucial aspects of EBOV infection resulting in EVD, consequently we wondered how infection with other another Ebola virus would affect this model. HuNSGA2 mice have been recently shown to successfully recapitulate human case fatality rates of different members of the *Ebolavirus* family (Escudero-Perez et al., 2019). We therefore also generated avatar mice engineered with RESTV. Mice lost weight, showed signs of disease, and 40% succumbed to disease. These results were in concordance with the results from RESTV infection in the previously mentioned study by Escudero et al. Moreover, a delay in RESTV viremia with respect to that of EBOV was demonstrated, which has been already shown in huNSGA2 mice (Escudero et al., 2019). This indicated that avatar mice are well suited to study pathogenesis of other Ebola viruses.

Avatar mice infected with LASV were also generated, as it has been shown that LASV also infects moDCs *in vitro* and T cell activation plays a major role in pathology (Oestereich et al., 2016; Port et al., 2020), but the mice survived the infection and showed no symptoms despite the presence of viremia and viral titers in organs. Interestingly, LASV-infected mice revealed high viral titers especially in the lung comparable to those in lethally EBOV-infected mice. Unfortunately, to date, there are no data on asymptomatic or mild-progression Lassa Fever cases in humans or in NHP models with which we can compare our data. Nevertheless, these results indicate that despite the described role of T cells in Lassa fever immunopathology, other immune cells beyond T cell – DC crosstalk might be required to recapitulate severe disease in

avatar mice. Most recent epidemiological data of LASV outbreaks also demonstrated that only 20% of Lassa fever cases develop symptoms and the infection with LASV seems to be less pathogenic for humans than for example EBOV (WHO. Lassa fever. *World Health Organization* https://www.who.int/health-topics/lassa-fever#tab=tab_1 ; 10.10.2023).

It can be assumed that with the help of the postulated mouse model, the role of T cells and DCs regarding pathology can be investigated for other viral infections. In this respect, Marburg viruses would suitable candidates for testing infection in avatar mice since they are able to infect DCs in a similar way to Ebola viruses (Bosio et al., 2003). In addition, MARV is also highly pathogenic for humans with a case fatality rate of up to 90% (https://www.cdc.gov/vhf/marburg/symptoms/index.html; 10.10.2023).

5.2 DC-TCR interaction is important

Previous studies have suggested that DCs and resident macrophages are primary targets of EBOV infection and migratory DCs are likely responsible for virus dissemination from the initial infection sites to the body (Lüdtke et al., 2017). One advantage of avatar mice was supposed to facilitate manipulating of the DC fraction to further characterize DC – T cell crosstalk and the influence of EBOV pathogenesis.

First, avatar mice were inoculated with different amounts of EBOV-infected moDCs and demonstrated that disease severity correlated with the dose of EBOV-infected moDCs. Reducing the number of EBOV-infected moDCs reduced morbidity and mortality in avatar mice. Moreover, this demonstrated that the DC fraction really influences disease progression and can easily be manipulated in avatar mice. It strengthens the role of DCs as “vessels” for infectious EBOV. So far, in human studies it could only be assumed that EBOV migrates through the body with the help of the migratory capacity of certain DC subsets. It was demonstrated that CD16+ monocytes were reduced in blood during acute EBOV infection in humans, but it is not proven that they were extravasating out of the blood vessels or were lost due to the infection with EBOV (Lüdtke et al., 2016; McElroy et al., 2020). A study in mice could identify alveolar macrophages, cDCs, inflammatory monocytes as viral targets *in vivo* (Lüdtke et al., 2017). This study hypothesized that due to the migratory capacity of these cell types, the virus can disseminate through the host. Finally, a sublethal humanized mouse

model for EVD could be generated, that facilitates the finding of more human correlates of survival or death.

The interaction between DCs and T cells or their dysfunction, appears to be a major driver of EVD pathogenesis and survival. To prove that both cell fractions are necessary to recapitulate EVD, NSG mice were infected without prior transplantation of PBLs with EBOV-infected moDCs. Despite the presence of virus titers, none of the infected animals showed any symptoms. Weight, body temperature and serum ASTs showed no measurable differences compared to non-infected animals. The lack of PBLs in the system was sufficient to abrogate all symptomatology in avatar mice. Our data are consistent with human clinical data demonstrating that severe EVD is associated with high levels of T cell activation and a loss of function in fatal cases (Ruibal et al., 2016; McElroy et al., 2015).

DC and T cell interaction is orchestrated through MHC and TCR interaction. MHC molecules are highly polymorphic ensuring a crucial role in self and antigen recognition. If the HLA type of the APC does not match that of the T cell donor, this interaction is disrupted. This concept was used to further investigate the mechanisms of crosstalk between DCs and T cells. Therefore, pathogenesis of NSG mice transplanted with HLA-A2 PBLs and infected either with HLA-A2-matched EBOV-infected moDCs or with moDCs from a non-HLA-A2 expressing donor was compared. Despite similar levels of viremia 80% of HLA-TCR-mismatched avatar mice survived. This indicated that the role of T cells in pathogenesis is dependent on TCR activation by cognate HLA-peptide complexes presented by DCs.

Taken together, these findings indicated that, in avatar mice, lethal EBOV infection can be achieved by transplantation of both huPBLs and DCs, but the severity of the model is dependent on HLA-TCR interactions. Furthermore, they provide a platform to manipulate the DC input so that other myeloid cells could also be evaluated for their role in EVD pathogenesis and viral dissemination. One experiment using a MUTZ-3 cell line was performed and these cells were derived into Langerin-expressing DCs and DC-SIGN-expressing moDCs. In this experiment, however, there was no difference in disease progression and outcome. This could be due to the fact that these cells are very heterogenous after differentiation (Masterson et al., 2002). MUTZ-3 cells would have to be sorted prior for Langerin+ or DC-SIGN-expression to ensure pure cell populations. It has been suggested in animal experiments that Langerin+ DCs were not infected with EBOV *in vivo* (Lüdtke et al., 2017).

5.3 Immune response in avatar mice

During the past decade the immune response during EVD in humans could be investigated more in depth due to better infrastructure during outbreak responses. These findings could be translated into therapeutics if better characterized. Therefore, the immune response in avatar mice during EBOV infection was analyzed to evaluate whether this model is suitable to study these different aspects.

Using flow cytometry, percentages of human cells in mock-infected and EBOV-infected avatar mice were compared. Percentages of human cells in both groups were similar until day 10 post infection. From this point EBOV-infected avatar mice showed lower levels of CD45+ cells in peripheral blood and lung. One observation that has been made in early outbreaks was that lymphocytes undergo apoptosis in fatal human EVD and is considered as a hallmark regarding T cell response during EBOV infection and affects circulating bystander $CD4^+$ and $CD8^+$ T cells in peripheral blood. The main triggers are presumably massive, uncontrolled release of pro-inflammatory mediators (cytokine storm) by DCs, macrophages, and monocytes, and poor DC function as a result from direct infection of the latter cells (Baize et al., 1999; Geisbert et al., 2000; Reed et al., 2004; Sanchez et al., 2004; Wauquier et al., 2010b).

From this data, it cannot be deducted if cells were apoptotic, or the infection inhibits replication of human cells in the model. Another explanation could be that cell migrate to organs that were not analyzed. In fact, the data from spleen was not entirely clear and displayed a trend towards a slight increase in human cells, but with high variability. Additional experiments with higher sample sizes examining more organs could clarify cell migration. Moreover, so-called “homing makers” could be measured using flow cytometry. These are expressed on T cells and mediate their dissemination to specific tissues and the sites of infection (Sackstein et al., 2017). Transcriptional analysis of samples from EVD samples revealed a different homing profile among fatal and survivor cases (Speranza et al., 2018). While in survivor samples expression of homing factors mediating T cells to the site of infection (CCL5/RANTES) was detected, analysis of fatal samples revealed high expression of the gut mucosa homing factor β7-integrin (Parra et al., 2014; Rott et al., 1997). Consequently, the gut would a good candidate to further investigate the migration of human T cells in avatar mice.

To also test whether replication is inhibited, or cells display an apoptotic phenotype, replication markers such as Ki67 and apoptotic markers [TRAIL (tumor necrosis factor-related apoptosis-inducing ligand), NO (nitric oxide) release, FasR] could be included in the analysis. The mechanistical background of lymphocyte death in human EVD lymphopenia is still debated. It is assumed that two mechanisms are involved. On the one hand the extrinsic apoptotic pathway through FasL/FasR receptor binding and the upregulation of TNF production might play a big role. On the other hand, the intrinsic pathway caused by viral induced damage of surrounding tissue might also be important (Geisbert et al., 2003b; Bradfute et al., 2010; Bradley et al., 2008; Geisbert et al., 2000; Wauqier et al., 2010; McElroy et al., 2015).

A Luminex-based assay to measure chemokines and cytokine release in plasma of mock-infected and EBOV-infected avatar mice was also performed. In fact, a trend was detected that pro-inflammatory cytokines and chemokines were upregulated in EBOV-infected animals, namely MIP1a and MIP1b, IP10, E-Selectin, and PECAM1 among others. E-Selectin and PECAM1 are associated with endothelial activation coagulation and were already shown to be up-regulated in severe EVD (McElroy et al., 2016; Kerber et al., 2018). Especially, IP10 can be associated with apoptosis. It is produced by various cell types (leukocytes, neutrophils, eosinophils, monocytes, epithelial, endothelial, and stromal cells, and keratinocytes) during viral infection (Dyer et al., 2009; Luster & Ravetch, 1987). Activated T and B lymphocytes express the CXCR3 receptor which can be activated by interaction with IP-10 and the interaction can then induce apoptosis among other things in these cells (Loetscher et al., 1996; Sallusto et al., 1998). In human EVD studies it also was upregulated in fatal cases (Kerber et al., 2018). This also applies to the pro-inflammatory chemokines MIP1a and MIP1b (Ruibal et al., 2016, Kerber et al., 2018; McElroy et al., 2016). They play an important role in pathology upon viral infections. They are involved in the recruitment of eosinophils and basophils to the site of infection. Their degranulation can cause tissue damage (Garofalo et al., 1992).

In human EVD high activation of T cells in both fatal cases and survivors could be demonstrated, but despite highly activated T cells only in survivors EBOV-specific T cells could be detected (Ruibal et al., 2016; McElroy et al., 2015). Therefore, T cell activation was also tested in avatar mice. Mock-infected mice were compared to EBOV-infected groups to see if avatar mice could help to better understand the underlying mechanisms. Even though a high basal activation in mock-infected mice

was observed, a trend was detected that EBOV-infected avatar mice displayed an even higher activated T cell phenotype.

One possible consequence of activation is a reversible phenomenon called “T cell exhaustion” rendering T cells ineffective and finally apoptotic. “Exhausted” T cells upregulate immune checkpoint molecules such as CTLA-4, PD-1, TIM-3, or LAG-3. Furthermore, they typically show impaired effector functions, poor recall responses, show clear differences on the transcriptional level compared to effector memory T cells, and more important fail to reach antigen-independent memory T cell status (Schietinger & Greenberg, 2014; Wherry, 2011). Under normal circumstances they function as immunological brakes limiting immunopathology (Waterhouse et al., 1995), but certain cancer types (Currie et al., 2009; Mao et al., 2010; H. Yu et al., 2015) and especially viruses causing chronic infections developed immune evasion mechanisms exploiting these molecules leading to dysfunctional T cells (Crawford & Wherry, 2009; Guidotti & Chisari, 2006; Kaufmann et al., 2007). Therefore, blockage of these molecules, especially PD-1 and CTLA-4, using so-called immune checkpoint inhibitors was studied extensively for the treatment of melanoma among others and resulted in their approval as cancer therapeutic (Balar et al., 2017; Rittmeyer et al., 2017; Robert et al., 2015). During fatal EVD it was also observed that T cell expressed higher levels of PD-1 and CTLA-4 than patients that cleared the virus (Ruibal et al., 2016; McElroy et al., 2015). Consequently, avatar mice were evaluated upon their PD-1 and CTLA-4 expression but were not able to detect significant differences between mock-infected and EBOV-infected avatar mice. Unfortunately, this model cannot be used to test those very inhibitors. Nevertheless, this therapeutic approach should be considered as a possible treatment of EVD. Currently, possibilities using immune checkpoint inhibitors around chronic viral infections such as HIV (Human immunodeficiency virus), HBV (hepatitis B virus) and HCV (hepatitis C virus) are being investigated (Fuller et al., 2013; Gardiner et al., 2013; Hagiwara et al., 2022). In one study, a HIV+ patient was treated for metastatic melanoma with Ipilimumab (a CTLA-4 inhibitor) resulting in the reactivation of latent HIV-infected CD4+ T cells. In turn, these could be detected by the immune system and removed (Wightman et al., 2015). In another trial with an anti-PD-L1 antibody in HIV^+ patients, HIV-specific T cells were activated after treatment (Gay et al., 2017). The upregulation of these markers could not only be detected in chronic viral infections but is also observed during acute influenza infections. PD-L1 is upregulated already within the first 24 h post infection in human primary airway epithelial cells (McNally et al., 2013). The upregulation of CTLA-4 on CD8+ T cells could also be correlated to reduced T-cell activation and influenza encephalopathy

(Ayukawa et al., 2004). So far, clinical studies with immune checkpoint inhibitors have not been initiated.

Moreover, antigen-specific T cell formation was investigated after EBOV infection in surviving mice from the dose experiments. A tetramer specific for the HLA-A2-restricted peptide FLSFASLFL was used that has been shown to be able to detect NP-specific T cells during the West African pandemic (Ruibal et al., 2016). It was not possible to detect antigen-specific T cell using this dextramer. This might be simply due to the donor so that EBOV-specific T cells specific for this peptide could not developed. Another reason could be that the pDCs are missing in avatar mice. This specific DC sub population are important type I IFN producers and can present antigens to activate adaptive immunity (Swiecki et al., 2015). Strikingly these cells are not susceptible to EBOV infection and therefore their functions are not affected by the virus in contrast to for example moDCs (Leung et al., 2011a). *In vitro* experiments showed as well that VP35, which demonstrates IFN-antagonistic activity, is not able to inhibit IFNa production by pDCs (Leung et al., 2011b). McElroy and colleagues demonstrated in four patients that were treated in the US and survived EVD that pDCs upregulated CD38 and therefore displayed an activated phenotype (McElroy et al., 2020). They hypothesize that these cells were active and functional during EVD in these four surviving patients. So far, it was not investigated in fatal cases if this cell population is somehow affected. Nevertheless, it could be interesting to investigate whether this cell type is present at all in avatar mice. One possible hypothesis would be that these cells are missing or only very rare since T cell mostly repopulate in avatar mice, which could be a reason why we have no antigen-specific T cells. Harui et al. demonstrated that it is possible to generate antigen-specific T cells with the help of adoptively transferred moDCs (Harui et al., 2011), but since it has already been demonstrated *in vitro* that EBOV infection affects their priming functions it might be possible that these are not sufficient to prime T cells in our experimental set up. Another possible explanation Another plausible explanation for the lack of development of antigen-specific T cells could simply be the predominant hyperactivated, exhausted phenotype.

Dissecting the immune response to EVD with its different aspects, how they interplay, and their underlying mechanism would be a tremendous opportunity for new therapeutic approaches. In summary, avatar mice recapitulate the human immune response to some extent. Differences in T cell activation was observed in EBOV-

infected mice as well as chemokine and cytokine production. One limitation of the conducted experiment is, of course, the low sample size of three animals per group.

However, it is also clear that the avatar model itself has its drawbacks due to the xenotransplantation of mature human PBLs into NSG mice. These mature immune cells, which we have shown to be highly activated independently of infection, act against the host. This condition, known as graft-versus-host disease (GvHD), not only limits the model by interfering with the immune response, but also limits the lifespan of mice transplanted with human mature lymphocytes. Avatar mice have therefore been used as a model to study GvHD (Ali et al., 2012; Ehx et al., 2018; King et al., 2009). King and colleagues showed that the underlying mechanisms of GvHD involve the interaction between human PBMCs and the host MHC I and II molecules (King et al., 2009). In their study they showed that MHC-deficiency in their recipient NSG mice showed a delayed onset of GvHD using MHC knockout NSG mice. There are already strains available that are depleted of murine HLA (NSG-(K^bD^b)^{null} and NOD *scid Il2ry*^{null} *B2m*^{null}) and are also available transgenic for human HLA molecules (NSG-HLA-A2/HHD) (Covassin et al., 2013; King et al., 2009; Shultz et al., 2010). Using these mouse strains could improve the avatar model by reducing human cell activation and prolonging the lifespan of these mice. Another approach could be to deplete the cells that drive GvHD before transplanting human cells into mice. Several studies in mouse models using BALB/c mice as recipient mice transplanted with cells from C57BL/6 mice (Chen et al., 2004; Dutt et al., 2007) or other laboratory mouse strains (Anderson et al., 2003) have shown that naïve T cells play a major role in GvHD. Indeed, depletion of this cell fraction actually resulted in a delayed onset of GvHD. In the case of humanized mice, Ishikawa and colleagues achieved similar results by depleting naïve CD4+ T cells in human PBMCs before injecting them into NSG mice (Y. Ishikawa et al., 2014). This also had a positive effect on the maintenance and functionality of B cells in these mice.

5.4 Evaluation of EBOV-specific immunological memory in avatar mice

While the innate immune response to EBOV infection most likely plays an important role in controlling early EBOV replication, the adaptive immune response seems to be the main driving factor for viral clearance and recovery from EVD. Properly regulated humoral and cellular immune responses including the generation of antigen-specific cells are associated with EVD survival (Ruibal et al., 2016; Speranza et al., 2018). The advantage of avatar mice is that they retain the immunological memory of the respective donor. It was therefore speculated that avatar mice could be used to evaluate whether pre-existing immunity would provide protection against an EBOV challenge.

To study different aspects of the immunological memory PBMCS and plasma samples from EVD survivors from the 2013 – 2016 West Africa outbreak were utilized. These samples were already analyzed regarding their T cell response to GP. Only samples were chosen that elucidated a high IFNy release upon restimulation (Tipton et al., 2021). In the first step avatar mice received only PBLs from EVD survivors and HLA-matched infected DCs. The mice lost weight rapidly, displayed elevated serum AST levels, and succumbed to the infection, which indicated that survivor PBLs were not sufficient to rescue the mice. Nevertheless, these animals revealed significantly reduced organ titers in liver, kidney, spleen, and heart. Interestingly, mice transplanted with PBLs from EVD survivors showed reduced T cell activation in their CD4+ compartment. This could indicate that bystander T cell activation is reduced and that a more specific T cell response was mounted in these mice but was not enough to protect the animals. Bystander T cell activation has been shown in EVD (Agrati et al., 2016; Bradfute et al., 2010). This also supports the hypothesis that in fatal cases the inflammation associated with EVD may lead to a response from bystander T cell clones rather than EBOV-specific T cell clones, thereby influencing the immunopathology and preventing viral clearance. EVD survivor in contrast tend to mount a highly poly-clonal mainly CD8+ T cell responses during the acute phase of EVD (McElroy et al., 2015; Ruibal et al., 2016; Speranza, Ruibal, et al., 2018; Thom et al., 2021). These might be reactivated during challenge in avatar mice.

Since the inoculation of survivor PBLs was not sufficient to rescue avatar mice, the next step was to inoculate the mice with antibodies isolated from high and low

neutralizing survivor plasma. Interestingly, only the combination of survivor PBLs and survivor antibodies or mAB KZ52 could rescue avatar mice from succumbing to EVD. The transfer of IgG alone had no influence on disease progression in avatar mice. A trial with convalescent plasma in West Africa already indicated that both antibody and T cell responses might be important in protection in humans. Here, a significant clinical benefit or a correlation between neutralization and efficacy could not be detected (van Griensven et al., 2016). In addition, the neutralizing capacity of the antibodies were not crucial on the outcome of the infection. Studies already suggested that effective humoral immune responses against EBOV may require NAB as well as other antibody functions mediated by the Fc receptor (Davis et al., 2019b; Ehrhardt et al., 2019; Gunn et al., 2021; Koch et al., 2020). EVD survivor antibodies display in addition to neutralizing capacity also ADCC and ADCP (antibody-dependent cellular phagocytosis) functions (Koch et al., 2020). In fact, Antibody cocktails for EVD treatment utilized in post exposure therapy are combinations of neutralizing and non-neutralizing antibodies (Wec et al., 2019).

This data could show for the first time *in vivo* that humoral and cellular components from EVD survivors together still have, at least in our avatar model, protective functions, and rescued mice from otherwise lethal EBOV infection. Of course, one must be careful to translate this into humans and involve EVD survivors as frontline workers in new outbreaks. Thom and colleagues revealed in an observational cohort study focusing on longitudinal antibody and T cell data in EVD survivors that in a small percentage the humoral immune response was absent. They suggest that this might be an explanation of the few registered re-infection or re-activation cases (Thom et al. 2021).

Nevertheless, avatar mice could help to further dissect the correlates of protection against EVD and especially the role of CD4+ and CD8+ T cells. In mice it was demonstrated that the depletion of CD4 cells had no impact on the survival of the mice while CD8 depleted mice succumbed to disease (Gupta et al. 2004; Ldtke et al., 2017) indicating that CD8 T cells play a major role in protection against EVD. The already mentioned study by Tipton and colleagues, who had the opportunity to evaluate long-term T cell responses regarding their epitope specificity also revealed that EBOV-specific T cells were CD8 T cell dominated. Avatar mice could be generated with only CD8+ or CD4+ T cells from EVD survivors and inoculated with antibodies to evaluate the protectivity of these T cell fractions. Moreover, in this study they identified a motif with EBOV GP, which elicited a CD8+ T cell response in EVD survivors. After enriching

this specific T cell clone *in vitro* avatar mice could provide an excellent platform for evaluating protectivity of those cells. Nevertheless, other studies have shown that the majority of EBOV-specific T cells are directed against NP epitopes, but so far this was not studied in detail (Sakabe et al., 2018; McElroy et al., 2015).

The dissection of T cell and B cell memory of EVD survivors including finding antibody functions and identifying immunodominant T cell epitopes, which are correlates of survival, could have major implications on vaccine development. With the aid of this data vaccines could be generated that not only display a strong humoral immunity but also specifically induce T cell immunity against immunodominant epitopes. Moreover, avatar mice could also be utilized to test whether these would also be protective against other *Ebolavirus* species.

5.5 Summary and Outlook

This study described the development of a new humanized mouse model to study EVD. NSG mice transgenic for human HLA-A2 transplanted with HLA-A2+ human PBLs and EBOV-infected moDCs infected animals showed drastic weight loss, high AST levels, high viremia, and hemorrhagic symptoms. The course of infection was dependent on the donor. Furthermore, it was demonstrated that this mouse platform was suitable to study other Ebola virus species (RESTV). RESTV infection, which has not been recorded in humans so far, of avatar mice displayed a similar disease progression as recently shown in another humanized mouse model. In contrast, avatar mice infected with LASV, also a hemorrhagic fever virus, did not show signs of disease, but a high viral load in the lung. Furthermore, DC- and T-cell interaction played a major role in EVD pathogenesis. It was demonstrated that NSG mice transplanted with EBOV-infected moDCs alone did not develop EVD, and that disrupting MHC-TCR interaction through utilizing HLA-mismatched moDCs. This highlighted that the only necessary cell types for developing EVD are infected moDCs and the matching PBLs fraction in our system. When dissecting the immune response, EBOV-infected avatar mice showed elevated pro-inflammatory cytokine levels, especially IP10, MIP1α, and MIPβ, and a higher percentage of activated T cells when compared to mock-infected mice. Furthermore, the repopulation of human cells was lower in EBOV-infected mice compared to mock-infected avatar mice. Moreover, these experiments showed the limitations of this mouse model to study immune responses due to the interaction of the engraftment and the host cells. The last part of this study showed the big capacity

of this model to study correlates of protection. Avatar mice transplanted with PBLs from EVD survivors had a decreased T cell activation and reduced viral titers, but still succumbed to the disease with a slight delay. When IgG isolated from EVD survivor plasma were additionally administered to avatar mice transplanted with EVD survivor PBLs, 100% of mice survived the challenge with EBOV.

These experiments suggest that avatar mice will be a great opportunity to dissect the role of T cells and DCs as well as the correlates of protection to EBOV. Moreover, other viral infections specifically viruses that also infect DCs and where T cells play a big role in pathogenesis can possibly be studied. MARV could be a suitable candidate for this model since it is also highly pathogenic for humans and infects moDCs (Bosio et al., 2003).

This model could also provide more information about the role of other DCs for example pDCs. *In vitro* infection of pDCs with EBOV showed that these were not susceptible and that their functions was not diminished by the virus (Swiecki et al., 2015; Leung et al., 2011a). PDCs could be sorted and utilized instead of moDCs in this model to evaluate their role in virus dissemination and pathogenesis during EBOV infection.

For future experiments transcriptome analysis on bulk human T cells or single cell level of different organs at different time points would also help to gain a better understanding of the immune response in avatar mice. Using flow cytometry so far, the differences that were detected were not significant. Gene expression analysis could help to decipher more differences between mock- and EBOV-infected avatar mice and also answer open questions for example whether T cell proliferation is affected by the infection. It could also help to understand the mechanisms behind the development of hemorrhagic symptoms in the intestines, which was not investigated in this study.

So far, avatar mice were only infected through retroorbital administration of EBOV-infected moDCs so that they directly enter the peripheral blood stream. The natural route of infection for EBOV is through direct contact with mucosal tissues or through skin lesions (Feldman & Geisbert, 2011). For this reason, intranasal infection is widely used in mouse models for EVD (Lüdtke et al., 2015, 2017). In fact, protocols to inoculate mice intranasally with different subsets of DCs have been developed. For example, it has been shown that murine antigen-loaded moDCs inoculated intranasally

in BALB/c mice could induce antigen-specific T cell response in lymphoid organs and cell could be trafficked in mice (Vilekar et al., 2010). This demonstrated that also with intranasal administration of moDCs a DC-T-cell interaction could be induced. This might be as well interesting to address in avatar mice to assess differences in lethality of EVD and dissemination of moDCs.

It was already demonstrated in avatar mice that EBOV-specific T cell memory and IgG isolated from EVD survivor was required for survival. These mice could provide a platform to evaluate EBOV-specific T cells clones or the combination of different T cell clones specific for immunodominant epitopes. For this T cell clones could be expanded *in vitro* and tested for their functionality. Avatar mice could be inoculated with strong clones and tested *in vivo* in combination with plasma IgG from EVD survivors. With this knowledge about naturally acquired immune responses and their protective functions vaccines could be developed including induction of a very specific T cell response.

One major limitation of this mouse model was the impact of GvHD on the T cell response and therefore it would be of big interest to improve the avatar model in this regard. Other studies utilized murine MHC-deficient and human HLA-A2 expressing NSG mice for the transplantation of human PBLs. This resulted in delayed onset of GvHD (Covassin et al., 2013; King et al., 2009; Shultz et al., 2010). Therefore, these mouse strains should be tested in the future for the avatar model generated in this study. It should also be investigated whether this would affect the activation and exhaustion of the transplanted human cells.

6. Material

6.1 General consumables

General consumables were obtained from Eppendorf, Sarstedt, Greiner Bio One, Quiagen, Thermo Scientific, Miltenyi, Sigma-Aldrich, Carl Roth and StemCell Technologies. Specific equipment is listed below:

Item	Manufacturer
Syringe 1 ml	Braun
Syringe 5 ml	Braun
Insulin Syringe	Braun
Needles	Braun
Tuberculin syringe	Braun
Surgical Blades (Carbon Steel Sterile No. 11)	Swann-Morton
Microvette z-Gel tubes	Hartmann
Microvette LiHep-Gel tubes	Sarstedt
EDTA tubes	Sarstedt

6.2 Viruses

Infections with EBOV (Ebola virus *H.sapiens*-tc/COD/1976/Yambuku-Mayinga) were conducted under BSL-4 containment by trained personnel at the Bernhard Nocht Institute, Hamburg. In one experiment recombinant wild-type Lassa virus (LASV Ba366) and Reston Ebola virus (RESTV, Pennsylvania strain) were used.

6.3 Cell lines

Cell line	Application
VeroE6 cells (African green monkey kidney cells)	Virus amplification Immunofluorescence Assay
MUTZ3 cell line	Infection

6.4 Mouse colonies

For reconstitution of mice with human peripheral blood lymphocytes highly immunodeficient mouse strains are required. In this study we used 5 – 11–week-old NOD.Cg-*Prkdc*^{scid} *Il2rg*^{tm1Wjl} Tg(HLA-A2.1) (NSG) mice from Jackson Laboratories (Bar Harbor, ME, USA). They were housed in individually ventilated cages (IVCs) and provided with autoclaved food, bedding, and acidified water. Due to lack of lymphocytes (B cells, T cells, NK cells) and deficiencies in cytokine signalling pathways engraftment with human cells was facilitated within these mice (Schultz et al., 2005; Ishikawa et al., 2005). Mouse colonies were maintained in the animal housing facility at HPI, Hamburg. All experiments were performed according to German animal protection law under the permit N043/2019.

6.5 Chemicals and reagents

Item	Manufacturer
β-Mercaptoethanol	Roth
Baytril	Bayer
Biocoll	Biochrom
Bovine serum albumin (BSA)	Sigma
Bromphenol blue	
Dulbecco's Modiefied Eagle Medium (DMEM)	Gibco
Dimythylsulfoxid (DMSO)	Roth
DNAseI	Sigma
Ethylenediaminetetra acetic acid (EDTA)	Roth
Fetal calf serum (FCS)	Biochrom
Gentamycin	Roth
Glycerol	Roth
Glutamine 200 mM	PAA
GolgiPlug™ Protein Transport Inhibitor	BD Bioscience
HEPES	Roth
Human Serum	Merck Millipore
Ionomycin	Sigma
Isoflurane (inhalation anaesthetic)	AbbVie Limited
L-glutamine (200 mM)	Gibco
Methanol	Roth
Paraformaldehyde (PFA)	Sigma
Penicillin / Streptomycin (P/S)	Gibco
Phorbol 12-myristate 13-acetate (PMA)	Sigma-Aldrich

Dulbecco's Phosphate Buffered Saline (PBS)	Sigma
Penicillin / Streptamycin	Gibco
Recombinant human GM-CSF	PeproTech
Recombinant human interleukin 4 (IL-4)	PeproTech
Roswell Park Memorial Institute (RPMI) 1640	Gibco
Sodium azide (NaN_3)	Sigma
Sodium chloride	Roth
Tris	Applichem
Triton X-100	Roth
Trypsin TrypLE™	Gibco
Tween-20	Roth

6.6 Buffers, media, kits

6.6.1 Buffers

MACS buffer……...	PBS
	1% Human serum
	2 mM EDTA
Washing buffer (blood)……	PBS
	0.02% Human serum
	2 mM EDTA
	100 U/ml Pen Strep

6.6.2 Media

Freezing media……	**DMSO**
	10% FCS
Growth Media……..	DMEM
	5% FCS
	100 U/ml Pen Strep
	2 mM L-glutamine
Infection media……	DMEM
	2% FCS
Mutz-3 complete media (100 ml)…….	60 ml MEM-alpha
	20 ml FCS
	20 ml 5637 conditioned media
	1 ml P/S

	1 ml L-glutamine
Mutz-3 Langerhans cell media……..	Mutz-3 complete media
	GM-CSF (100 ng / ml)
	TGF-β (10 ng / ml)
	TNF-α (2.5 ng / ml)
Mutz-3 moDC media……..	Mutz-3 complete media
	GM-CSF (100 ng / ml)
	IL-4 (20 ng / ml)
	TNF-α (2.5 ng / ml)
moDC differentiation media……...	RPMI 1640
	10% Human serum
	500 ng/ml gentamycin
	2 mM L-Glutamine
	100 mg/m IL-4
	200 mg/ml GM-CSF
	2 µM beta-mercaptoethanol

6.6.3 Kits

Reagent	**Manufacturer**
CD14 MicroBeads, human	Miltenyi Biotech
CompBeads	BD Biosciences
Fixation / Permeabilization Solution Kit	BD Biosciences
Fuji DRI-CHEM AST (GOT8) test chips	Fujifilm
ProcartaPlex Mix & Match Human 19-plex	Thermo Fisher Scientific
Zombie Red Fixable Viability Kit	Biolegend

6.7Antibodies

6.7.1 Flow cytometry antibodies

Reactivity	**Antibody**	**Conjugated Fluorophore**	**Clone**	**Manufacturer**
α-human	CCR7	APC	G043H7	Biolegend
α-human	CD14	PE-Texas Red	HCD14	Biolegend
α-human	CD16	PE-Texas Red	3G	Biolegend
α-human	CD19	PE-Texas Red	HIB19	Biolegend
α-human	CD20	PE-Texas Red	2H7	Biolegend

α-human	CD3	APC-Cy7	UCHT1	Biolegend
α-human	CD38	BV785	HIT2	Biolegend
α-human	CD4	BUV395	SK3	BD Biosciences
α-human	CD45	AlexaFluor700	HI30	Biolegend
α-human	CD45RA	PerCP-Cy5.5	HI100	Biolegend
α-human	CD56	PE-Texas Red	HCD56	Biolegend
α-human	CD8	BV650	RPA-T8	Biolegend
α-human	CTLA-4	PE	L3D10	Biolegend
α-human	HLA-DR	PE-Cy7	L243	Biolegend
α-human	HLA-A*0201-FLSFASLFL	PE	Tetramer	Immudex
α-human	HLA-A*0201-FLSFASLFL	APC	Tetramer	Immudex
α-human	PD-1	BV605	EH12-2HT	Biolegend

6.7.2 Other antibodies

Reagent	**Manufacturer**
KZ52 anti-EBOV GP antibody	Absolute Antibodies
Polyclonal mouse α-EBOV antibody	BNITM
Sheep α-mouse IgG peroxidase-conjugated (H+L) antibody	Jackson Immuno Research

6.8 Laboratory Equipment

Instrument	**Manufacturer**
Animal rack	Techniplast
Biosafety animal changing station	Techniplast
Cell counter LUNA-FL	Logos Biosystems
Centrifuge 541SC	Eppendorf
CKX41 microscope	Olympus
Clini Tray	KLINIKA Medical
DRI-CHEM NX500 Chemistry Analyzer	Fuji
Autoclave (bench-top)	Tuttnauer Systec
Class 2 safety cabinet	Kojair
F1-ClipTip (10-100µl)(30-300µl)	Thermo Fisher Scientific
Fast-Prep-24 – Tissue homogenator	mpbio

FlowSafe C-[MaxPro]^3-130 safety cabinet	Berner
Fortessa flow cytometer	BD
Freezer (-20 °C)	Bosch
Freezer (-20 °C) profi line	Liebherr
Fridge	Bosch
Fridge	Liebherr
HydroFlex - Microplate Washers	Tecan
Heracell 150 incubator	Thermo Fisher Scientific
Innova CO-170 incubator	New Brunswick Scientific
IKA Vortex 3	IKA
Infrared light	HT instruments
Isoflurane vaporizer Univentor 410 and inhalator chamber	UNO BV
Luminex™ 200™ Instrument System	Millipore
Microwave	Sharp
Mini Start table centrifuge	VWR
NanoDrop	Thermo Fisher Scientific
Photo scanner Reflection V550	Epson
Pipette (1-2 µl)/-20 µl)), (20-200 µl), (100-1000µl)	Gilson
Plate shaker 3006	GFL
Precision scale PCB	Kern
Red Tube Tailvein Restrainer	Braintree Scientific
Refrigerated centrifuge; swing buckets 15 & 50 ml (Rotina 420R)	Hettich
Refrigerated centrifuge; 1.5 – 2 ml (5417R)	Eppendorf
SpotChem	Axonlab
Thermocouple with rectal probe (BIO-TK8851 & BIO-BRET-3)	Bioseb
Thermomixer 5436	Eppendorf
ThermoMixer C	Eppendorf
TwinGuard freezer	PHCBI
Vortex-genie2	Scientific Industries
Waterbath M20	Lauda

6.9 Software

Name	**Manufacturer**
FlowJo Version 10	BD / FlowJo LLC
GraphPad Prism Version 9	GraphPad
Microsoft Excel 16	Microsoft
Microsoft Word 16	Microsoft

Microsoft PowerPoint 16 (with material from https://smart.servier.com/)	Microsoft
FACS Diva	BD
Mendeley	Mendeley

.

7. Methods

7.1 BSL-4 experiments

Experiments with infectious virus were carried out in the BSL-4 laboratory at the Bernhard Nocht Institute for tropical medicine, Hamburg, Germany.

7.2 Virus amplification

10^6 Vero-E6 cells seeded in 20 ml growth medium in T-75 cm2 flasks and incubated at 37 °C and 5% CO_2 for 24 h. Cells were infected with an MOI of 0.01 in 3 ml of infection medium (DMEM with 2% FCS) and incubated at 37 °C 5% CO_2 for 1 hour. Inoculum was removed, 20 ml growth media was added, and cells were stored at 37 °C and 5% CO_2 for 5 days. After this incubation period supernatant was harvested and centrifuged at 1500 x g for 5 min. The resulting virus stock was aliquoted and stored at -80 °C.

7.3 Focus formation assay

Focus formation assay was utilized for quantification of viral titers in virus cultures and blood or organs of infected animals. 1 x 10^6 Vero-E6 cells were seeded in a 24-well plate in growth media and incubated for 24 hours at 37 °C and 5% CO_2. On the next day samples were harvested or thawed and logarithmic dilutions were prepared in infection medium on 96-well u-bottom plates. Blood was prediluted 1:20 in DMEM. Cell culture media was removed and 200 µl sample dilutions were transferred to the cells without touching the cell layer. 24-well plates were incubated at 37 °C and 5% CO_2 for one hour. The inoculum was removed, cells were covered with overlay medium (2/3 DMEM with 10% FCS and 1/3 methylcellulose) and incubated at 37 °C and 5% CO_2 for 6 days. Cells incubated with LASV were incubated for 5 days. After incubation overlay medium was removed and cells were fixated and inactivated for BSL-4 removal. For this, plates were completely covered with 4% formaldehyde in PBS for 45 min at RT. After fixation, plates were removed from the BSL-4 laboratory and rinsed under running H_2O. For permeabilization, cells were incubated with 0.5% Triton X-100 at RT on a shaker with mild agitation for 30 min and rinsed again under running water. Blocking was obtained by incubation with 10% FCS in PBS on a shaker at RT for 1 hour. Blocking buffer was removed and cells were incubated with primary polyclonal anti-EBOV antibody (1:5000 in PBS with 10% FCS) at RT for 1 hour or at 4 °C

overnight. This was followed by a thorough washing step under running water. In the next step the secondary anti-mouse antibody coupled with HRP (horseradish peroxidase) was added (1:1000 in PBS with 5% FCS) and incubated at RT for 1 hour. For the final detection of the foci, cells were washed with H_2O and incubated with TMB substrate (3,3',5,5'-Tetramethylbenzidine). The resulting blue foci were counted manually.

7.4 Generation of avatar mice

7.4.1 Isolation of lymphocytes from whole blood

Buffy coats from HLA-A2 positive donors were obtained from the transfusion medicine department at the University Hospital Eppendorf. Approval to obtain blood samples from healthy donors was granted by the Medical Ethics committee of Hamburg.

The following steps were performed under sterile conditions. The obtained buffy coats were initially isolated from 500 ml whole blood and still contained erythrocytes residues. Accordingly, cells had to be purified. Buffy coats were collected in flasks and washing buffer was added for a total volume of 750 ml (1:1.5 dilution of initial whole blood) and 35 ml of dilution were carefully layered on 15 ml of biocoll separating solution (Biochrom) in a 50 ml polypropylene tube. This biocoll has a density of 1.077 g/ml and centrifugation at 2000 rpm, 45 min, 20°C at minimal acceleration leads to separation of the blood components. The cell pellet under the biocoll layer contains erythrocytes and granulocytes, whereas peripheral blood mononuclear cells (PBMCs) form the so-called buffy coat on top of the biocoll layer. Plasma forms the topmost layer of the gradient. This separation method is called density gradient centrifugation (Bøyum, 1976). Buffy coats were carefully collected with a pipette, transferred to a 50 ml polypropylene tube, and washed with washing buffer. Cells were centrifuged for 10 min with 1500 rpm at 4 °C. After this step, cell numbers were determined with an automated cell counter (Countess, Invitrogen), isolated PBMCs were cryopreserved in FCS with 10% DMSO or directly used for further experiments.

7.4.2 Separation of $CD14^+$ and $CD14^-$ cells

Magnetic-activated cell sorting is a cell separation method using magnetic beads, which are conjugated with antibodies against cell surface antigens. In a cell suspension the antibody binds to all cells expressing these antigens. The cell

suspension can be transferred to a column, which is attached to a magnetic field. Labelled cells are retained in the column and undesired cells flow through the column. To obtain the cells the column is removed from the magnetic field and subsequently flushed.

For separation of $CD14^+$ and $CD14^-$ cells fresh or thawed PBMCs (section 7.4.1) were washed with PBS, passed through a cell strainer, and counted. For the whole procedure ice cold buffers were used. After centrifugation for 5 min, 4 °C, 1700 g, supernatant was discarded. Cells were resuspended in 80 µl of MACS buffer (PBS, 1% human serum, 2 mM EDTA) per 10^7 total cells. In this case positive selection (meaning that desired cell population stays in the column) was carried out. 20 µl of human CD14 microbeads (Miltenyi Biotec) were added per 10^7 cells and well mixed with the cells. An incubation step of 15 min at 4°C followed. Cells were washed by adding 1 ml of MACS buffer per 10^7 cells, centrifuged for 5 min (1700 rpm, 4 °C), resuspended in 500 µl MACS buffer, and applied into a MACS column (MS column, Miltenyi Biotec) placed in a magnetic field (OctoMACS, Miltenyi Biotec). The column was washed three times with MACS buffer and flow through containing unlabelled $CD14^-$cells was collected in a 15 ml polypropylene tube that was placed in a 50 ml polypropylene tube filled with ice. The column was removed from the magnetic field and placed on a new tube. The $CD14^+$ fraction was eluted in 1 ml MACS buffer. Both cell fractions were counted and either cryopreserved or directly used.

7.4.3 Reconstitution of avatar mice

To adoptively transfer donor-specific PBLs into immunodeficient mice, 10^7 human $CD14^-$ PBLs were resuspended in 20 µl PBS and injected retroorbitally (r.o.) into 5 – 11 weeks old NSG mice. During the whole procedure mice were kept under isoflurane anaesthesia. Recipient mice were transplanted with 50 µl cell suspension intravenously (i.v.) via the retro-orbital sinus. Mice were anesthetized using isoflurane and placed on their ventral side on a heating pad (37 – 38 °C). To avoid injection injures of the experimenter the head was fixed carefully using padded forceps. A tuberculin syringe with little resistance and 30 G-cannula was carefully inserted through the cornea at the inner canthus at a 20 – 40 ° degree until the retro orbital sinus and then the cell suspension was applied. The animals were closely monitored to ensure their wellbeing after reconstitution.

7.4.4 Differentiation of moDCs

(Sallusto & Lanzavecchia, 1994)Dendritic cells (DCs) are the only cell type among antigen-presenting cells that can prime naïve T cells (Banchereau and Steinman, 1998). A particular subset of inflammatory DCs derive from monocyte precursors ($CD14^+$) into immature monocyte-derived dendritic (moDCs) cells during inflammation and are defined phenotypically as $CD14^-$, $CD11c^+$, $HLA\text{-}DR^+$ and $CD86^-$. Generation of moDCs *in vitro* has been established for a long time (Sallusto & Lanzavecchia, 1994) and fulfils the necessity to manipulate DCs *ex vivo*. We have successfully derived moDCs in culture using the following protocol.

Freshly isolated $CD14^+$ cells (section 2.4.2) were cultured at a density of $3*10^6$ cells / ml in DC differentiation medium on a 6-well plate and kept at 37°C, 5% CO_2 for five days. On day 3 half of the medium was replaced with DC medium with doubled cytokine concentration without disturbing the cells. The cells were harvested on day 5 for further experiments.

7.4.5 Mutz-3 cell culture

Mutz-3 cells are a human cell line for cytokine-induced differentiation of dendritic cells. They behave as an immortalized equivalent of $CD34^+$ DC precursors and express human HLA-A2. The cell line can acquire phenotypes consistent with either interstitial- or Langerhans-like DCs through specific cytokine cocktails (Masterson et al., 2002)

MUTZ-3 cells were obtained from Dr. Tanja D. de Grujil (Amsterdam UMC) and were differentiated into interstitial DC-like cells expressing DC-SIGN or Langerhans-like cells expressing Langerin using cytokine-conditioned media as previously described.
For routine passaging of undifferentiated Mutz-3 cells, cells are gently resuspended in each well and collected in 50 ml falcon tubes. After centrifugation at 180 – 200 x g for 6 – 8 min, the supernatant was discarded, and cells were resuspended in 1 – 5 ml Mutz3 complete media for counting. Cells were replated at a density of 1.5×10^5 cells per ml with 1 ml total volume per well on a 24 – well plate and kept for at 37 °C, 5% CO_2 for 3 – 4 days.

For induction of an immature Langerhans cell phenotype cells were harvested as described above, but instead of replacing media with Mutz3-complete media, Langerhans media was used after spinning down. Cells were again seeded at a density of 1.5×10^5 cells / ml. Cytokines were refreshed at day 4 and day 8 of culture

through removing half the media and replacing it with fresh media). Cells were cultured for 10 days total. If cells became adherent over time, ice cold PBS + 0.02% EDTA solution was used for detaching cells before or after infection.

The immature moDC phenotype was induced using moDC media after harvesting. Cells were seeded at a density of 1.5 x 10^5 cells / ml and cultured for 6 – 7 days, refreshing the media as described above on day 3.

7.5 Animal experiments in the BSL-4 laboratory

7.5.1 *In vivo* infection

7.5.1.1 Intranasal infection

Virus stocks were diluted to a concentration of 1 000 PFUs EBOV / 20 µl. Mice were anesthetized using an isoflurane chamber. When breathing slowed down, mice were placed on their backs on a heating mat (37 °C) and virus suspension was administered with a pipette dropwise into the nasal cavity. Mice were then turned on their side and monitored until fully awake.

7.5.1.2 Infection with moDCs

MoDCs were infected *ex vivo* prior to administration into huPBL mice. After five days of culture moDCs were harvested, centrifuged for 10 min at RT 300 x g and washed with PBS to remove serum residues and spun down again. Cells were resuspended in virus stock to reach an MOI of 1 and incubated at 37 °C, 5% CO_2 for one hour. Then the cells were washed again with PBS and adjusted to a concentration of 5 x 10^5 moDCs / 50 µl. Recipient mice were transplanted with 50 µl cell suspension intravenously (i.v.) via the retro-orbital sinus. Mice were anesthetized using isoflurane and placed on their ventral side on a heating pad (37 – 38 °C). To avoid injection injures of the experimenter the head was fixed carefully using padded forceps. A tuberculin syringe with little resistance and 30 G-cannula was carefully inserted through the cornea at the inner canthus at a 20 – 40 ° degree until the retro orbital sinus and then the cell suspension was applied.

7.5.1.3 Monitoring and Scoring

Mice were sacrificed on specific time point as described in the respective experiment or when termination criteria were met. Blood and organs were harvested for analysis of immune cell populations, as well as AST serum levels, viremia, and viral titers. Mice were monitored daily to evaluate weight, temperature, and the outer appearance. Temperature was measured using a rectal probe. Mice were euthanized through an isoflurane overdose followed by cervical dislocation.

7.5.2 Blood draw

To collect small amounts of blood during experiments mice were bled 2 – 3 times from the tail vein. To dilate veins and increase their visibility mice were kept under infrared light for 2 min prior to bleeding. For venipuncture, mice were restrained in a specific mouse restraining device and the lateral vein was punctured with a small scalpel blade. Three drops of whole blood were collected in a heparin tube, subsequently diluted 1:20 in DMEM on a 96-well u-bottom plate, and frozen until titration at – 20 °C. To obtain serum, whole blood was directly collected in serum tubes. These were centrifuged at 12 000 x g for 3 min and stored at – 20 °C until further analysis. Bleeding was stopped by applying pressure with a sterile tissue.

7.5.3 Organ preparation

Viral titers were determined in liver, kidney, spleen, lung, and heart. For this, animals were sacrificed via isoflurane narcosis and cervical dislocation, organs were harvested, and stored at – 80 °C until titration. For processing, organs were thawed, weighted, and transferred into Lysing matrix D tubes filled prefilled with 1 ml DMEM. Organs were homogenized with a FastPrep homogenizer (3 x 30 sec, level 5, 2 x). Tubes were centrifuged at 5 000 x g and then logarithmic dilutions were prepared and frozen at – 80 °C until titration.

7.5.4 Clinical parameters

Levels of ASTs in serum were analysed with a commercial kit and using a Fujifilm machine. Sera were diluted 1:10 or higher (if sample was out of range) with a 0.9% saline solution (v/v). The normal range of AST in humanized mice has been determined as < 200 U/l.

7.5.5 Luminex

Analysis of cytokine concentrations was performed using ProcartaPlex Multiplex Immunoassay magnetic bead panel premix 19 plex according to manufacturer's instructions. The Luminex principle works as following: a sample (in this case serum) is added to a mixture of colour-coded magnetic beads, which are pre-coated with analyte-specific capture antibodies. These antibodies can bind to the analyte of interest if present. In the next step, biotinylated detection antibodies specific for the analytes of interests are added and form an antibody-antigen sandwich. In the end phycoerythrin (PE)-conjugated streptavidin is added and binds to the biotinylated detection antibodies. A dual-laser flow-based detection instrument can read the beads, which can determine on the one hand the analyte and on the other hand the magnitude of the PE-derived signal, which is in direct proportion to the amount of analyte bound.

7.5.5.1 Sample preparation

To analyse cytokine concentrations in serum of avatar mice, samples were thawed and centrifuged for 10 min at maximum speed at RT. Samples were diluted 1:1 with 1 x universal assay buffer (diluted with ddH_2O) and kept on a master plate at -80 °C until assay was performed.

7.5.5.2 Preparation of antigen standards

Antigen standard set vials were centrifuged at 2 000 x g for 10 seconds. 50 µl of 1 x universal buffer was added into 5 different standard set vials, which were gently vortexed for 30 seconds and centrifuged at 2 000 x g for 10 seconds to remove solution from lids and collect content at the bottom of the vials. Afterwards, vials were incubated on ice for 10 more minutes to ensure complete reconstitution. The entire content of one vial was transferred to the sixth antigen standard vial (for this specific kit 6 different standard vials were provided) and the reconstitution steps were repeated. This ensured that the final volume of 250 µl was not exceeded. All standard vials were pooled into one vial, gently vortexed for 30 seconds, and centrifuged at 2 000 x g for 10 seconds. From this pool 4-fold serial dilutions were prepared using PCR 8-tube strips. Standards were prepared as duplicates. 200 µl of the reconstituted antigen standards were pipetted into the first tube of each strip (tube 1), while 50 µl of 1 x universal buffer were added into the remaining empty tubes (tubes 2 – 7). For the first dilution50 µl of the reconstituted antigen standards from tube 1 was transferred into tube 2 and mixed by pipetting up and down for a total of 10 times. 50 µl of the standard mix was transferred from tube 2 into tube 3. These steps were repeated for tubes 3 –

7. Tube 8 received 200 µl 1x universal buffer and served as blank. Dilutions were kept on ice until assay was performed.

7.5.5.3 Assay protocol

After the plate set up was planned, magnetic beads were prepared. For this, the vial with beads was vortexed for 30 seconds and 50 µl of bead solution was added to each well of the plate using a multichannel pipette. Magnetic beads were washed with 1 x wash buffer (10 x wash buffer diluted with ddH_2O) using an automated plate washer (Tecan). After the washing buffer was removed, 25 µl of universal assay buffer (1x) was loaded into each well followed by 25 µl of prepared standards or samples into dedicated wells. For wells assigned as blanks 25 µl of universal assay buffer (1x) was used. The plate was sealed with a provided plate seal, covered with a black microplate lid, and incubated for 30 min at RT at 500 rpm on a shaker, then transferred to 4 °C overnight. After overnight incubation, the plate was placed for 30 min on shaker at 500 rpm. Afterwards, two wash cycles using an automated plate washer were followed by the addition of detection antibody mix (25 µl per well). The Plate was sealed again with a new plate seal, covered with a black lid, and incubated for 30 min on a plate shaker at RT at 500 rpm, followed by 2 x washing with the automated plate washer. The next step included the addition of 50 µl streptavidin-PE (SA-PE) to each well, followed by sealing, covering with the black lid, and incubating for 30 min on a plate shaker at RT at 500 rpm. After that, two more washing cycles were conducted, and the plate was prepared for the final analysis on a Luminex instrument. In this case a Luminex 200 system (Millipore) was used for data acquisition. 120 µl reading buffer was loaded into each well, the plate was sealed with a new seal, covered with the black lid, and incubated for 5 min on a plate shaker at RT for 500 rpm. After removal of plate seal, the plate was run on Luminex instrument.

7.5.6 Sample preparation for flow cytometry

7.5.6.1 Blood

Blood was analysed through flow cytometry after mice have been euthanized. After sacrifice, blood was collected through heart puncture using 1ml U-100 insulin syringes and transferred into EDTA tubes to prevent clotting. To lysing erythrocytes blood was pipetted into a 15 ml falcon tube containing 5 ml 1 x red blood cell (RBC) lysis buffer (diluted in dH_20) for 5 min. The reaction was stopped with 10 ml PBS and cell

suspension was centrifuged at 300 x g for 5 min. The cell pellet was resuspended in PBS and kept at 4 °C until staining.

7.5.6.2 Organs

Spleen and lungs were harvested in DMEM for flow cytometry in 2 ml Eppendorf tubes containing 1 ml DMEM. To obtain single cell suspension organs were transferred into 2 ml Eppendorf tubes containing Collagenase D / DNAse I solution (2 mg/ml collagenase D, 50 µg/ml DNAseI), cut into small pieces with scissors, and incubated at 37 °C, 650 rpm on a ThermoMixer C (Eppendorf) for 30 min. Organ pieces were poured and mashed through a 70 nm cell straining with the aid of a plunger into 50 ml falcon tubes. Cell strainers were washed with PBS and cells were centrifuged at 500 x g for 5 min, followed by a 1 min red blood cell lysis in 1 ml 1 x RBC lysis buffer at RT. The reaction was stopped with PBS and cells were washed with PBS twice at 500 x g for 5 min. The cell pellet was resuspended in PBS and kept at 4 °C until staining.

7.6 Avatar mice from human EVD survivors

EDTA blood samples of EVD survivors were collected in Guéckédou, Guinea, under the Ethics protocols approved by both the Guinean National Committee for Research and Health (33/CNERS/15) and the Medical Ethics Commission of the state of Hamburg (PV5309).

7.6.1 Generation of survivor avatar mice and infection

To evaluate protection of the immunological memory of EVD survivors huPBL Avatar mice were generated with PBLs from EVD survivors. $CD14^+$ cells were separated as described previously and 10^7 PBLs were administered to the mice. Since the yield of monocytes was too low to generate the appropriate amount of moDCs, monocytes from naïve donors were isolated and cultured. The infection experiments were conducted as previously described.

7.6.2 IgG isolation

Bulk IgG was isolated through affinity-purification using Protein G beads (GE Healthcare) from plasma of EVD survivors. Beads were washed three times with binding buffer (20 mM sodium phosphate, pH 7) and incubated with plasma for 2h at RT. Columns were washed with binding buffer and incubated beads were applied to column. After plasma passed the column columns were rinsed 2 x with binding buffer.

For IgG elution 15ml polypropylene tubes were filled with 500 µl (10% v/v) of neutralization buffer (Tris 1M, pH 8) and placed under the column on ice. The columns were sealed and incubated for 5 min with 4.5 ml elution buffer (0.1 M glycine buffer, pH 2.8). For final elution of IgG, seal was removed and flow through was collected in prepared tubes. IgG concentration was determined with a Nanodrop system and antibodies were stored at -80°C until use.

7.6.3 IgG administration into mice

For antibody protection studies, isolated IgG with a concentration of 10 mg/kg of body weight was administered i.p. per mouse directly after infection (Duehr at al., 2017). As a control anti-Ebola GP clone KZ52 (Absolute Antibodies) was used at the same concentration. For i.p. injections mice were anesthetized using an isoflurane chamber. When breathing slowed down, mice were restrained appropriately in a head-down position. Needles were carefully inserted with bevel facing up into the lower right quadrant of the abdomen towards the head at a 30 – 40° angle to horizontal up to a depth in which the entire bevel was within the abdominal cavity. The plunger was depressed until the virus suspension has been fully administered and the needle was pulled straight out again. Mice were then placed on a heating mat and turned on their side and monitored until fully awake.

7.7 Flow cytometry

Flow cytometry is a widely used method in immunology to discriminate cell population according to their expression of surface molecules, also referred to as cluster of discrimination (CD). A cell suspension is incubated with specific antibodies conjugated with fluorophores and applied to a flow cytometer. Single cells pass beams of different lasers in the cytometer and fluorescent signals are detected. Besides the division by cell surface marker, flow cytometer can also separate populations by characteristics like cell size (forward scatter, FSC) and granularity of the cell (sideward scatter, SSC).

7.7.1 Staining protocol

7.7.1.1 Sample preparation

Samples (blood cell or organ cell suspensions) were washed with either PBS or PBS + 2% FCS and centrifuged at 300 x g for 5 min and the supernatant was removed. Cells were either stained in 2 ml Eppendorf tubes or on 96-well v-bottom plates. Murine

cells were directly stained after isolation and human PBMCs after cryopreservation. If cells were cryopreserved prior DNase I was added in each staining step until fixation.

7.7.1.2 Extracellular staining

All staining steps were conducted at 4 °C omitted from light. In between staining steps cells were washed with PBS and centrifugation was performed at 300 x g for 5 min. If antigen-specific T cells were detected through dextramer staining, an additional staining step was included at the beginning. For this, cells were incubated with a dextramer for 30 min in 50 µl PBS (10% FCS) at 37 °C. Otherwise, the staining started with staining of dead cells through a Zombie dye (Biolegend) diluted 1:500 in PBS for 20 min at 4 °C to distinguish between live and dead cells. Afterwards unspecific binding sites were blocked with an Fc block 1:100 diluted in PBS for 10 min at 4 °C. Extracellular staining was performed with antibody cocktails diluted in 50 µl PBS according to section 2.9.2 for 45 min at 4 °C.

7.7.1.3 Fixation and intracellular staining

After extracellular staining samples were washed and at the same time fixed and inactivated with 400 µl Cytofix/Cytoperm (BD) containing additional 4% formaldehyde solution for 30 min. If intracellular marker were included in the panel, cells were washed twice with 1 x PermWash solution (BD) diluted in ddH_20 and stained for 30 min with intracellular antibodies in 50 µl PermWash solution. Samples were washed twice with PBS and passed through cell strainers into FACS tubes and acquired using a Fortessa (BD) flow cytometer.

7.7.2 T cell phenotyping antibody panel

Table 2: T cell phenotyping antibody panel with Fortessa laser setup.

Laser (excitation)	Detector / Filter	Fluorochrome	Marker	Dilution
UV-Laser (355nm)	740/35 690	BUV 737		
	380/14	BUV395	CD4	1:200
Yellow/Green Laser (561 nm)	780/60 750	PE-Cy7	HLA-DR	1:100
	670/30 635	PE-Cy5		
	610/20 600	PE-Texas Red	Dump (CD14, CD19, CD20, CD56, CD16, Zombie Red)	1:200
	586/15	PE	CTLA-4 (intra) / Tetramer	1:100 / 1:50
Violet Laser (405 nm)	780/60 735	BV785	CD38	1:100
	710/40 670	BV711		
	675/50 635	BV650	CD8	1:400
	610/20 600	BV605	PD-1	1:100
	586/15 570	BV570		
	525/50 505	BV510		
	450/50	BV421		
Red Laser (640 nm)	780/60 750	APC-Cy7	CD3	1:400
	730/45 690	AlexaFluor700	CD45	1:200
	670/14	APC	CCR7 / Tetramer	1:100 / 1:50
Blue Laser (488 nm)	710/40 685	PerCP-Cy5.5	CD45RA	1:200
	530/30 595	FITC		

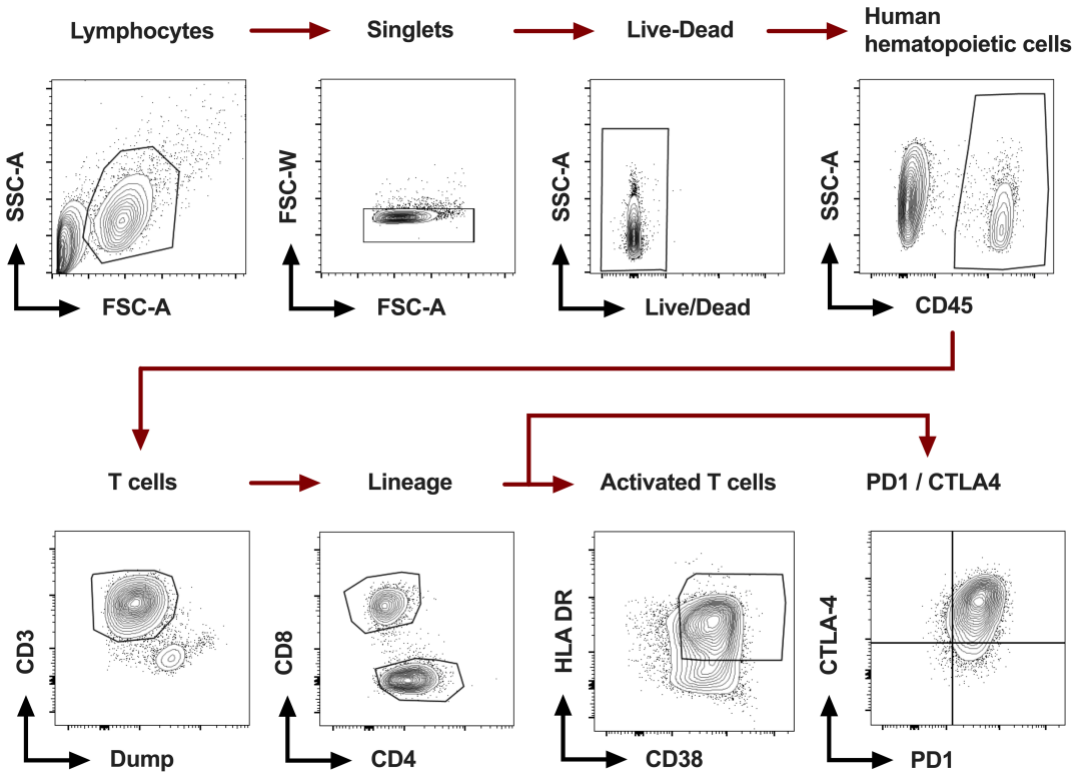

Figure 29: Human T cell gating strategy: Lymphocytes were gated based on FSC and SSC followed by doublet exclusion and live cell gating. To discriminate between mouse and human cells, CD45+ cells were gated. In the next step, T lymphocytes were separated from B cell, NK cell, and myeloid cells (dump). T lymphocytes were then separated according to their lineage into CD4 and CD8 T cells. Within these two lineages activation status was evaluated or the expression of PD-1 and CTLA-4.

7.8 Statistical analysis

Statistical analysis was performed with GraphPad Prism 9 software. Differences in survival rate were evaluated using Mantel-Cox test. Differences in weight, AST levels, and serum or virus titers in blood over time were evaluated with two-way ANOVA, followed by Dunnett's multiple comparison test. To compare virus titers in organs Kruskal-Wallis test was carried out. Significance levels are presented as follows: *, $p \leq 0.05$, **, $p \leq 0.01$, ***, $p \leq 0.001$, and ****, $p \leq 0.0001$. Data are presented as mean and the standard error of mean (SEM).

8. Supplemental Material

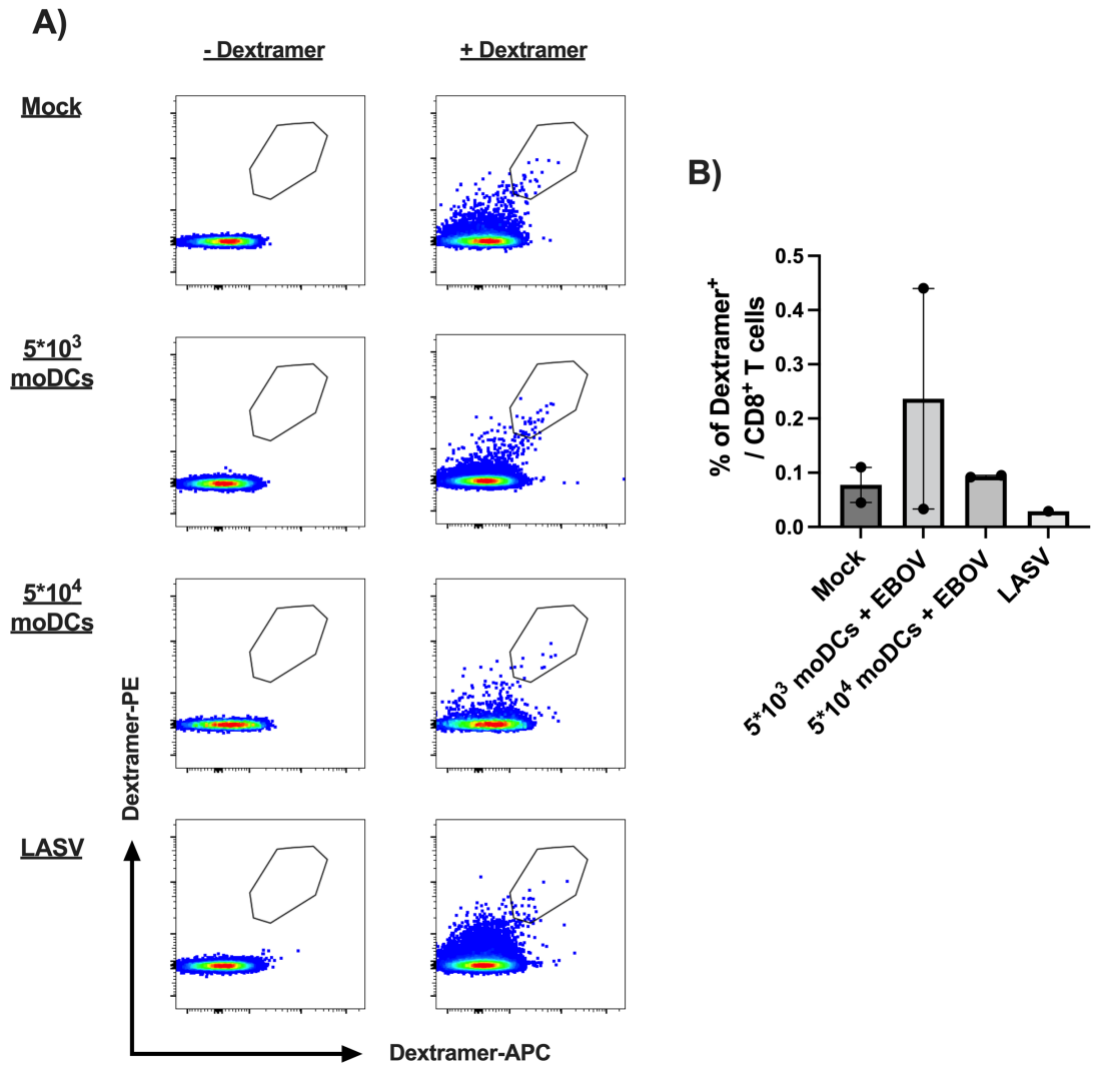

Supp. Fig. 1: Dextramer-staining of huPBL-Avatar mice. Surviving mice from experiments 5.1.4 and 5.1.5 were evaluated for generation of EBOV-specific CD8+ T cells. Briefly, avatar mice were infected with 5*104 or 5*103 EBOV-infected moDCs, or 5*105 LASV-infected moDCs 5 days post transplantation. Mock mice received mock-infected moDCs. Mice were sacrificed 21 days post infection and frequency of EBOV-specific CD8+ T cells specific for the HLA-A*02:01-resticted peptide FLSFASLFL were assessed through flow cytometry dextramer staining. A) Representative plots from dextramer-specific CD8+ T cells (gate: lymphocytes, single cells, live cells, CD45+ cells, dump-, CD3+, CD8+) mock, EBOV-infected, and LASV-infected mice. Mock and LASV-infected mice were included as background. Left plots display dextramer-FMO and right plots dextramer+ staining. B) Bar graph displays frequencies of dextramer+ CD8+ T cells. Mean and SEM are shown.

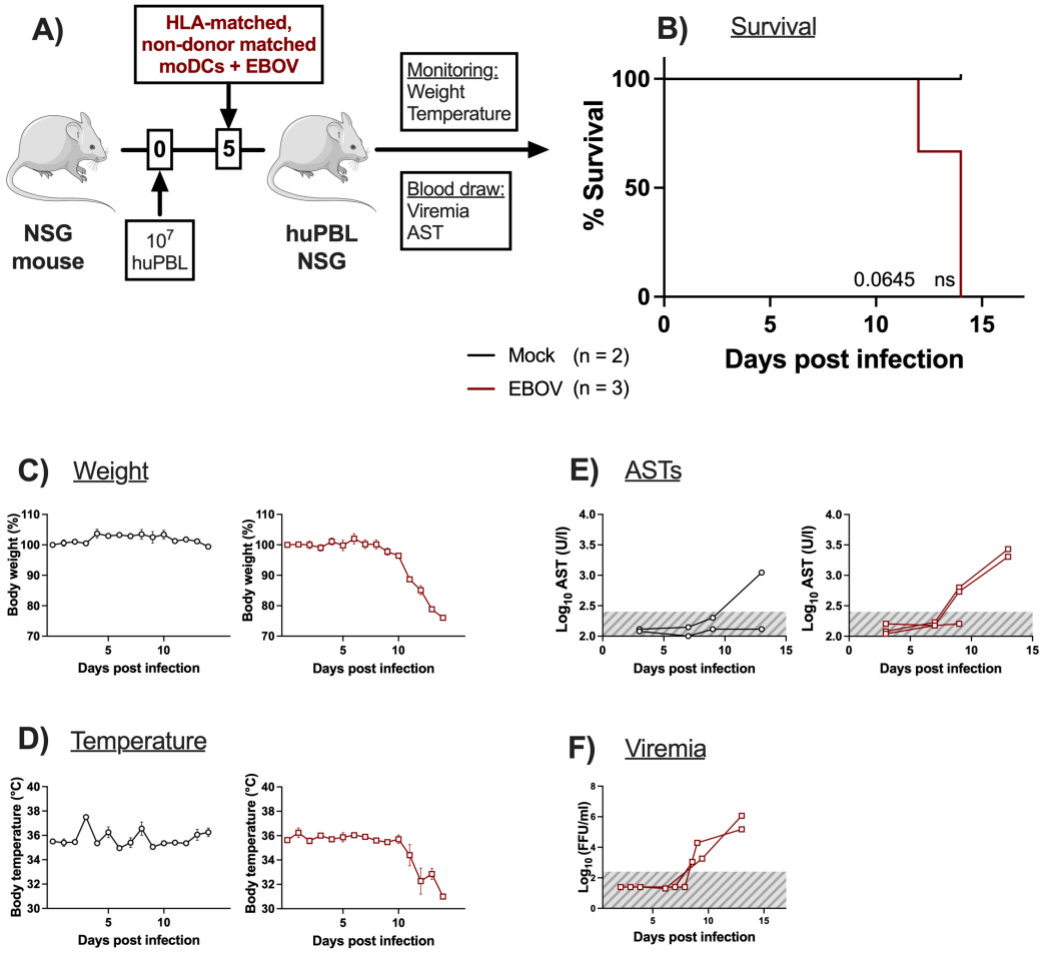

Suppl. Fig. 2: EBOV infection of avatar mice with HLA-A2⁺ non-donor-matched moDCs. (A) 5 mice were inoculated with 10^7 PBLs from a healthy donor. 5 days post inoculation mice were transplanted with $5*10^5$ *in vitro* generated either mock-infected (black; n = 2) or EBOV-infected moDCs (red; n = 3) from a different HLA-A2⁺ donor. Survival, weight, and temperature were monitored daily (B – D), blood and serum were collected at indicated time points for detection of AST levels and viremia (E / F). The normal range for AST and the limit of detection for viremia are shaded in grey. Mean and SEM are shown unless individual data points are depicted. Statistical significance was analyzed using LogRank (Mantel-Cox) test. Levels of significance were interpreted as follows: NS (not significant) $p > 0.05$, * $p \leq 0.05$, ** $p \leq 0.01$, *** $p \leq 0.001$, and **** $p \leq 0.0001$.

9. Literature

Agrati, C., Castilletti, C., Casetti, R., Sacchi, A., Falasca, L., Turchi, F., Tumino, N., Bordoni, V., Cimini, E., Viola, D., Lalle, E., Bordi, L., Lanini, S., Martini, F., Nicastri, E., Petrosillo, N., Puro, V., Piacentini, M., Di Caro, A., … Capobianchi, M. R. (2016). Longitudinal characterization of dysfunctional T cell-activation during human acute Ebola infection. *Cell Death and Disease*, *7*(3). https://doi.org/10.1038/cddis.2016.55

Akira, S., Uematsu, S., & Takeuchi, O. (2006). Pathogen recognition and innate immunity. In *Cell* (Vol. 124, Issue 4, pp. 783–801). https://doi.org/10.1016/j.cell.2006.02.015

Akkaya, M., Kwak, K., & Pierce, S. K. (2020). B cell memory: building two walls of protection against pathogens. In *Nature Reviews Immunology* (Vol. 20, Issue 4, pp. 229–238). Nature Research. https://doi.org/10.1038/s41577-019-0244-2

Alcántara-Hernández, M., & Idoyaga, J. (2021). Mass cytometry profiling of human dendritic cells in blood and tissues. In *Nature Protocols* (Vol. 16, Issue 10, pp. 4855–4877). Nature Research. https://doi.org/10.1038/s41596-021-00599-x

Ali, N., Flutter, B., Sanchez Rodriguez, R., Sharif-Paghaleh, E., Barber, L. D., Lombardi, G., & Nestle, F. O. (2012). Xenogeneic Graft-versus-Host-Disease in NOD-scid IL-2Rγnull Mice Display a T-Effector Memory Phenotype. *PLoS ONE*, *7*(8). https://doi.org/10.1371/journal.pone.0044219

Altin, J. G., & Sloan, E. K. (1997). The role of CD45 and CD45-associated molecules in T cell activation. In *Immunology and Cell Biology* (Vol. 75).

Alvarez, C. P., Lasala, F., Carrillo, J., Muñiz, O., Corbí, A. L., & Delgado, R. (2002). C-type lectins DC-SIGN and L-SIGN mediate cellular entry by Ebola virus in cis and in trans. *Journal of Virology*, *76*(13), 6841–6844. https://doi.org/10.1128/jvi.76.13.6841-6844.2002

Anderson, B. E., McNiff, J., Yan, J., Doyle, H., Mamula, M., Shlomchik, M. J., & Shlomchik, W. D. (2003). Memory CD4+ T cells do not induce graft-versus-host disease. *The Journal of Clinical Investigation*, *112*(1), 101–108. https://doi.org/10.1172/JCI17601

Askenase, M. H., Han, S.-J., Byrd, A. L., Morais da Fonseca, D., Bouladoux, N., Wilhelm, C., Konkel, J. E., Hand, T. W., Lacerda-Queiroz, N., Su, X., Trinchieri, G., Grainger, J. R., & Belkaid, Y. (2015). Bone-Marrow-Resident NK Cells Prime Monocytes for Regulatory Function during Infection. *Immunity*, *42*(6), 1130–1142. https://doi.org/10.1016/j.immuni.2015.05.011

Ayukawa, H., Matsubara, T., Kaneko, M., Hasegawa, M., Ichiyama, T., & Furukawa, S. (2004). Expression of CTLA-4 (CD152) in peripheral blood T cells of children with influenza virus infection including encephalopathy in comparison with respiratory syncytial virus infection. *Clinical and Experimental Immunology*, *137*(1), 151–155. https://doi.org/10.1111/j.1365-2249.2004.02502.x

Baize, S., Leroy, E. M., Georges, A. J., Georges-Courbot, M.-C., Capron, M., Bedjabaga, I., Lansoud-Soukate, J., & Mavoungou, E. (2002). Inflammatory responses in Ebola virus-infected patients. *Clinical and Experimental Immunology*, *128*(1), 163–168. https://doi.org/10.1046/j.1365-2249.2002.01800.x

Baize, S., Leroy, E. M., Georges-Courbot, M.-C., Capron, M., Lansoud-Soukate, J., Debré, P., Fisher-Hoch, S. P., McCormick, J. B., & Georges, A. J. (1999). Defective humoral responses and extensive

intravascular apoptosis are associated with fatal outcome in Ebola virus-infected patients. *Nature Medicine*, *5*(4), 423–426. https://doi.org/10.1038/7422

Baize, S., Pannetier, D., Oestereich, L., Rieger, T., Koivogui, L., Magassouba, N., Soropogui, B., Sow, M. S., Keïta, S., De Clerck, H., Tiffany, A., Dominguez, G., Loua, M., Traoré, A., Kolié, M., Malano, E. R., Heleze, E., Bocquin, A., Mély, S., … Günther, S. (2014). Emergence of Zaire Ebola Virus Disease in Guinea. *New England Journal of Medicine*, *371*(15), 1418–1425. https://doi.org/10.1056/NEJMoa1404505

Balar, A. V, Galsky, M. D., Rosenberg, J. E., Powles, T., Petrylak, D. P., Bellmunt, J., Loriot, Y., Necchi, A., Hoffman-Censits, J., Perez-Gracia, J. L., Dawson, N. A., van der Heijden, M. S., Dreicer, R., Srinivas, S., Retz, M. M., Joseph, R. W., Drakaki, A., Vaishampayan, U. N., Sridhar, S. S., … Bajorin, D. F. (2017). Atezolizumab as first-line treatment in cisplatin-ineligible patients with locally advanced and metastatic urothelial carcinoma: a single-arm, multicentre, phase 2 trial. *The Lancet*, *389*(10064), 67–76. https://doi.org/10.1016/S0140-6736(16)32455-2

Banchereau, J., & Steinman, R. M. (1998). Dendritic cells and the control of immunity. *Nature*, *392*(6673), 245–252. https://doi.org/10.1038/32588

Bao, M., & Liu, Y. J. (2013). Regulation of TLR7/9 signaling in plasmacytoid dendritic cells. In *Protein and Cell* (Vol. 4, Issue 1, pp. 40–52). Higher Education Press Limited Company. https://doi.org/10.1007/s13238-012-2104-8

Baseler, L., Chertow, D. S., Johnson, K. M., Feldmann, H., & Morens, D. M. (2017). The Pathogenesis of Ebola Virus Disease∗. In *Annual Review of Pathology: Mechanisms of Disease* (Vol. 12, pp. 387–418). Annual Reviews Inc. https://doi.org/10.1146/annurev-pathol-052016-100506

Basler, C. F., Mikulasova, A., Martinez-Sobrido, L., Paragas, J., Mühlberger, E., Bray, M., Klenk, H.-D., Palese, P., & García-Sastre, A. (2003). The Ebola Virus VP35 Protein Inhibits Activation of Interferon Regulatory Factor 3. *Journal of Virology*, *77*(14), 7945–7956. https://doi.org/10.1128/jvi.77.14.7945-7956.2003

Basler, C. F., Wang, X., Mü Hlberger †, E., Volchkov, V., Paragas, J., Klenk, H.-D., García-Sastre, A., & Palese, P. (2000). *The Ebola virus VP35 protein functions as a type I IFN antagonist*. www.pnas.org

Bernard, A., & Boumsell, L. (1984). The clusters of differentiation (CD) defined by the First International Workshop on human leucocyte differentiation antigens. *Human Immunology*, *11*(1), 1–10. https://doi.org/10.1016/0198-8859(84)90051-X

Bird, B. H., Spengler, J. R., Chakrabarti, A. K., Khristova, M. L., Sealy, T. K., Coleman-McCray, J. D., Martin, B. E., Dodd, K. A., Goldsmith, C. S., Sanders, J., Zaki, S. R., Nichol, S. T., & Spiropoulou, C. F. (2015). Humanized mouse model of Ebola virus disease mimics the immune responses in human disease. *Journal of Infectious Diseases*, *212*(11), 703–711. https://doi.org/10.1093/infdis/jiv538

Bornholdt, Z. A., Ndungo, E., Fusco, M. L., Bale, S., Flyak, A. I., Crowe, J. E., Chandran, K., & Saphire, E. O. (2016). Host-Primed Ebola Virus GP Exposes a Hydrophobic NPC1 Receptor-Binding Pocket, Revealing a Target for Broadly Neutralizing Antibodies. *MBio*, *7*(1), e02154-15. https://doi.org/10.1128/mBio.02154-15

Bosio, C. M., Aman, M. J., Grogan, C., Hogan, R., Ruthel, G., Negley, D., Mohamadzadeh, M., Bavari, S., & Schmaljohn, A. (2003). Ebola and Marburg Viruses Replicate in Monocyte-Derived Dendritic Cells without Inducing the Production of Cytokines and Full Maturation. In *The Journal of Infectious Diseases* (Vol. 188). https://academic.oup.com/jid/article/188/11/1630/862409

Bowen, E. T., Platt, G. S., Simpson, D. I., McArdell, L. B., & Raymond, R. T. (1978). Ebola haemorrhagic fever: experimental infection of monkeys. *Transactions of the Royal Society of Tropical Medicine and Hygiene*, *72*(2), 188–191. https://doi.org/10.1016/0035-9203(78)90058-5

Bowie, A. G., & Unterholzner, L. (2008). Viral evasion and subversion of pattern-recognition receptor signalling. In *Nature Reviews Immunology* (Vol. 8, Issue 12, pp. 911–922). https://doi.org/10.1038/nri2436

Bradfute, S. B., Swanson, P. E., Smith, M. A., Watanabe, E., McDunn, J. E., Hotchkiss, R. S., & Bavari, S. (2010). Mechanisms and Consequences of Ebolavirus-Induced Lymphocyte Apoptosis. *The Journal of Immunology*, *184*(1), 327–335. https://doi.org/10.4049/jimmunol.0901231

Bradfute, S. B., Warfield, K. L., & Bray, M. (2012). Mouse models for filovirus infections. In *Viruses* (Vol. 4, Issue 9, pp. 1477–1508). https://doi.org/10.3390/v4091477

Brannan, J. M., Froude, J. W., Prugar, L. I., Bakken, R. R., Zak, S. E., Daye, S. P., Wilhelmsen, C. E., & Dye, J. M. (2015). Interferon α/β Receptor-Deficient Mice as a Model for Ebola Virus Disease. *The Journal of Infectious Diseases*, *212 Suppl 2*, S282-94. https://doi.org/10.1093/infdis/jiv215

Bray, M. (2001). The role of the Type I interferon response in the resistance of mice to filovirus infection. *The Journal of General Virology*, *82*(Pt 6), 1365–1373. https://doi.org/10.1099/0022-1317-82-6-1365

Bray, M., Davis, K., Geisbert, T., Schmaljohn, C., & Huggins, J. (1998). A mouse model for evaluation of prophylaxis and therapy of Ebola hemorrhagic fever. *The Journal of Infectious Diseases*, *178*(3), 651–661. https://doi.org/10.1086/515386

Bray, M., & Geisbert, T. W. (2005). Ebola virus: The role of macrophages and dendritic cells in the pathogenesis of Ebola hemorrhagic fever. *The International Journal of Biochemistry & Cell Biology*, *37*(8), 1560–1566. https://doi.org/10.1016/j.biocel.2005.02.018

Bray, M., Hatfill, S., Hensley, L., & Huggins, J. W. (2001). Haematological, biochemical and coagulation changes in mice, guinea-pigs and monkeys infected with a mouse-adapted variant of Ebola Zaire virus. *Journal of Comparative Pathology*, *125*(4), 243–253. https://doi.org/10.1053/jcpa.2001.0503

Cantoni, D., Hamlet, A., Michaelis, M., Wass, M. N., & Rossman, J. S. (2016). Risks Posed by Reston, the Forgotten Ebolavirus. *MSphere*, *1*(6). https://doi.org/10.1128/msphere.00322-16

Cárdenas, W. B., Loo, Y.-M., Gale, M., Hartman, A. L., Kimberlin, C. R., Martínez-Sobrido, L., Saphire, E. O., & Basler, C. F. (2006). Ebola Virus VP35 Protein Binds Double-Stranded RNA and Inhibits Alpha/Beta Interferon Production Induced by RIG-I Signaling. *Journal of Virology*, *80*(11), 5168–5178. https://doi.org/10.1128/jvi.02199-05

Carette, J. E., Raaben, M., Wong, A. C., Herbert, A. S., Obernosterer, G., Mulherkar, N., Kuehne, A. I., Kranzusch, P. J., Griffin, A. M., Ruthel, G., Dal Cin, P., Dye, J. M., Whelan, S. P., Chandran, K., & Brummelkamp, T. R. (2011). Ebola virus entry requires the cholesterol transporter Niemann-Pick C1. *Nature*, *477*(7364), 340–343. https://doi.org/10.1038/nature10348

Cella, M., Jarrossay, D., Facchetti, F., Alebardi, O., Nakajima, H., Lanzavecchia, A., & Colonna, M. (1999). Plasmacytoid monocytes migrate to inflamed lymph nodes and produce large amounts of type I interferon. *Nature Medicine*, *5*(8), 919–923. https://doi.org/10.1038/11360

Chen, B. J., Cui, X., Sempowski, G. D., Liu, C., & Chao, N. J. (2004). Transfer of allogeneic CD62L–memory T cells without graft-versus-host disease. *Blood*, *103*(4), 1534–1541. https://doi.org/10.1182/blood-2003-08-2987

Connolly, B. M., Steele, K. E., Davis, K. J., Geisbert, T. W., Kell, W. M., Jaax, N. K., & Jahrling, P. B. (1999). Pathogenesis of experimental Ebola virus infection in guinea pigs. *The Journal of Infectious Diseases*, *179 Suppl 1*, S203-17. https://doi.org/10.1086/514305

Corti, D., Misasi, J., Mulangu, S., Stanley, D. A., Kanekiyo, M., Wollen, S., Ploquin, A., Doria-Rose, N. A., Staupe, R. P., Bailey, M., Shi, W., Choe, M., Marcus, H., Thompson, E. A., Cagigi, A., Silacci, C., Fernandez-Rodriguez, B., Perez, L., Sallusto, F., … Sullivan, N. J. (2016). Protective monotherapy against lethal Ebola virus infection by a potently neutralizing antibody. *Science (New York, N.Y.)*, *351*(6279), 1339–1342. https://doi.org/10.1126/science.aad5224

Côté, M., Misasi, J., Ren, T., Bruchez, A., Lee, K., Filone, C. M., Hensley, L., Li, Q., Ory, D., Chandran, K., & Cunningham, J. (2011). Small molecule inhibitors reveal Niemann-Pick C1 is essential for Ebola virus infection. *Nature*, *477*(7364), 344–348. https://doi.org/10.1038/nature10380

Covassin, L., Jangalwe, S., Jouvet, N., Laning, J., Burzenski, L., Shultz, L. D., & Brehm, M. A. (2013). Human immune system development and survival of non-obese diabetic (NOD) - scid IL2r *γnull* (NSG) mice engrafted with human thymus and autologous haematopoietic stem cells. *Clinical and Experimental Immunology*, *174*(3), 372–388. https://doi.org/10.1111/cei.12180

Cox, N. J., Mccormick, J. B., Johnson, K. M., & Kiley, M. P. (1983). Evidence for Two Subtypes of Ebola Virus Based on Oligonucleotide Mapping of RNA. In *THE JOURNAL OF INFECTIOUS DISEASES* • (Vol. 147, Issue 2). http://jid.oxfordjournals.org/

Crawford, A., & Wherry, E. J. (2009). The diversity of costimulatory and inhibitory receptor pathways and the regulation of antiviral T cell responses. *Current Opinion in Immunology*, *21*(2), 179–186. https://doi.org/10.1016/j.coi.2009.01.010

Cross, R. W., Fenton, K. A., Geisbert, J. B., Mire, C. E., & Geisbert, T. W. (2015). Modeling the Disease Course of Zaire ebolavirus Infection in the Outbred Guinea Pig. *The Journal of Infectious Diseases*, *212 Suppl 2*, S305-15. https://doi.org/10.1093/infdis/jiv237

Currie, A. J., Prosser, A., McDonnell, A., Cleaver, A. L., Robinson, B. W. S., Freeman, G. J., & van der Most, R. G. (2009). Dual control of antitumor CD8 T cells through the programmed death-1/programmed death-ligand 1 pathway and immunosuppressive CD4 T cells: regulation and counterregulation. *Journal of Immunology (Baltimore, Md.: 1950)*, *183*(12), 7898–7908. https://doi.org/10.4049/jimmunol.0901060

Davis, C. W., Jackson, K. J. L., McElroy, A. K., Halfmann, P., Huang, J., Chennareddy, C., Piper, A. E., Leung, Y., Albariño, C. G., Crozier, I., Ellebedy, A. H., Sidney, J., Sette, A., Yu, T., Nielsen, S. C. A., Goff, A. J., Spiropoulou, C. F., Saphire, E. O., Cavet, G., … Ahmed, R. (2019a). Longitudinal Analysis of the Human B Cell Response to Ebola Virus Infection. *Cell*, *177*(6), 1566-1582.e17. https://doi.org/10.1016/j.cell.2019.04.036

Davis, C. W., Jackson, K. J. L., McElroy, A. K., Halfmann, P., Huang, J., Chennareddy, C., Piper, A. E., Leung, Y., Albariño, C. G., Crozier, I., Ellebedy, A. H., Sidney, J., Sette, A., Yu, T., Nielsen, S. C. A., Goff, A. J., Spiropoulou, C. F., Saphire, E. O., Cavet, G., … Ahmed, R. (2019b). Longitudinal Analysis of the Human B Cell Response to Ebola Virus Infection. *Cell*, *177*(6), 1566-1582.e17. https://doi.org/10.1016/j.cell.2019.04.036

De La Vega, M. A., Caleo, G., Audet, J., Qiu, X., Kozak, R. A., Brooks, J. I., Kern, S., Wolz, A., Sprecher, A., Greig, J., Lokuge, K., Kargbo, D. K., Kargbo, B., Di Caro, A., Grolla, A., Kobasa, D., Strong, J. E., Ippolito, G., Van Herp, M., & Kobinger, G. P. (2015). Ebola viral load at diagnosis associates with patient outcome and outbreak evolution. *Journal of Clinical Investigation*, *125*(12), 4421–4428. https://doi.org/10.1172/JCI83162

de Wit, E., Munster, V. J., Metwally, S. A., & Feldmann, H. (2011). Assessment of Rodents as Animal Models for Reston Ebolavirus. *The Journal of Infectious Diseases*, *204*(suppl_3), S968–S972. https://doi.org/10.1093/infdis/jir330

Dowell, S. F., Mukunu, R., Ksiazek, T. G., Khan, A. S., Rollin, P. E., & Peters, C. J. (1999a). Transmission of Ebola hemorrhagic fever: a study of risk factors in family members, Kikwit, Democratic Republic of the Congo, 1995. Commission de Lutte contre les Epidémies à Kikwit. *The Journal of Infectious Diseases*, *179 Suppl 1*, S87-91. https://doi.org/10.1086/514284

Dowell, S. F., Mukunu, R., Ksiazek, T. G., Khan, A. S., Rollin, P. E., & Peters, C. J. (1999b). Transmission of Ebola hemorrhagic fever: a study of risk factors in family members, Kikwit, Democratic Republic of the Congo, 1995. Commission de Lutte contre les Epidémies à Kikwit. *The Journal of Infectious Diseases*, *179 Suppl 1*, S87-91. https://doi.org/10.1086/514284

Duehr, J., Wohlbold, T. J., Oestereich, L., Chromikova, V., Amanat, F., Rajendran, M., Gomez-Medina, S., Mena, I., Tenoever, B. R., García-Sastre, A., Basler, C. F., Munoz-Fontela, C., & Krammer, F. (2017). *Novel Cross-Reactive Monoclonal Antibodies against Ebolavirus Glycoproteins Show Protection in a Murine Challenge Model VACCINES AND ANTIVIRAL AGENTS crossm*. *91*, 652–669. https://doi.org/10.1128/JVI

Durand, M., Walter, T., Pirnay, T., Naessens, T., Gueguen, P., Goudot, C., Lameiras, S., Chang, Q., Talaei, N., Ornatsky, O., Vassilevskaia, T., Baulande, S., Amigorena, S., & Segura, E. (2019). Human lymphoid organ cDC2 and macrophages play complementary roles in T follicular helper responses. *The Journal of Experimental Medicine*, *216*(7), 1561–1581. https://doi.org/10.1084/jem.20181994

Dutt, S., Tseng, D., Ermann, J., George, T. I., Liu, Y. P., Davis, C. R., Fathman, C. G., & Strober, S. (2007). Naive and memory T cells induce different types of graft-versus-host disease. *Journal of Immunology (Baltimore, Md.: 1950)*, *179*(10), 6547–6554. https://doi.org/10.4049/jimmunol.179.10.6547

Dyer, K. D., Percopo, C. M., Fischer, E. R., Gabryszewski, S. J., & Rosenberg, H. F. (2009). Pneumoviruses infect eosinophils and elicit MyD88-dependent release of chemoattractant cytokines and interleukin-6. *Blood*, *114*(13), 2649–2656. https://doi.org/10.1182/blood-2009-01-199497

Ebihara, H., Takada, A., Kobasa, D., Jones, S., Neumann, G., Theriault, S., Bray, M., Feldmann, H., & Kawaoka, Y. (2006). Molecular determinants of Ebola virus virulence in mice. *PLoS Pathogens*, *2*(7), e73. https://doi.org/10.1371/journal.ppat.0020073

Ebihara, H., Zivcec, M., Gardner, D., Falzarano, D., LaCasse, R., Rosenke, R., Long, D., Haddock, E., Fischer, E., Kawaoka, Y., & Feldmann, H. (2013). A Syrian golden hamster model recapitulating ebola hemorrhagic fever. *The Journal of Infectious Diseases*, *207*(2), 306–318. https://doi.org/10.1093/infdis/jis626

Eguíluz-Gracia, I., Bosco, A., Dollner, R., Melum, G. R., Lexberg, M. H., Jones, A. C., Dheyauldeen, S. A., Holt, P. G., Bækkevold, E. S., & Jahnsen, F. L. (2016). Rapid recruitment of CD14+ monocytes in experimentally induced allergic rhinitis in human subjects. *Journal of Allergy and Clinical Immunology*, *137*(6), 1872-1881.e12. https://doi.org/10.1016/j.jaci.2015.11.025

Ehrhardt, S. A., Zehner, M., Krähling, V., Cohen-Dvashi, H., Kreer, C., Elad, N., Gruell, H., Ercanoglu, M. S., Schommers, P., Gieselmann, L., Eggeling, R., Dahlke, C., Wolf, T., Pfeifer, N., Addo, M. M., Diskin, R., Becker, S., & Klein, F. (2019). Polyclonal and convergent antibody response to Ebola virus vaccine rVSV-ZEBOV. *Nature Medicine*, *25*(10), 1589–1600. https://doi.org/10.1038/s41591-019-0602-4

Ehx, G., Somja, J., Warnatz, H. J., Ritacco, C., Hannon, M., Delens, L., Fransolet, G., Delvenne, P., Muller, J., Beguin, Y., Lehrach, H., Belle, L., Humblet-Baron, S., & Baron, F. (2018). Xenogeneic

Graft-Versus-Host Disease in Humanized NSG and NSG-HLA-A2/HHD Mice. *Frontiers in Immunology*, *9*. https://doi.org/10.3389/fimmu.2018.01943

Ellebedy, A. H., Jackson, K. J. L., Kissick, H. T., Nakaya, H. I., Davis, C. W., Roskin, K. M., McElroy, A. K., Oshansky, C. M., Elbein, R., Thomas, S., Lyon, G. M., Spiropoulou, C. F., Mehta, A. K., Thomas, P. G., Boyd, S. D., & Ahmed, R. (2016). Defining antigen-specific plasmablast and memory B cell subsets in human blood after viral infection or vaccination. *Nature Immunology*, *17*(10), 1226–1234. https://doi.org/10.1038/ni.3533

Emanuel, J., Marzi, A., & Feldmann, H. (2018). Filoviruses: Ecology, Molecular Biology, and Evolution. In *Advances in Virus Research* (Vol. 100, pp. 189–221). Academic Press Inc. https://doi.org/10.1016/bs.aivir.2017.12.002

Emond, R. T., Evans, B., Bowen, E. T., & Lloyd, G. (1977). A case of Ebola virus infection. *BMJ*, *2*(6086), 541–544. https://doi.org/10.1136/bmj.2.6086.541

Epstein, L., Wong, K. K., Kallen, A. J., & Uyeki, T. M. (2015). Post-Ebola Signs and Symptoms in U.S. Survivors. *New England Journal of Medicine*, *373*(25), 2484–2486. https://doi.org/10.1056/NEJMc1506576

Escudero-Pérez, B., Ruibal, P., Rottstegge, M., Lödtke, A., Port, J. R., Hartmann, K., Gómez-Medina, S., Möller-Guhl, J., Nelson, E. V., Krasemann, S., Rodríguez, E., & Munoz-Fontela, C. (2019). Comparative pathogenesis of Ebola virus and Reston virus infection in humanized mice. *JCI Insight*, *4*(21). https://doi.org/10.1172/jci.insight.126070

Feldmann, H., & Geisbert, T. (2011). Ebola haemorrhagic fever. *The Lancet*, *377*(9768), 849–862. https://www.sciencedirect.com/science/article/pii/S0140673610606678

Feldmann, H., Sprecher, A., & Geisbert, T. W. (2020). Ebola. *New England Journal of Medicine*, *382*(19), 1832–1842. https://doi.org/10.1056/NEJMra1901594

Feng, J., Pucella, J. N., Jang, G., Alcántara-Hernández, M., Upadhaya, S., Adams, N. M., Khodadadi-Jamayran, A., Lau, C. M., Stoeckius, M., Hao, S., Smibert, P., Tsirigos, A., Idoyaga, J., & Reizis, B. (2022). Clonal lineage tracing reveals shared origin of conventional and plasmacytoid dendritic cells. *Immunity*, *55*(3), 405-422.e11. https://doi.org/10.1016/j.immuni.2022.01.016

Fisher-Hoch, S. P., Brammer, T. L., Trappier, S. G., Hutwagner, L. C., Farrar, B. B., Ruo, S. L., Brown, B. G., Hermann, L. M., Perez-Oronoz, G. I., Goldsmith, C. S., Hanes, M. A., & McCormick, J. B. (1992). Pathogenic Potential of Filoviruses: Role of Geographic Origin of Primate Host and Virus Strain. *Journal of Infectious Diseases*, *166*(4), 753–763. https://doi.org/10.1093/infdis/166.4.753

Fisher-Hoch, S. P., Platt, G. S., Neild, G. H., Southee, T., Baskerville, A., Raymond, R. T., Lloyd, G., & Simpson, D. I. H. (1985). Pathophysiology of Shock and Hemorrhage in a Fulminating Viral Infection (Ebola). *Journal of Infectious Diseases*, *152*(5), 887–894. https://doi.org/10.1093/infdis/152.5.887

Frame, J. D., Baldwin, J. M., Gocke, D. J., & Troup, J. M. (1970). Lassa fever, a new virus disease of man from West Africa. I. Clinical description and pathological findings. *The American Journal of Tropical Medicine and Hygiene*, *19*(4), 670–676. https://doi.org/10.4269/ajtmh.1970.19.670

Franco, A., Guidotti, L. G., Hobbs, M. V, Pasquetto, V., & Chisari, F. V. (1997). Pathogenetic effector function of CD4-positive T helper 1 cells in hepatitis B virus transgenic mice. *Journal of Immunology (Baltimore, Md. : 1950)*, *159*(4), 2001–2008.

Fuller, M. J., Callendret, B., Zhu, B., Freeman, G. J., Hasselschwert, D. L., Satterfield, W., Sharpe, A. H., Dustin, L. B., Rice, C. M., Grakoui, A., Ahmed, R., & Walker, C. M. (2013). Immunotherapy of chronic hepatitis C virus infection with antibodies against programmed cell death-1 (PD-1). *Proceedings of the National Academy of Sciences of the United States of America*, *110*(37), 15001–15006. https://doi.org/10.1073/pnas.1312772110

Gałas, A. (2014). The determinants of spread of Ebola virus disease - an evidence from the past outbreak experiences. *Folia Medica Cracoviensia*, *54*(3), 17–25.

García-Sastre, A., & Biron, C. A. (2006). Type 1 interferons and the virus-host relationship: A lesson in détente. In *Science* (Vol. 312, Issue 5775, pp. 879–882). https://doi.org/10.1126/science.1125676

Gardiner, D., Lalezari, J., Lawitz, E., DiMicco, M., Ghalib, R., Reddy, K. R., Chang, K.-M., Sulkowski, M., Marro, S. O., Anderson, J., He, B., Kansra, V., McPhee, F., Wind-Rotolo, M., Grasela, D., Selby, M., Korman, A. J., & Lowy, I. (2013). A randomized, double-blind, placebo-controlled assessment of BMS-936558, a fully human monoclonal antibody to programmed death-1 (PD-1), in patients with chronic hepatitis C virus infection. *PloS One*, *8*(5), e63818. https://doi.org/10.1371/journal.pone.0063818

Garofalo, R., Kimpen, J. L. L., Welliver, R. C., & Ogra, P. L. (1992). Eosinophil degranulation in the respiratory tract during naturally acquired respiratory syncytial virus infection. *The Journal of Pediatrics*, *120*(1), 28–32. https://doi.org/10.1016/S0022-3476(05)80592-X

Gay, C. L., Bosch, R. J., Ritz, J., Hataye, J. M., Aga, E., Tressler, R. L., Mason, S. W., Hwang, C. K., Grasela, D. M., Ray, N., Cyktor, J. C., Coffin, J. M., Acosta, E. P., Koup, R. A., Mellors, J. W., Eron, J. J., & AIDS Clinical Trials 5326 Study Team. (2017). Clinical Trial of the Anti-PD-L1 Antibody BMS-936559 in HIV-1 Infected Participants on Suppressive Antiretroviral Therapy. *The Journal of Infectious Diseases*, *215*(11), 1725–1733. https://doi.org/10.1093/infdis/jix191

Geisbert, T. W., Hensley, L. E., Gibb, T. R., Steele, K. E., Jaax, N. K., & Jahrling, P. B. (2000). Apoptosis induced in vitro and in vivo during infection by Ebola and Marburg viruses. *Laboratory Investigation; a Journal of Technical Methods and Pathology*, *80*(2), 171–186. https://doi.org/10.1038/labinvest.3780021

Geisbert, T. W., Hensley, L. E., Jahrling, P. B., Larsen, T., Geisbert, J. B., Paragas, J., Young, H. A., Fredeking, T. M., Rote, W. E., & Vlasuk, G. P. (2003a). Treatment of Ebola virus infection with a recombinant inhibitor of factor VIIa/tissue factor: a study in rhesus monkeys. *Lancet (London, England)*, *362*(9400), 1953–1958. https://doi.org/10.1016/S0140-6736(03)15012-X

Geisbert, T. W., Hensley, L. E., Larsen, T., Young, H. A., Reed, D. S., Geisbert, J. B., Scott, D. P., Kagan, E., Jahrling, P. B., & Davis, K. J. (2003b). Pathogenesis of Ebola Hemorrhagic Fever in Cynomolgus Macaques Evidence that Dendritic Cells Are Early and Sustained Targets of Infection. In *American Journal of Pathology* (Vol. 163, Issue 6).

Geisbert, T. W., Strong, J. E., & Feldmann, H. (2015). Considerations in the Use of Nonhuman Primate Models of Ebola Virus and Marburg Virus Infection. In *Journal of Infectious Diseases* (Vol. 212, pp. S91–S97). Oxford University Press. https://doi.org/10.1093/infdis/jiv284

Geisbert, T. W., Young, H. A., Jahrling, P. B., Davis, K. J., Kagan, E., & Hensley, L. E. (2003c). Mechanisms Underlying Coagulation Abnormalities in Ebola Hemorrhagic Fever: Overexpression of Tissue Factor in Primate Monocytes/Macrophages Is a Key Event. In *The Journal of Infectious Diseases* (Vol. 188). https://academic.oup.com/jid/article/188/11/1618/862287

Geissmann, F., Manz, M. G., Jung, S., Sieweke, M. H., Merad, M., & Ley, K. (2010). Development of Monocytes, Macrophages, and Dendritic Cells. *Science*, *327*(5966), 656–661. https://doi.org/10.1126/science.1178331

Gibb, T. R., Bray, M., Geisbert, T. W., Steele, K. E., Kell, W. M., Davis, K. J., & Jaax, N. K. (2001). Pathogenesis of Experimental Ebola Zaire Virus Infection in BALB/c Mice. *Journal of Comparative Pathology*, *125*(4), 233–242. https://doi.org/10.1053/jcpa.2001.0502

Goldstein, T., Anthony, S. J., Gbakima, A., Bird, B. H., Bangura, J., Tremeau-Bravard, A., Belaganahalli, M. N., Wells, H. L., Dhanota, J. K., Liang, E., Grodus, M., Jangra, R. K., DeJesus, V. A., Lasso, G.,

Smith, B. R., Jambai, A., Kamara, B. O., Kamara, S., Bangura, W., … Mazet, J. A. K. (2018). The discovery of Bombali virus adds further support for bats as hosts of ebolaviruses. *Nature Microbiology*, *3*(10), 1084–1089. https://doi.org/10.1038/s41564-018-0227-2

Guidotti, L. G., & Chisari, F. V. (2001). *Noncytolytic Control Of Viral Infections By The Innate And Adaptive Immune Response*. www.annualreviews.org

Guidotti, L. G., & Chisari, F. V. (2006). Immunobiology and pathogenesis of viral hepatitis. In *Annual Review of Pathology* (Vol. 1, pp. 23–61). Annual Reviews Inc. https://doi.org/10.1146/annurev.pathol.1.110304.100230

Guidotti, L. G., Ishikawa, T., Hobbs, M. V, Matzke, B., Schreiber, R., & Chisari, F. V. (1996). Intracellular inactivation of the hepatitis B virus by cytotoxic T lymphocytes. *Immunity*, *4*(1), 25–36. https://doi.org/10.1016/s1074-7613(00)80295-2

Gunn, B. M., Lu, R., Slein, M. D., Ilinykh, P. A., Huang, K., Atyeo, C., Schendel, S. L., Kim, J., Cain, C., Roy, V., Suscovich, T. J., Takada, A., Halfmann, P. J., Kawaoka, Y., Pauthner, M. G., Momoh, M., Goba, A., Kanneh, L., Andersen, K. G., … Alter, G. (2021). A Fc engineering approach to define functional humoral correlates of immunity against Ebola virus. *Immunity*, *54*(4), 815-828.e5. https://doi.org/10.1016/j.immuni.2021.03.009

Gupta, M., Greer, P., Mahanty, S., Shieh, W.-J., Zaki, S. R., Ahmed, R., & Rollin, P. E. (2005). CD8-mediated protection against Ebola virus infection is perforin dependent. *Journal of Immunology (Baltimore, Md. : 1950)*, *174*(7), 4198–4202. https://doi.org/10.4049/jimmunol.174.7.4198

Gupta, M., MacNeil, A., Reed, Z. D., Rollin, P. E., & Spiropoulou, C. F. (2012). Serology and cytokine profiles in patients infected with the newly discovered Bundibugyo ebolavirus. *Virology*, *423*(2), 119–124. https://doi.org/10.1016/j.virol.2011.11.027

Gupta, M., Mahanty, S., Ahmed, R., & Rollin, P. E. (2001). Monocyte-derived human macrophages and peripheral blood mononuclear cells infected with Ebola virus secrete MIP-1α and TNF-α and inhibit poly-IC-induced IFN-α in vitro. *Virology*, *284*(1), 20–25. https://doi.org/10.1006/viro.2001.0836

Gupta, M., Spiropoulou, C., & Rollin, P. E. (2007). Ebola virus infection of human PBMCs causes massive death of macrophages, CD4 and CD8 T cell sub-populations in vitro. *Virology*, *364*(1), 45–54. https://doi.org/10.1016/j.virol.2007.02.017

Hagiwara, S., Nishida, N., Ida, H., Ueshima, K., Minami, Y., Takita, M., Aoki, T., Morita, M., Chishina, H., Komeda, Y., Yoshida, A., Hayashi, H., Nakagawa, K., & Kudo, M. (2022). Clinical implication of immune checkpoint inhibitor on the chronic hepatitis B virus infection. *Hepatology Research : The Official Journal of the Japan Society of Hepatology*, *52*(9), 754–761. https://doi.org/10.1111/hepr.13798

Hale, J. S., Youngblood, B., Latner, D. R., Mohammed, A. U. R., Ye, L., Akondy, R. S., Wu, T., Iyer, S. S., & Ahmed, R. (2013). Distinct memory CD4+ T cells with commitment to T follicular helper- and T helper 1-cell lineages are generated after acute viral infection. *Immunity*, *38*(4), 805–817. https://doi.org/10.1016/j.immuni.2013.02.020

Harui, A., Kiertscher, S. M., & Roth, M. D. (2011). Reconstitution of huPBL-NSG mice with donor-matched dendritic cells enables antigen-specific T-cell activation. *Journal of Neuroimmune Pharmacology*, *6*(1), 148–157. https://doi.org/10.1007/s11481-010-9223-x

Huber, S. R., van Beek, J., de Jonge, J., Luytjes, W., & van Baarle, D. (2014). T cell responses to viral infections - opportunities for peptide vaccination. In *Frontiers in Immunology* (Vol. 5, Issue APR). Frontiers Research Foundation. https://doi.org/10.3389/fimmu.2014.00171

Hugo, M., Declerck, H., Fitzpatrick, G., Severy, N., Gbabai, O. B.-M., Decroo, T., & Van Herp, M. (2015). Post-Traumatic Stress Reactions in Ebola Virus Disease Survivors in Sierra Leone. *Emergency Medicine: Open Access*, *05*(06). https://doi.org/10.4172/2165-7548.1000285

Huppa, J. B., & Davis, M. M. (2003). T-cell-antigen recognition and the immunological synapse. In *Nature Reviews Immunology* (Vol. 3, Issue 12, pp. 973–983). European Association for Cardio-Thoracic Surgery. https://doi.org/10.1038/nri1245

Ishikawa, F., Yasukawa, M., Lyons, B., Yoshida, S., Miyamoto, T., Yoshimoto, G., Watanabe, T., Akashi, K., Shultz, L. D., & Harada, M. (2005). Development of functional human blood and immune systems in NOD/SCID/IL2 receptor γ chainnull mice. *Blood*, *106*(5), 1565–1573. https://doi.org/10.1182/BLOOD-2005-02-0516

Ishikawa, Y., Usui, T., Shiomi, A., Shimizu, M., Murakami, K., & Mimori, T. (2014). Functional engraftment of human peripheral T and B cells and sustained production of autoantibodies in NOD/LtSzscid/IL-2Rγ-/- mice. *European Journal of Immunology*, *44*(11), 3453–3463. https://doi.org/10.1002/eji.201444729

Ivashkiv, L. B., & Donlin, L. T. (2014). Regulation of type I interferon responses. *Nature Reviews. Immunology*, *14*(1), 36–49. https://doi.org/10.1038/nri3581

Iwasaki, A., & Medzhitov, R. (2004). Toll-like receptor control of the adaptive immune responses. *Nature Immunology*, *5*(10), 987–995. https://doi.org/10.1038/ni1112

Jaax, N. K., Davis, K. J., Geisbert, T. J., Vogel, P., Jaax, G. P., Topper, M., & Jahrling, P. B. (1996). Lethal experimental infection of rhesus monkeys with Ebola-Zaire (Mayinga) virus by the oral and conjunctival route of exposure. *Archives of Pathology & Laboratory Medicine*, *120*(2), 140–155.

Jacob, S. T., Crozier, I., Fischer, W. A., Hewlett, A., Kraft, C. S., Vega, M. A. de La, Soka, M. J., Wahl, V., Griffiths, A., Bollinger, L., & Kuhn, J. H. (2020). Ebola virus disease. In *Nature Reviews Disease Primers* (Vol. 6, Issue 1). Nature Research. https://doi.org/10.1038/s41572-020-0147-3

Jacobs, M., Rodger, A., Bell, D. J., Bhagani, S., Cropley, I., Filipe, A., Gifford, R. J., Hopkins, S., Hughes, J., Jabeen, F., Johannessen, I., Karageorgopoulos, D., Lackenby, A., Lester, R., Liu, R. S. N., MacConnachie, A., Mahungu, T., Martin, D., Marshall, N., … Thomson, E. C. (2016). Late Ebola virus relapse causing meningoencephalitis: a case report. *The Lancet*, *388*(10043), 498–503. https://doi.org/10.1016/S0140-6736(16)30386-5

Jahrling, P. B., Geisbert, T. W., Johnson, E. D., Peters, C. J., Dalgard, D. W., & Hall, W. C. (1990). Preliminary report: isolation of Ebola virus from monkeys imported to USA. *The Lancet*, *335*(8688), 502–505. https://doi.org/10.1016/0140-6736(90)90737-P

Jasenosky, L. D., Neumann, G., Lukashevich, I., & Kawaoka, Y. (2001). Ebola virus VP40-induced particle formation and association with the lipid bilayer. *Journal of Virology*, *75*(11), 5205–5214. https://doi.org/10.1128/JVI.75.11.5205-5214.2001

Jenner, W., Motwani, M., Veighey, K., Newson, J., Audzevich, T., Nicolaou, A., Murphy, S., MacAllister, R., & Gilroy, D. W. (2014). Characterisation of Leukocytes in a Human Skin Blister Model of Acute Inflammation and Resolution. *PLoS ONE*, *9*(3), e89375. https://doi.org/10.1371/journal.pone.0089375

Johnson, D. M., Brasel, T., Massey, S., Smith, J., Garron, T., Wallace, S., Yu, X., Beasley, D. W., & Comer, J. E. (2023). Characterization of Ebola Virus Mucosal Challenge Routes in Cynomolgus Macaques. *Journal of Virology*, *97*(5). https://doi.org/10.1128/jvi.01888-22

Johnson, K. M., Lange, J. V., Webb, P. A., & Murphy, F. A. (1977). ISOLATION AND PARTIAL CHARACTERISATION OF A NEW VIRUS CAUSING ACUTE HÆMORRHAGIC FEVER IN ZAIRE. *The Lancet*, *309*(8011), 569–571. https://doi.org/10.1016/S0140-6736(77)92000-1

Jongbloed, S. L., Kassianos, A. J., McDonald, K. J., Clark, G. J., Ju, X., Angel, C. E., Chen, C.-J. J., Dunbar, P. R., Wadley, R. B., Jeet, V., Vulink, A. J. E., Hart, D. N. J., & Radford, K. J. (2010). Human CD141+ (BDCA-3)+ dendritic cells (DCs) represent a unique myeloid DC subset that cross-presents necrotic cell antigens. *The Journal of Experimental Medicine*, *207*(6), 1247–1260. https://doi.org/10.1084/jem.20092140

Jouvenet, N., Neil, S. J. D., Zhadina, M., Zang, T., Kratovac, Z., Lee, Y., McNatt, M., Hatziioannou, T., & Bieniasz, P. D. (2009). Broad-spectrum inhibition of retroviral and filoviral particle release by tetherin. *Journal of Virology*, *83*(4), 1837–1844. https://doi.org/10.1128/JVI.02211-08

Kaletsky, R. L., Francica, J. R., Agrawal-Gamse, C., & Bates, P. (2009). Tetherin-mediated restriction of filovirus budding is antagonized by the Ebola glycoprotein. *Proceedings of the National Academy of Sciences of the United States of America*, *106*(8), 2886–2891. https://doi.org/10.1073/pnas.0811014106

Kaufmann, D. E., Kavanagh, D. G., Pereyra, F., Zaunders, J. J., Mackey, E. W., Miura, T., Palmer, S., Brockman, M., Rathod, A., Piechocka-Trocha, A., Baker, B., Zhu, B., Le Gall, S., Waring, M. T., Ahern, R., Moss, K., Kelleher, A. D., Coffin, J. M., Freeman, G. J., … Walker, B. D. (2007). Upregulation of CTLA-4 by HIV-specific CD4+ T cells correlates with disease progression and defines a reversible immune dysfunction. *Nature Immunology*, *8*(11), 1246–1254. https://doi.org/10.1038/ni1515

Kerber, R., Krumkamp, R., Korva, M., Rieger, T., Wurr, S., Duraffour, S., Oestereich, L., Gabriel, M., Sissoko, D., Anglaret, X., Malvy, D., May, J., Zupanc, T. A., Muñoz-Fontela, C., & Günther, S. (2018). Kinetics of Soluble Mediators of the Host Response in Ebola Virus Disease. *Journal of Infectious Diseases*, *218*, S496–S503. https://doi.org/10.1093/infdis/jiy429

Khan, A. S., Tshioko, F. K., Heymann, D. L., Le Guenno, B., Nabeth, P., Kerstiëns, B., Fleerackers, Y., Kilmarx, P. H., Rodier, G. R., Nkuku, O., Rollin, P. E., Sanchez, A., Zaki, S. R., Swanepoel, R., Tomori, O., Nichol, S. T., Peters, C. J., Muyembe-Tamfum, J. J., & Ksiazek, T. G. (1999). The reemergence of Ebola hemorrhagic fever, Democratic Republic of the Congo, 1995. Commission de Lutte contre les Epidémies à Kikwit. *The Journal of Infectious Diseases*, *179 Suppl 1*, S76-86. https://doi.org/10.1086/514306

King, M. A., Covassin, L., Brehm, M. A., Racki, W., Pearson, T., Leif, J., Laning, J., Fodor, W., Foreman, O., Burzenski, L., Chase, T. H., Gott, B., Rossini, A. A., Bortell, R., Shultz, L. D., & Greiner, D. L. (2009). Human peripheral blood leucocyte non-obese diabetic-severe combined immunodeficiency interleukin-2 receptor gamma chain gene mouse model of xenogeneic graft-versus-host-like disease and the role of host major histocompatibility complex. *Clinical and Experimental Immunology*, *157*(1), 104–118. https://doi.org/10.1111/j.1365-2249.2009.03933.x

Koch, T., Rottstegge, M., Ruibal, P., Gomez-Medina, S., Nelson, E. V., Escudero-Pérez, B., Pillny, M., Ly, M. L., Koundouno, F. R., Bore, J. A., Magassouba, N., Dahlke, C., Günther, S., Carroll, M. W., Addo, M. M., & Muñoz-Fontela, C. (2020). Ebola virus disease survivors show more efficient antibody immunity than vaccinees despite similar levels of circulating immunoglobulins. *Viruses*, *12*(9). https://doi.org/10.3390/v12090915

Koyama, S., Ishii, K. J., Coban, C., & Akira, S. (2008). Innate immune response to viral infection. In *Cytokine* (Vol. 43, Issue 3, pp. 336–341). https://doi.org/10.1016/j.cyto.2008.07.009

Kreuels, B., Wichmann, D., Emmerich, P., Schmidt-Chanasit, J., de Heer, G., Kluge, S., Sow, A., Renné, T., Günther, S., Lohse, A. W., Addo, M. M., & Schmiedel, S. (2014). A Case of Severe Ebola Virus Infection Complicated by Gram-Negative Septicemia. *New England Journal of Medicine*, *371*(25), 2394–2401. https://doi.org/10.1056/nejmoa1411677

Ksiazek, T. G., Rollin, P. E., Williams, A. J., Bressler, D. S., Martin, M. L., Swanepoel, R., Burt, F. J., Leman, P. A., Khan, A. S., Rowe, A. K., Mukunu, R., Sanchez, A., & Peters, C. J. (1999). Clinical Virology of Ebola Hemorrhagic Fever (EHF): Virus, Virus Antigen, and IgG and IgM Antibody Findings among EHF Patients in Kikwit, Democratic Republic of the Congo, 1995. *The Journal of Infectious Diseases*, *179*(s1), S177–S187. https://doi.org/10.1086/514321

Kuhn, J. H., Amarasinghe, G. K., Basler, C. F., Bavari, S., Bukreyev, A., Chandran, K., Crozier, I., Dolnik, O., Dye, J. M., Formenty, P. B. H., Griffiths, A., Hewson, R., Kobinger, G. P., Leroy, E. M., Mühlberger, E., Netesov, S. V., Palacios, G., Palyi, B., Pawęska, J. T., … Orton, R. J. (2019). ICTV virus taxonomy profile: Filoviridae. *Journal of General Virology*, *100*(6), 911–912. https://doi.org/10.1099/jgv.0.001252

Kumar, H., Kawai, T., & Akira, S. (2011). Pathogen recognition by the innate immune system. *International Reviews of Immunology*, *30*(1), 16–34. https://doi.org/10.3109/08830185.2010.529976

Kurosaki, T., Kometani, K., & Ise, W. (2015). Memory B cells. *Nature Reviews Immunology*, *15*(3), 149–159. https://doi.org/10.1038/nri3802

Lanini, S., Portella, G., Vairo, F., Kobinger, G. P., Pesenti, A., Langer, M., Kabia, S., Brogiato, G., Amone, J., Castilletti, C., Miccio, R., Zumla, A., Capobianchi, M. R., Di Caro, A., Strada, G., & Ippolito, G. (2015). Blood kinetics of Ebola virus in survivors and nonsurvivors. *Journal of Clinical Investigation*, *125*(12), 4692–4698. https://doi.org/10.1172/JCI83111

Laydon, D. J., Bangham, C. R. M., & Asquith, B. (2015). Estimating T-cell repertoire diversity: limitations of classical estimators and a new approach. *Philosophical Transactions of the Royal Society of London. Series B, Biological Sciences*, *370*(1675). https://doi.org/10.1098/rstb.2014.0291

Le Bon, A., & Tough, D. F. (2002). Links between innate and adaptive immunity via type I interferon. *Current Opinion in Immunology*, *14*(4), 432–436. https://doi.org/10.1016/S0952-7915(02)00354-0

Le Guenno, B., Formenty, P., Wyers, M., Gounon, P., Walker, F., & Boesch, C. (1995). Isolation and partial characterisation of a new strain of Ebola virus. *The Lancet*, *345*(8960), 1271–1274. https://doi.org/10.1016/S0140-6736(95)90925-7

Leligdowicz, A., Fischer, W. A., Uyeki, T. M., Fletcher, T. E., Adhikari, N. K. J., Portella, G., Lamontagne, F., Clement, C., Jacob, S. T., Rubinson, L., Vanderschuren, A., Hajek, J., Murthy, S., Crozier, I., Ibrahima, E., Lamah, M. C., Schieffelin, J. S., Brett-Major, D., Bausch, D. G., … Fowler, R. A. (2016). Ebola virus disease and critical illness. *Critical Care*, *20*(1). https://doi.org/10.1186/s13054-016-1325-2

Leroy, E. M., Epelboin, A., Mondonge, V., Pourrut, X., Gonzalez, J.-P., Muyembe-Tamfum, J.-J., & Formenty, P. (2009). Human Ebola outbreak resulting from direct exposure to fruit bats in Luebo, Democratic Republic of Congo, 2007. *Vector Borne and Zoonotic Diseases (Larchmont, N.Y.)*, *9*(6), 723–728. https://doi.org/10.1089/vbz.2008.0167

Leroy, E. M., Kumulungui, B., Pourrut, X., Rouquet, P., Hassanin, A., Yaba, P., Délicat, A., Paweska, J. T., Gonzalez, J.-P., & Swanepoel, R. (2005). Fruit bats as reservoirs of Ebola virus. *Nature*, *438*(7068), 575–576. https://doi.org/10.1038/438575a

Leung, L. W., Martinez, O., Reynard, O., Volchkov, V. E., & Basler, C. F. (2011a). Ebola Virus Failure to Stimulate Plasmacytoid Dendritic Cell Interferon Responses Correlates With Impaired Cellular Entry. *The Journal of Infectious Diseases*, *204*(suppl_3), S973–S977. https://doi.org/10.1093/infdis/jir331

Leung, L. W., Park, M.-S., Martinez, O., Valmas, C., López, C. B., & Basler, C. F. (2011b). Ebolavirus VP35 suppresses IFN production from conventional but not plasmacytoid dendritic cells. *Immunology and Cell Biology*, *89*(7), 792–802. https://doi.org/10.1038/icb.2010.169

Levy, D. E., & García-Sastre, A. (2001). The virus battles: IFN induction of the antiviral state and mechanisms of viral evasion. In *Cytokine & Growth Factor Reviews* (Vol. 12). www.elsevier.com/locate/cytogfr

Lindgren, T., Ahlm, C., Mohamed, N., Evander, M., Ljunggren, H.-G., & Björkström, N. K. (2011). Longitudinal Analysis of the Human T Cell Response during Acute Hantavirus Infection. *Journal of Virology*, *85*(19), 10252–10260. https://doi.org/10.1128/JVI.05548-11

Loetscher, M., Gerber, B., Loetscher, P., Jones, S. A., Piali, L., Clark-Lewis, I., Baggiolini, M., & Moser, B. (1996). Chemokine receptor specific for IP10 and mig: structure, function, and expression in activated T-lymphocytes. *The Journal of Experimental Medicine*, *184*(3), 963–969. https://doi.org/10.1084/jem.184.3.963

Lu, L. L., Suscovich, T. J., Fortune, S. M., & Alter, G. (2018). Beyond binding: Antibody effector functions in infectious diseases. In *Nature Reviews Immunology* (Vol. 18, Issue 1, pp. 46–61). Nature Publishing Group. https://doi.org/10.1038/nri.2017.106

Luczkowiak, J., Lasala, F., Mora-Rillo, M., Arribas, J. R., & Delgado, R. (2018). Broad Neutralizing Activity Against Ebolaviruses Lacking the Mucin-Like Domain in Convalescent Plasma Specimens from Patients with Ebola Virus Disease. *Journal of Infectious Diseases*, *218*, S574–S581. https://doi.org/10.1093/infdis/jiy302

Lüdtke, A., Oestereich, L., Ruibal, P., Wurr, S., Pallasch, E., Bockholt, S., Ip, W. H., Rieger, T., Gómez-Medina, S., Stocking, C., Rodríguez, E., Günther, S., & Muñoz-Fontela, C. (2015). Ebola Virus Disease in Mice with Transplanted Human Hematopoietic Stem Cells. *Journal of Virology*, *89*(8), 4700–4704. https://doi.org/10.1128/jvi.03546-14

Lüdtke, A., Ruibal, P., Becker-Ziaja, B., Rottstegge, M., Wozniak, D. M., Cabeza-Cabrerizo, M., Thorenz, A., Weller, R., Kerber, R., Idoyaga, J., Magassouba, N., Gabriel, M., Günther, S., Oestereich, L., & Muñoz-Fontela, C. (2016). Ebola Virus Disease Is Characterized by Poor Activation and Reduced Levels of Circulating CD16 $^{+}$ Monocytes. *Journal of Infectious Diseases*, *214*(suppl 3), S275–S280. https://doi.org/10.1093/infdis/jiw260

Lüdtke, A., Ruibal, P., Wozniak, D. M., Pallasch, E., Wurr, S., Bockholt, S., Gómez-Medina, S., Qiu, X., Kobinger, G. P., Rodríguez, E., Günther, S., Krasemann, S., Idoyaga, J., Oestereich, L., & Muñoz-Fontela, C. (2017). Ebola virus infection kinetics in chimeric mice reveal a key role of T cells as barriers for virus dissemination. *Scientific Reports*, *7*. https://doi.org/10.1038/srep43776

Luster, A. D., & Ravetch, J. V. (1987). Genomic characterization of a gamma-interferon-inducible gene (IP-10) and identification of an interferon-inducible hypersensitive site. *Molecular and Cellular Biology*, *7*(10), 3723–3731. https://doi.org/10.1128/mcb.7.10.3723-3731.1987

Mahanty, S., Gupta, M., Paragas, J., Bray, M., Ahmed, R., & Rollin, P. E. (2003a). Protection from lethal infection is determined by innate immune responses in a mouse model of Ebola virus infection. *Virology*, *312*(2), 415–424. https://doi.org/10.1016/S0042-6822(03)00233-2

Mahanty, S., Hutchinson, K., Agarwal, S., Mcrae, M., Rollin, P. E., & Pulendran, B. (2003b). *IMMUNOLOGY Cutting Edge: Impairment of Dendritic Cells and Adaptive Immunity by Ebola and Lassa Viruses 1*. http://journals.aai.org/jimmunol/article-pdf/170/6/2797/1170521/2797.pdf

Mao, H., Zhang, L., Yang, Y., Zuo, W., Bi, Y., Gao, W., Deng, B., Sun, J., Shao, Q., & Qu, X. (2010). New insights of CTLA-4 into its biological function in breast cancer. *Current Cancer Drug Targets*, *10*(7), 728–736. https://doi.org/10.2174/156800910793605811

Maruyama, T., Rodriguez, L. L., Jahrling, P. B., Sanchez, A., Khan, A. S., Nichol, S. T., Peters, C. J., Parren, P. W. H. I., & Burton, D. R. (1999). Ebola Virus Can Be Effectively Neutralized by Antibody Produced in Natural Human Infection. In *JOURNAL OF VIROLOGY* (Vol. 73, Issue 7).

Masterson, A. J., Sombroek, C. C., de Gruijl, T. D., Graus, Y. M. F., van der Vliet, H. J. J., Lougheed, S. M., van den Eertwegh, A. J. M., Pinedo, H. M., & Scheper, R. J. (2002). MUTZ-3, a human cell line model for the cytokine-induced differentiation of dendritic cells from CD34+precursors. *Blood*, *100*(2), 701–703. https://doi.org/10.1182/blood.V100.2.701

Mate, S. E., Kugelman, J. R., Nyenswah, T. G., Ladner, J. T., Wiley, M. R., Cordier-Lassalle, T., Christie, A., Schroth, G. P., Gross, S. M., Davies-Wayne, G. J., Shinde, S. A., Murugan, R., Sieh, S. B., Badio, M., Fakoli, L., Taweh, F., de Wit, E., van Doremalen, N., Munster, V. J., … Palacios, G. (2015). Molecular Evidence of Sexual Transmission of Ebola Virus. *New England Journal of Medicine*, *373*(25), 2448–2454. https://doi.org/10.1056/NEJMoa1509773

McCormick, J. B., Bauer, S. P., Elliott, L. H., Webb, P. A., & Johnson, K. M. (1983). Biologic Differences Between Strains of Ebola Virus from Zaire and Sudan. *Journal of Infectious Diseases*, *147*(2), 264–267. https://doi.org/10.1093/infdis/147.2.264

McElroy, A. K., Akondy, R. S., Davis, C. W., Ellebedy, A. H., Mehta, A. K., Kraft, C. S., Lyon, G. M., Ribner, B. S., Varkey, J., Sidney, J., Sette, A., Campbell, S., Ströher, U., Damon, I., Nichol, S. T., Spiropoulou, C. F., & Ahmed, R. (2015). Human Ebola virus infection results in substantial immune activation. *Proceedings of the National Academy of Sciences of the United States of America*, *112*(15), 4719–4724. https://doi.org/10.1073/pnas.1502619112

McElroy, A. K., Akondy, R. S., Mcllwain, D. R., Chen, H., Bjornson-Hooper, Z., Mukherjee, N., Mehta, A. K., Nolan, G., Nichol, S. T., & Spiropoulou, C. F. (2020). Immunologic timeline of Ebola virus disease and recovery in humans. *JCI Insight*, *5*(10). https://doi.org/10.1172/JCI.INSIGHT.137260

McMichael, A. J., Gotch, F. M., Noble, G. R., & Beare, P. A. (1983). Cytotoxic T-cell immunity to influenza. *The New England Journal of Medicine*, *309*(1), 13–17. https://doi.org/10.1056/NEJM198307073090103

McNally, B., Ye, F., Willette, M., & Flaño, E. (2013). Local Blockade of Epithelial PDL-1 in the Airways Enhances T Cell Function and Viral Clearance during Influenza Virus Infection. *Journal of Virology*, *87*(23), 12916–12924. https://doi.org/10.1128/JVI.02423-13

Mehedi, M., Falzarano, D., Seebach, J., Hu, X., Carpenter, M. S., Schnittler, H.-J., & Feldmann, H. (2011). A New Ebola Virus Nonstructural Glycoprotein Expressed through RNA Editing. *Journal of Virology*, *85*(11), 5406–5414. https://doi.org/10.1128/JVI.02190-10

Meylan, E., Tschopp, J., & Karin, M. (2006). Intracellular pattern recognition receptors in the host response. In *Nature* (Vol. 442, Issue 7098, pp. 39–44). Nature Publishing Group. https://doi.org/10.1038/nature04946

Miller, J. D., van der Most, R. G., Akondy, R. S., Glidewell, J. T., Albott, S., Masopust, D., Murali-Krishna, K., Mahar, P. L., Edupuganti, S., Lalor, S., Germon, S., Del Rio, C., Mulligan, M. J., Staprans, S. I., Altman, J. D., Feinberg, M. B., & Ahmed, R. (2008). Human effector and memory CD8+ T cell responses to smallpox and yellow fever vaccines. *Immunity*, *28*(5), 710–722. https://doi.org/10.1016/j.immuni.2008.02.020

Mohammed, A., Sheikh, T. L., Gidado, S., Poggensee, G., Nguku, P., Olayinka, A., Ohuabunwo, C., Waziri, N., Shuaib, F., Adeyemi, J., Uzoma, O., Ahmed, A., Doherty, F., Nyanti, S. B., Nzuki, C. K., Nasidi, A., Oyemakinde, A., Oguntimehin, O., Abdus-Salam, I. A., & Obiako, R. O. (2015). An evaluation of psychological distress and social support of survivors and contacts of Ebola virus disease infection and their relatives in Lagos, Nigeria: A cross sectional study - 2014. *BMC Public Health*, *15*(1). https://doi.org/10.1186/s12889-015-2167-6

Moreau, M., Spencer, C., Gozalbes, J. G., Colebunders, R., Lefevre, A., Gryseels, S., Borremans, B., Gunther, S., Becker, D., Bore, J. A., Koundouno, F. R., Di Caro, A., Wölfel, R., Decroo, T., Van

Herp, M., Peetermans, L., & Camara, A. M. (2015). Lactating mothers infected with Ebola virus: EBOV RT-PCR of blood only may be insufficient. *Eurosurveillance*, *20*(3). https://doi.org/10.2807/1560-7917.ES2015.20.3.21017

Mühlberger, E., Weik, M., Volchkov, V. E., Klenk, H.-D., & Becker, S. (1999). Comparison of the Transcription and Replication Strategies of Marburg Virus and Ebola Virus by Using Artificial Replication Systems. *Journal of Virology*, *73*(3), 2333–2342. https://doi.org/10.1128/JVI.73.3.2333-2342.1999

Murphy, F.A., van der Groen, G., Whitfield, S.G., an Lange, J.V. (1978). Ebola and Marburg virus morphology and taxonomy. *Ebola virus haemorrhagic fever*, 61-82.

Nanyonga, M., Saidu, J., Ramsay, A., Shindo, N., & Bausch, D. G. (2016). Sequelae of Ebola Virus Disease, Kenema District, Sierra Leone. In *Clinical Infectious Diseases* (Vol. 62, Issue 1, pp. 125–126). Oxford University Press. https://doi.org/10.1093/cid/civ795

Neil, S. J. D. (2013). *The Antiviral Activities of Tetherin* (pp. 67–104). https://doi.org/10.1007/978-3-642-37765-5_3

Nicastri, E., Kobinger, G., Vairo, F., Montaldo, C., Mboera, L. E. G., Ansunama, R., Zumla, A., & Ippolito, G. (2019). Ebola Virus Disease: Epidemiology, Clinical Features, Management, and Prevention. In *Infectious Disease Clinics of North America* (Vol. 33, Issue 4, pp. 953–976). W.B. Saunders. https://doi.org/10.1016/j.idc.2019.08.005

Nicolini, F. E., Cashman, J. D., Hogge, D. E., Humphries, R. K., & Eaves, C. J. (2004). NOD/SCID mice engineered to express human IL-3, GM-CSF and Steel factor constitutively mobilize engrafted human progenitors and compromise human stem cell regeneration. *Leukemia*, *18*(2), 341–347. https://doi.org/10.1038/sj.leu.2403222

Noda, T., Hagiwara, K., Sagara, H., & Kawaoka, Y. (2010). Characterization of the Ebola virus nucleoprotein-RNA complex. *The Journal of General Virology*, *91*(Pt 6), 1478–1483. https://doi.org/10.1099/vir.0.019794-0

Noda, T., Sagara, H., Suzuki, E., Takada, A., Kida, H., & Kawaoka, Y. (2002). Ebola virus VP40 drives the formation of virus-like filamentous particles along with GP. *Journal of Virology*, *76*(10), 4855–4865. https://doi.org/10.1128/jvi.76.10.4855-4865.2002

Oestereich, L., Lüdtke, A., Ruibal, P., Pallasch, E., Kerber, R., Rieger, T., Wurr, S., Bockholt, S., Pérez-Girón, J. V., Krasemann, S., Günther, S., & Muñoz-Fontela, C. (2016). Chimeric Mice with Competent Hematopoietic Immunity Reproduce Key Features of Severe Lassa Fever. *PLOS Pathogens*, *12*(5), e1005656. https://doi.org/10.1371/journal.ppat.1005656

Oswald, W. B., Geisbert, T. W., Davis, K. J., Geisbert, J. B., Sullivan, N. J., Jahrling, P. B., Parren, P. W. H. I., & Burton, D. R. (2007). Neutralizing antibody fails to impact the course of Ebola virus infection in monkeys. *PLoS Pathogens*, *3*(1), 0062–0066. https://doi.org/10.1371/journal.ppat.0030009

Parra, M., Herrera, D., Calvo-Calle, J. M., Stern, L. J., Parra-López, C. A., Butcher, E., Franco, M., & Angel, J. (2014). Circulating human rotavirus specific CD4 T cells identified with a class II tetramer express the intestinal homing receptors α4β7 and CCR9. *Virology*, *452–453*, 191–201. https://doi.org/10.1016/j.virol.2014.01.014

Parren, P. W. H. I., Geisbert, T. W., Maruyama, T., Jahrling, P. B., & Burton, D. R. (2002). Pre- and Postexposure Prophylaxis of Ebola Virus Infection in an Animal Model by Passive Transfer of a Neutralizing Human Antibody. *Journal of Virology*, *76*(12), 6408–6412. https://doi.org/10.1128/jvi.76.12.6408-6412.2002

Pattyn, S., Groen, G. vander, Jacob, W., Piot, P., & Courteille, G. (1977). ISOLATION OF MARBURG-LIKE VIRUS FROM A CASE OF HÆMORRHAGIC FEVER IN ZAIRE. *The Lancet*, *309*(8011), 573–574. https://doi.org/10.1016/S0140-6736(77)92002-5

Peters, P. J., Borst, J., Oorschot, V., Fukuda, M., Krähenbühl, O., Tschopp, J., Slot, J. W., & Geuze, H. J. (1991). Cytotoxic T lymphocyte granules are secretory lysosomes, containing both perforin and granzymes. *The Journal of Experimental Medicine*, *173*(5), 1099–1109. https://doi.org/10.1084/jem.173.5.1099

Ploquin, A., Zhou, Y., & Sullivan, N. J. (2018). Ebola Immunity: Gaining a Winning Position in Lightning Chess. *The Journal of Immunology*, *201*(3), 833–842. https://doi.org/10.4049/jimmunol.1700827

Port, J. R., Wozniak, D. M., Oestereich, L., Pallasch, E., Becker-Ziaja, B., Müller, J., Rottstegge, M., Olal, C., Gómez-Medina, S., Oyakhliome, J., Ighodalo, Y., Omomoh, E., Olokor, T., Adomeh, D. I., Asogun, D., Ogbani-Emovon, E., Hartmann, K., Krasemann, S., Nelson, E. V., … Muñoz-Fontela, C. (2020). Severe Human Lassa Fever Is Characterized by Nonspecific T-Cell Activation and Lymphocyte Homing to Inflamed Tissues. *Journal of Virology*, *94*(21). https://doi.org/10.1128/JVI.01367-20

Prescott, J., Falzarano, D., & Feldmann, H. (2015). Natural Immunity to Ebola Virus in the Syrian Hamster Requires Antibody Responses. *The Journal of Infectious Diseases*, *212 Suppl 2*(Suppl 2), S271-6. https://doi.org/10.1093/infdis/jiv203

Qureshi, A. I., Chughtai, M., Loua, T. O., Pe Kolie, J., Camara, H. F. S., Ishfaq, M. F., N'Dour, C. T., & Beavogui, K. (2015). Study of Ebola Virus Disease Survivors in Guinea. *Clinical Infectious Diseases*, *61*(7), 1035–1042. https://doi.org/10.1093/cid/civ453

Raymond, J., Bradfute, S., & Bray, M. (2011). Filovirus infection of STAT-1 knockout mice. *Journal of Infectious Diseases*, *204*(SUPPL. 3). https://doi.org/10.1093/infdis/jir335

Reardon, S. (2015). Ebola's mental-health wounds linger in Africa. *Nature*, *519*(7541), 13–14. https://doi.org/10.1038/519013a

Reed, D. S., Hensley, L. E., Geisbert, J. B., Jahrling, P. B., & Geisbert, T. W. (2004). Depletion of peripheral blood T lymphocytes and NK cells during the course of ebola hemorrhagic Fever in cynomolgus macaques. *Viral Immunology*, *17*(3), 390–400. https://doi.org/10.1089/vim.2004.17.390

Reed, D. S., Lackemeyer, M. G., Garza, N. L., Sullivan, L. J., & Nichols, D. K. (2011). Aerosol exposure to Zaire ebolavirus in three nonhuman primate species: differences in disease course and clinical pathology. *Microbes and Infection*, *13*(11), 930–936. https://doi.org/10.1016/j.micinf.2011.05.002

Reid, S. P., Leung, L. W., Hartman, A. L., Martinez, O., Shaw, M. L., Carbonnelle, C., Volchkov, V. E., Nichol, S. T., & Basler, C. F. (2006). Ebola virus VP24 binds karyopherin alpha1 and blocks STAT1 nuclear accumulation. *Journal of Virology*, *80*(11), 5156–5167. https://doi.org/10.1128/JVI.02349-05

Report of a WHO/International Study Team. (1978). Ebola haemorrhagic fever in Sudan, 1976. Report of a WHO/International Study Team. *Bulletin of the World Health Organization*, *56*(2), 247–270.

Report of an International Commission. (1978). Ebola haemorrhagic fever in Zaire, 1976. *Bulletin of the World Health Organization*, *56*(2), 271–293.

Rittmeyer, A., Barlesi, F., Waterkamp, D., Park, K., Ciardiello, F., von Pawel, J., Gadgeel, S. M., Hida, T., Kowalski, D. M., Dols, M. C., Cortinovis, D. L., Leach, J., Polikoff, J., Barrios, C., Kabbinavar, F., Frontera, O. A., De Marinis, F., Turna, H., Lee, J.-S., … Gandara, D. R. (2017). Atezolizumab versus docetaxel in patients with previously treated non-small-cell lung cancer (OAK): a phase 3, open-

label, multicentre randomised controlled trial. *The Lancet*, *389*(10066), 255–265. https://doi.org/10.1016/S0140-6736(16)32517-X

Robert, C., Schachter, J., Long, G. V., Arance, A., Grob, J. J., Mortier, L., Daud, A., Carlino, M. S., McNeil, C., Lotem, M., Larkin, J., Lorigan, P., Neyns, B., Blank, C. U., Hamid, O., Mateus, C., Shapira-Frommer, R., Kosh, M., Zhou, H., … Ribas, A. (2015). Pembrolizumab versus Ipilimumab in Advanced Melanoma. *New England Journal of Medicine*, *372*(26), 2521–2532. https://doi.org/10.1056/NEJMoa1503093

Roels, T. H., Bloom, A. S., Buffington, J., Muhungu, G. L., Mac Kenzie, W. R., Khan, A. S., Ndambi, R., Noah, D. L., Rolka, H. R., Peters, C. J., & Ksiazek, T. G. (1999). Ebola Hemorrhagic Fever, Kikwit, Democratic Republic of the Congo, 1995: Risk Factors for Patients without a Reported Exposure. *The Journal of Infectious Diseases*, *179*(s1), S92–S97. https://doi.org/10.1086/514286

Rojek, A., Horby, P., & Dunning, J. (2017). Insights from clinical research completed during the west Africa Ebola virus disease epidemic. In *The Lancet Infectious Diseases* (Vol. 17, Issue 9, pp. e280–e292). Lancet Publishing Group. https://doi.org/10.1016/S1473-3099(17)30234-7

Rott, L. S., Rosé, J. R., Bass, D., Williams, M. B., Greenberg, H. B., & Butcher, E. C. (1997). Expression of mucosal homing receptor alpha4beta7 by circulating CD4+ cells with memory for intestinal rotavirus. *Journal of Clinical Investigation*, *100*(5), 1204–1208. https://doi.org/10.1172/JCI119633

Rottstegge, M. (2016). Developing of tools for functional analysis of human Ebola virus immunology. University of Lübeck

Rowe, A. K., Bertolli, J., Khan, A. S., Mukunu, R., Muyembe-Tamfum, J. J., Bressler, D., Williams, A. J., Peters, C. J., Rodriguez, L., Feldmann, H., Nichol, S. T., Rollin, P. E., & Ksiazek, T. G. (1999). Clinical, Virologic, and Immunologic Follow-Up of Convalescent Ebola Hemorrhagic Fever Patients and Their Household Contacts, Kikwit, Democratic Republic of the Congo. *The Journal of Infectious Diseases*, *179*(s1), S28–S35. https://doi.org/10.1086/514318

Ruibal, P., Oestereich, L., Ludtke, A., Becker-Ziaja, B., Wozniak, D. M., Kerber, R., Korva, M., Cabeza-Cabrerizo, M., Bore, J. A., Koundouno, F. R., Duraffour, S., Weller, R., Thorenz, A., Cimini, E., Viola, D., Agrati, C., Repits, J., Afrough, B., Cowley, L. A., … Munoz-Fontela, C. (2016). Unique human immune signature of Ebola virus disease in Guinea. *Nature*, *533*(7601), 100–104. https://doi.org/10.1038/nature17949

Sackstein, R., Schatton, T., & Barthel, S. R. (2017). T-lymphocyte homing: an underappreciated yet critical hurdle for successful cancer immunotherapy. *Laboratory Investigation*, *97*(6), 669–697. https://doi.org/10.1038/labinvest.2017.25

Sadler, A. J., & Williams, B. R. G. (2008). Interferon-inducible antiviral effectors. *Nature Reviews. Immunology*, *8*(7), 559–568. https://doi.org/10.1038/nri2314

Saito, T., & Gale, M. (2007). Principles of intracellular viral recognition. In *Current Opinion in Immunology* (Vol. 19, Issue 1, pp. 17–23). https://doi.org/10.1016/j.coi.2006.11.003

Sakabe, S., Sullivan, B. M., Hartnett, J. N., Robles-Sikisaka, R., Gangavarapu, K., Cubitt, B., Ware, B. C., Kotliar, D., Branco, L. M., Goba, A., Momoh, M., Sandi, J. D., Kanneh, L., Grant, D. S., Garry, R. F., Andersen, K. G., De La Torre, J. C., Sabeti, P. C., Schieffelin, J. S., & Oldstone, M. B. A. (2018). Analysis of CD8+ T cell response during the 2013–2016 Ebola epidemic in West Africa. *Proceedings of the National Academy of Sciences of the United States of America*, *115*(32), E7578–E7586. https://doi.org/10.1073/pnas.1806200115

Sallusto, F., & Lanzavecchia, A. (1994). Efficient presentation of soluble antigen by cultured human dendritic cells is maintained by granulocyte/macrophage colony-stimulating factor plus interleukin 4

and downregulated by tumor necrosis factor alpha. *The Journal of Experimental Medicine*, *179*(4), 1109–1118. https://doi.org/10.1084/jem.179.4.1109

Sallusto, F., Lenig, D., Mackay, C. R., & Lanzavecchia, A. (1998). Flexible Programs of Chemokine Receptor Expression on Human Polarized T Helper 1 and 2 Lymphocytes. *The Journal of Experimental Medicine*, *187*(6), 875–883. https://doi.org/10.1084/jem.187.6.875

Samuel, C. E. (2001). Antiviral actions of interferons. In *Clinical Microbiology Reviews* (Vol. 14, Issue 4, pp. 778–809). https://doi.org/10.1128/CMR.14.4.778-809.2001

Sanchez, A., Kiley, M. P., Holloway, B. P., & Auperin, D. D. (1993). Sequence analysis of the Ebola virus genome: organization, genetic elements, and comparison with the genome of Marburg virus. *Virus Research*, *29*(3), 215–240. https://doi.org/10.1016/0168-1702(93)90063-S

Sanchez, A., Lukwiya, M., Bausch, D., Mahanty, S., Sanchez, A. J., Wagoner, K. D., & Rollin, P. E. (2004). Analysis of human peripheral blood samples from fatal and nonfatal cases of Ebola (Sudan) hemorrhagic fever: cellular responses, virus load, and nitric oxide levels. *Journal of Virology*, *78*(19), 10370–10377. https://doi.org/10.1128/JVI.78.19.10370-10377.2004

Schietinger, A., & Greenberg, P. D. (2014). Tolerance and exhaustion: defining mechanisms of T cell dysfunction. *Trends in Immunology*, *35*(2), 51–60. https://doi.org/10.1016/j.it.2013.10.001

Schnittler, H., & Feldmann, H. (1998). Marburg and Ebola Hemorrhagic Fevers: Does the Primary Course of Infection Depend on the Accessibility of Organ-Specific Macrophages? *Clinical Infectious Diseases*, *27*(2), 404–406. https://doi.org/10.1086/517704

Sharma, P., & Allison, J. P. (2015). Immune checkpoint targeting in cancer therapy: toward combination strategies with curative potential. *Cell*, *161*(2), 205–214. https://doi.org/10.1016/j.cell.2015.03.030

Shultz, L. D., Lyons, B. L., Burzenski, L. M., Gott, B., Chen, X., Chaleff, S., Kotb, M., Gillies, S. D., King, M., Mangada, J., Greiner, D. L., & Handgretinger, R. (2005). Human lymphoid and myeloid cell development in NOD/LtSz-scid IL2R gamma null mice engrafted with mobilized human hemopoietic stem cells. *Journal of Immunology (Baltimore, Md.: 1950)*, *174*(10), 6477–6489. https://doi.org/10.4049/jimmunol.174.10.6477

Shultz, L. D., Saito, Y., Najima, Y., Tanaka, S., Ochi, T., Tomizawa, M., Doi, T., Sone, A., Suzuki, N., Fujiwara, H., Yasukawa, M., & Ishikawa, F. (2010). Generation of functional human T-cell subsets with HLA-restricted immune responses in HLA class I expressing NOD/SCID/IL2rγnull humanized mice. *Proceedings of the National Academy of Sciences of the United States of America*, *107*(29), 13022–13027. https://doi.org/10.1073/pnas.1000475107

Siegert, R., Shu, H.-L., Slenczka, W., Peters, D., & Müller, G. (1967). Zur Ätiologie einer unbekannten, von Affen ausgegangenen menschlichen Infektionskrankheit. *DMW - Deutsche Medizinische Wochenschrift*, *92*(51), 2341–2343. https://doi.org/10.1055/s-0028-1106144

Simmons, G., Reeves, J. D., Grogan, C. C., Vandenberghe, L. H., Baribaud, F., Whitbeck, J. C., Burke, E., Buchmeier, M. J., Soilleux, E. J., Riley, J. L., Doms, R. W., Bates, P., & Pöhlmann, S. (2003). DC-SIGN and DC-SIGNR bind Ebola glycoproteins and enhance infection of macrophages and endothelial cells. *Virology*, *305*(1), 115–123. https://doi.org/10.1006/viro.2002.1730

Six, A., Mariotti-Ferrandiz, M. E., Chaara, W., Magadan, S., Pham, H.-P., Lefranc, M.-P., Mora, T., Thomas-Vaslin, V., Walczak, A. M., & Boudinot, P. (2013). The past, present, and future of immune repertoire biology - the rise of next-generation repertoire analysis. *Frontiers in Immunology*, *4*, 413. https://doi.org/10.3389/fimmu.2013.00413

Spengler, J. R., Lavender, K. J., Martellaro, C., Carmody, A., Kurth, A., Keck, J. G., Saturday, G., Scott, D. P., Nichol, S. T., Hasenkrug, K. J., Spiropoulou, C. F., Feldmann, H., & Prescott, J. (2016). Ebola Virus Replication and Disease Without Immunopathology in Mice Expressing Transgenes to

Support Human Myeloid and Lymphoid Cell Engraftment. *Journal of Infectious Diseases*, *214*, S308–S318. https://doi.org/10.1093/infdis/jiw248

Spengler, J. R., Saturday, G., Lavender, K. J., Martellaro, C., Keck, J. G., Nichol, S. T., Spiropoulou, C. F., Feldmann, H., & Prescott, J. (2017). Severity of Disease in Humanized Mice Infected With Ebola Virus or Reston Virus Is Associated With Magnitude of Early Viral Replication in Liver. *The Journal of Infectious Diseases*, *217*(1), 58–63. https://doi.org/10.1093/infdis/jix562

Speranza, E., Bixler, S. L., Altamura, L. A., Arnold, C. E., Pratt, W. D., Taylor-Howell, C., Burrows, C., Aguilar, W., Rossi, F., Shamblin, J. D., Wollen, S. E., Zelko, J. M., Minogue, T., Nagle, E., Palacios, G., Arthur, †, Goff, J., & Connor, J. H. (2018a). *A conserved transcriptional response to intranasal Ebola virus exposure in nonhuman primates prior to onset of fever*. http://stm.sciencemag.org/

Speranza, E., Ruibal, P., Port, J. R., Feng, F., Burkhardt, L., Grundhoff, A., Günther, S., Oestereich, L., Hiscox, J. A., Connor, J. H., & Muñoz-Fontela, C. (2018b). T-Cell Receptor Diversity and the Control of T-Cell Homeostasis Mark Ebola Virus Disease Survival in Humans. *Journal of Infectious Diseases*, *218*, S508–S518. https://doi.org/10.1093/infdis/jiy352

Subissi, L., Keita, M., Mesfin, S., Rezza, G., Diallo, B., Van Gucht, S., Musa, E. O., Yoti, Z., Keita, S., Djingarey, M. H., Diallo, A. B., & Fall, I. S. (2018). Ebola Virus Transmission Caused by Persistently Infected Survivors of the 2014-2016 Outbreak in West Africa. *Journal of Infectious Diseases*, *218*, S287–S291. https://doi.org/10.1093/infdis/jiy280

Sullivan, N. J., Hensley, L., Asiedu, C., Geisbert, T. W., Stanley, D., Johnson, J., Honko, A., Olinger, G., Bailey, M., Geisbert, J. B., Reimann, K. A., Bao, S., Rao, S., Roederer, M., Jahrling, P. B., Koup, R. A., & Nabel, G. J. (2011). CD8+ cellular immunity mediates rAd5 vaccine protection against Ebola virus infection of nonhuman primates. *Nature Medicine*, *17*(9), 1128–1131. https://doi.org/10.1038/nm.2447

Sundar, K., Boesen, A., & Coico, R. (2007). Computational prediction and identification of HLA-A2.1-specific Ebola virus CTL epitopes. *Virology*, *360*(2), 257–263. https://doi.org/10.1016/j.virol.2006.09.042

Swiecki, M., & Colonna, M. (2015). The multifaceted biology of plasmacytoid dendritic cells. *Nature Reviews Immunology*, *15*(8), 471–485. https://doi.org/10.1038/nri3865

Takada, A., Fujioka, K., Tsuiji, M., Morikawa, A., Higashi, N., Ebihara, H., Kobasa, D., Feldmann, H., Irimura, T., & Kawaoka, Y. (2004). Human Macrophage C-Type Lectin Specific for Galactose and N -Acetylgalactosamine Promotes Filovirus Entry . *Journal of Virology*, *78*(6), 2943–2947. https://doi.org/10.1128/jvi.78.6.2943-2947.2004

Teijaro, J. R. (2016). Too much of a good thing: Sustained type 1 interferon signaling limits humoral responses to secondary viral infection. *European Journal of Immunology*, *46*(2), 300–302. https://doi.org/10.1002/eji.201546224

Thom, R., Tipton, T., Strecker, T., Hall, Y., Akoi Bore, J., Maes, P., Raymond Koundouno, F., Fehling, S. K., Krähling, V., Steeds, K., Varghese, A., Bailey, G., Matheson, M., Kouyate, S., Coné, M., Moussa Keita, B., Kouyate, S., Richard Ablam, A., Laenen, L., … Carroll, M. W. (2021). Longitudinal antibody and T cell responses in Ebola virus disease survivors and contacts: an observational cohort study. *The Lancet Infectious Diseases*, *21*(4), 507–516. https://doi.org/10.1016/S1473-3099(20)30736-2

Thorson, A. E., Deen, G. F., Bernstein, K. T., Liu, W. J., Yamba, F., Habib, N., Sesay, F. R., Gaillard, P., Massaquoi, T. A., McDonald, S. L. R., Zhang, Y., Durski, K. N., Singaravelu, S., Ervin, E., Liu, H., Coursier, A., Marrinan, J. E., Ariyarajah, A., Carino, M., … Broutet, N. (2021). Persistence of Ebola

virus in semen among Ebola virus disease survivors in Sierra Leone: A cohort study of frequency, duration, and risk factors. *PLoS Medicine*, *18*(2). https://doi.org/10.1371/JOURNAL.PMED.1003273

Tiffany, A., Vetter, P., Mattia, J., Dayer, J. A., Bartsch, M., Kasztura, M., Sterk, E., Tijerino, A. M., Kaiser, L., & Ciglenecki, I. (2016). Ebola virus disease complications as experienced by survivors in Sierra Leone. *Clinical Infectious Diseases*, *62*(11), 1360–1366. https://doi.org/10.1093/cid/ciw158

Tipton, T. R. W., Hall, Y., Bore, J. A., White, A., Sibley, L. S., Sarfas, C., Yuki, Y., Martin, M., Longet, S., Mellors, J., Ewer, K., Günther, S., Carrington, M., Kondé, M. K., & Carroll, M. W. (2021). Characterisation of the T-cell response to Ebola virus glycoprotein amongst survivors of the 2013–16 West Africa epidemic. *Nature Communications*, *12*(1). https://doi.org/10.1038/s41467-021-21411-0

Towner, J. S., Pourrut, X., Albariño, C. G., Nkogue, C. N., Bird, B. H., Grard, G., Ksiazek, T. G., Gonzalez, J.-P., Nichol, S. T., & Leroy, E. M. (2007). Marburg Virus Infection Detected in a Common African Bat. *PLoS ONE*, *2*(8), e764. https://doi.org/10.1371/journal.pone.0000764

Towner, J. S., Sealy, T. K., Khristova, M. L., Albariño, C. G., Conlan, S., Reeder, S. A., Quan, P. L., Lipkin, W. I., Downing, R., Tappero, J. W., Okware, S., Lutwama, J., Bakamutumaho, B., Kayiwa, J., Comer, J. A., Rollin, P. E., Ksiazek, T. G., & Nichol, S. T. (2008). Newly discovered Ebola virus associated with hemorrhagic fever outbreak in Uganda. *PLoS Pathogens*, *4*(11). https://doi.org/10.1371/journal.ppat.1000212

Twenhafel, N. A., Mattix, M. E., Johnson, J. C., Robinson, C. G., Pratt, W. D., Cashman, K. A., Wahl-Jensen, V., Terry, C., Olinger, G. G., Hensley, L. E., & Honko, A. N. (2013). Pathology of experimental aerosol Zaire ebolavirus infection in rhesus macaques. *Veterinary Pathology*, *50*(3), 514–529. https://doi.org/10.1177/0300985812469636

van der Groen, G., Jacob, W., & Pattyn, S. R. (1979). Ebola virus virulence for newborn mice. *Journal of Medical Virology*, *4*(3), 239–240. https://doi.org/10.1002/jmv.1890040309

van Griensven, J., Edwards, T., de Lamballerie, X., Semple, M. G., Gallian, P., Baize, S., Horby, P. W., Raoul, H., Magassouba, N., Antierens, A., Lomas, C., Faye, O., Sall, A. A., Fransen, K., Buyze, J., Ravinetto, R., Tiberghien, P., Claeys, Y., De Crop, M., … Haba, N. (2016). Evaluation of Convalescent Plasma for Ebola Virus Disease in Guinea. *New England Journal of Medicine*, *374*(1), 33–42. https://doi.org/10.1056/nejmoa1511812

Varkey, J. B., Shantha, J. G., Crozier, I., Kraft, C. S., Lyon, G. M., Mehta, A. K., Kumar, G., Smith, J. R., Kainulainen, M. H., Whitmer, S., Ströher, U., Uyeki, T. M., Ribner, B. S., & Yeh, S. (2015). Persistence of Ebola Virus in Ocular Fluid during Convalescence. *New England Journal of Medicine*, *372*(25), 2423–2427. https://doi.org/10.1056/nejmoa1500306

Velásquez, G. E., Aibana, O., Ling, E. J., Diakite, I., Mooring, E. Q., & Murray, M. B. (2015). Time from Infection to Disease and Infectiousness for Ebola Virus Disease, a Systematic Review. In *Clinical Infectious Diseases* (Vol. 61, Issue 7, pp. 1135–1140). Oxford University Press. https://doi.org/10.1093/cid/civ531

Vernet, M.-A., Reynard, S., Fizet, A., Schaeffer, J., Pannetier, D., Guedj, J., Rives, M., Georges, N., Garcia-Bonnet, N., Sylla, A. I., Grovogui, P., Kerherve, J.-Y., Savio, C., Savio-Coste, S., de Séverac, M.-L., Zloczewski, P., Linares, S., Harouna, S., Abdoul, B. M., … Baize, S. (2017). Clinical, virological, and biological parameters associated with outcomes of Ebola virus infection in Macenta, Guinea. *JCI Insight*, *2*(6), e88864. https://doi.org/10.1172/jci.insight.88864

Vetter, P., Kaiser, L., Schibler, M., Ciglenecki, I., & Bausch, D. G. (2016). Sequelae of Ebola virus disease: the emergency within the emergency. In *The Lancet Infectious Diseases* (Vol. 16, Issue 6, pp. e82–e91). Lancet Publishing Group. https://doi.org/10.1016/S1473-3099(16)00077-3

Vilekar, P., Awasthi, V., Lagisetty, P., King, C., Shankar, N., & Awasthi, S. (2010). In vivo trafficking and immunostimulatory potential of an intranasally-administered primary dendritic cell-based vaccine. *BMC Immunology*, *11*. https://doi.org/10.1186/1471-2172-11-60

Villar, J., & Segura, E. (2020). Decoding the Heterogeneity of Human Dendritic Cell Subsets. *Trends in Immunology*, *41*(12), 1062–1071. https://doi.org/10.1016/j.it.2020.10.002

Villinger, F., Rollin, P. E., Brar, S. S., Chikkala, N. F., Winter, J., Sundstrom, J. B., Zaki, S. R., Swanepoel, R., Ansari, A. A., & Peters, C. J. (1999). Markedly Elevated Levels of Interferon (IFN)-g, IFN-a, Interleukin (IL)-2, IL-10, and Tumor Necrosis Factor-a Associated with Fatal Ebola Virus Infection cording to a previously described protocol [6-8] with primers. In *The Journal of Infectious Diseases* (Vol. 179, Issue 1). https://academic.oup.com/jid/article/179/Supplement_1/S188/881048

Volchkov, V. E., Becker, S., Volchkova, V. A., Ternovoj, V. A., Kotov, A. N., Netesov, S. V., & Klenk, H.-D. (1995). GP mRNA of Ebola Virus Is Edited by the Ebola Virus Polymerase and by T7 and Vaccinia Virus Polymerases1. *Virology*, *214*(2), 421–430. https://doi.org/10.1006/viro.1995.0052

Warfield, K. L., Bosio, C. M., Welcher, B. C., Deal, E. M., Mohamadzadeh, M., Schmaljohn, A., Aman, M. J., & Bavari, S. (2003). Ebola virus-like particles protect from lethal Ebola virus infection. *Proceedings of the National Academy of Sciences of the United States of America*, *100*(26), 15889–15894. https://doi.org/10.1073/pnas.2237038100

Waterhouse, P., Penninger, J. M., Timms, E., Wakeham, A., Shahinian, A., Lee, K. P., Thompson, C. B., Griesser, H., & Mak, T. W. (1995). Lymphoproliferative disorders with early lethality in mice deficient in Ctla-4. *Science (New York, N.Y.)*, *270*(5238), 985–988. https://doi.org/10.1126/science.270.5238.985

Wauquier, N., Becquart, P., Padilla, C., Baize, S., & Leroy, E. M. (2010a). Human fatal zaire ebola virus infection is associated with an aberrant innate immunity and with massive lymphocyte apoptosis. *PLoS Neglected Tropical Diseases*, *4*(10). https://doi.org/10.1371/journal.pntd.0000837

Wauquier, N., Becquart, P., Padilla, C., Baize, S., & Leroy, E. M. (2010b). Human Fatal Zaire Ebola Virus Infection Is Associated with an Aberrant Innate Immunity and with Massive Lymphocyte Apoptosis. *PLoS Neglected Tropical Diseases*, *4*(10), e837. https://doi.org/10.1371/journal.pntd.0000837

Wec, A. Z., Bornholdt, Z. A., He, S., Herbert, A. S., Goodwin, E., Wirchnianski, A. S., Gunn, B. M., Zhang, Z., Zhu, W., Liu, G., Abelson, D. M., Moyer, C. L., Jangra, R. K., James, R. M., Bakken, R. R., Bohorova, N., Bohorov, O., Kim, D. H., Pauly, M. H., … Chandran, K. (2019). Development of a Human Antibody Cocktail that Deploys Multiple Functions to Confer Pan-Ebolavirus Protection. *Cell Host & Microbe*, *25*(1), 39-48.e5. https://doi.org/10.1016/j.chom.2018.12.004

Wherry, E. J. (2011). T cell exhaustion. In *Nature Immunology* (Vol. 12, Issue 6, pp. 492–499). https://doi.org/10.1038/ni.2035

Wherry, E. J., & Ahmed, R. (2004). Memory CD8 T-Cell Differentiation during Viral Infection. *Journal of Virology*, *78*(11), 5535–5545. https://doi.org/10.1128/jvi.78.11.5535-5545.2004

Wightman, F., Solomon, A., Kumar, S. S., Urriola, N., Gallagher, K., Hiener, B., Palmer, S., Mcneil, C., Garsia, R., & Lewin, S. R. (2015). Effect of ipilimumab on the HIV reservoir in an HIV-infected individual with metastatic melanoma. *AIDS (London, England)*, *29*(4), 504–506. https://doi.org/10.1097/QAD.0000000000000562

Wolf, T., Kann, G., Becker, S., Stephan, C., Brodt, H. R., De Leuw, P., Grünewald, T., Vogl, T., Kempf, V. A. J., Keppler, O. T., & Zacharowski, K. (2015). Severe Ebola virus disease with vascular leakage and multiorgan failure: Treatment of a patient in intensive care. *The Lancet*, *385*(9976), 1428–1435. https://doi.org/10.1016/S0140-6736(14)62384-9

Wong, G., Qiu, X., Richardson, J. S., Cutts, T., Collignon, B., Gren, J., Aviles, J., Embury-Hyatt, C., & Kobinger, G. P. (2015). Ebola Virus Transmission in Guinea Pigs. *Journal of Virology*, *89*(2), 1314–1323. https://doi.org/10.1128/JVI.02836-14

Xiong, H., & Pamer, E. G. (2015). Monocytes and infection: Modulator, messenger and effector. *Immunobiology*, *220*(2), 210–214. https://doi.org/10.1016/j.imbio.2014.08.007

Ye, L., Schnepf, D., & Staeheli, P. (2019). Interferon-λ orchestrates innate and adaptive mucosal immune responses. *Nature Reviews. Immunology*, *19*(10), 614–625. https://doi.org/10.1038/s41577-019-0182-z

Yu, C. I., Becker, C., Metang, P., Marches, F., Wang, Y., Toshiyuki, H., Banchereau, J., Merad, M., & Palucka, A. K. (2014). Human CD141+ dendritic cells induce CD4+ T cells to produce type 2 cytokines. *Journal of Immunology (Baltimore, Md.: 1950)*, *193*(9), 4335–4343. https://doi.org/10.4049/jimmunol.1401159

Yu, H., Yang, J., Jiao, S., Li, Y., Zhang, W., & Wang, J. (2015). Cytotoxic T lymphocyte antigen 4 expression in human breast cancer: implications for prognosis. *Cancer Immunology, Immunotherapy : CII*, *64*(7), 853–860. https://doi.org/10.1007/s00262-015-1696-2

Zhang, A. P. P., Bornholdt, Z. A., Liu, T., Abelson, D. M., Lee, D. E., Li, S., Woods, V. L., & Saphire, E. O. (2012). The Ebola Virus Interferon Antagonist VP24 Directly Binds STAT1 and Has a Novel, Pyramidal Fold. *PLoS Pathogens*, *8*(2), e1002550. https://doi.org/10.1371/journal.ppat.1002550

Acknowledgement

First, I would like to thank César for the interesting topic and the unique opportunities I had during my PhD. Not many people in this world have the opportunity to work with one of the deadliest pathogen and go to very rural places to meet people who actually survived encountering Ebola. Moreover, meeting people from MSF or other scientists (Anita, Ian, and Billy), who are very involved in the topic or experienced the virus himself, are moments I will never forget. Thank you for this!

Very importantly, I would like to thank Prof. Redecke, who helped, supported, and motivated on every level that he could. Thank you as well for taking over the supervision on the University site.

Thank you Prof. Schaible and Prof. König for being part of my thesis committee.